DETECTING GENETIC VARIANTS IN RADIATION-INDUCED LUNG DISEASE

Mihaela Alexandra Paun

Department of Human Genetics

McGill University, Montreal

June 2013

A thesis submitted to McGill University in partial fulfillment of the requirements of the degree of Doctor of Philosophy

To Daniel, my everything

ABSTRACT

Thoracic radiotherapy, a common treatment modality for thoracic cancers, has pulmonary side-effects of either excessive inflammation (alveolitis), or pulmonary fibrosis consisting of uncontrolled deposition of collagen in the lungs, for which no cure exists. Prior knowledge, before radiotherapy, of patients genetically predisposed to fibrosis would improve cancer treatments. Based on the known similarities between human and mouse responses to lung irradiation, we used a murine model to detect molecular pathways, immune mechanisms and genetic variants associated with the development of fibrosis.

Through a gene expression study in the lungs of fibrosis-prone C57Bl/6J and alveolitis-prone A/J and C3H/HeJ mice we found that several inflammatory pathways are significantly altered and differentiate between alveolitis- and fibrosis-prone mice and that Cell Adhesion Molecule signaling is the most significantly perturbed pathway in all strains. The differences in fibrosis between inbred mice led us to perform a genome-wide association analysis in a panel of 27 strains. We found several variants in immune genes associated with fibrosis, among which several SNPs upstream of Cell adhesion molecule 1 (*Cadm1*), a promising potential candidate gene for susceptibility to fibrosis. The role of immunity in lung disease prompted the investigation of mice lacking Tlr2 and/or Tlr4 receptors in response to thoracic irradiation. While *Tlr2*-/- and *Tlr4*-/- mice did not differ from C57Bl/6J wildtype, *Tlr2,4*-/- mice have decreased survival and more severe fibrosis compared to irradiated wildtype animals. Subsequent analyses of lymphocytes infiltrating the lungs after thoracic irradiation revealed the more severe fibrosis in the *Tlr2,4*-/- strain to be due to increased production of Il6, Tgfβ and Il17 and lack of protective Ifnγ. These studies also showed the pro-fibrotic role of Il17, as *Il17*-/- mice do not develop the disease.

To summarize, in this thesis we identified immune pathways and several candidate genes associated with the presence of fibrosis following thoracic radiation. We also showed that disease development is dictated, in part, by Tlr signaling and disequilibrium between pro- and anti-fibrotic cytokines.

RÉSUMÉ

La radiothérapie thoracique, un traitement commun pour les cancers de la cavité thoracique, a des effets secondaires au niveau des poumons: l'inflammation excessive (alvéolite) ou la fibrose pulmonaire qui consiste d'un dépôt incontrôlable de collagène dans les poumons, et pour laquelle aucun traitement n'existe. La connaissance a priori, avant l'administration de la radiothérapie, des patients susceptibles au développement de la fibrose, améliorerait considérablement les traitements du cancer. Étant données les similarités des réponses à la radiation entre l'homme et la souris, nous avons utilisé un modèle murin pour la détection des voies moléculaires, mécanismes immunitaires et des variantes génétiques associés avec le développement de la fibrose pulmonaire.

A travers une étude d'expression des gènes sur les poumons des souris susceptibles à la fibrose, C57Bl/6J et à l'alvéolite, A/J and C3H/HeJ, nous avons identifié certaines voies inflammatoires significativement impactées par le traitement et différentient entre les souches susceptibles à la fibrose, et celles succombant à l'alvéolite. Parmi celles-ci, la voie de Signalisation des Molécules d'Adhésion Cellulaire est la plus perturbée dans toutes les souches. Pour déterminer la composante génétique qui détermine les différences en degré de fibrose parmi les souches des souris consanguines, nous avons fait une analyse d'association pan-génomique sur un groupe de 27 souches de souris. Nous avons identifiés plusieurs variants associés à la fibrose, situés dans des gènes immunitaires, parmi lesquels, plusieurs SNPs dans le gène *Cadm1* (Cell Adhesion Molecule 1). Étant donné le rôle de l'immunité dans la maladie pulmonaire, nous avons testé la réponse des souris manquant les récepteurs Tlr2 et/ou Tlr4 à la radiation thoracique. Tandis que les souris *Tlr2*-/- et *Tlr4*-/- ne diffèrent pas dans leur phénotype de la souche sauvage C57Bl/6J, les souris *Tlr2,4*-/- succombent plus tôt, a une fibrose plus sévère que les souris sauvages. Des analyses ultérieures sur les lymphocytes qui s'infiltrent dans les poumons à la suite de la radiation, ont démontré que la fibrose plus sévère chez les souris *Tlr2,4*-/- est due à une

production augmentée des cytokines Il6, Il17 et Tgfβ et à l'absence du Ifnγ qui a un rôle protecteur. Ces études ont aussi montré le rôle pro-fibrotique du Il17, étant donné que les souris *Il17*-/- ne développent pas la maladie.

Pour conclure, dans cette thèse nous avons identifié des voies de signalisation immunitaires et plusieurs gènes candidats associés avec la présence de la fibrose suivant la radiation thoracique. Nous avons aussi montré que le développement de la maladie est dicté, en partie, par la voie de signalisation des récepteurs Tlr et aussi par un déséquilibre entre les cytokines pro- et anti-fibrotiques.

ACKNOWLEDGEMENTS

There are no proper words to convey my deep gratitude and respect for my supervisor, Dr. Christina Haston. She has been a wonderful mentor throughout these five years, providing guidance for all the scientific projects and at the same time allowing me to test new ideas. I have learnt a lot under her supervision, and I could not have asked for a more inspirational, supportive and patient mentor. I hope one day to become a scientist as passionate and dedicated as Dr. Haston.

I would also like to thank my Supervisory Committee members, Dr. Ciro Piccirillo and Dr. Salman Qureshi, both amazing scientists whose advice on how to better my projects was invaluable. They have provided thoughtful and detailed comments during all my Supervisory Committee Meetings at the end of which I always felt inspired, my mind filled with new and exciting scientific ideas. I am particularly grateful for their input in areas pertaining to the vast and complex field of immunology.

This work would not have been possible without the financial support of our funding sources, Canadian Institute for Health Research, Canadian Cancer Society, McGill University Health Center, Faculty of Medicine and Quebec Respiratory Health Training Network.

A huge “Thank you!” to all my current and former lab mates: Amit, Anguel, Lisa, Mark, Jess, Tom and Anne-Marie. They are all such lovely people, with whom I have tied strong friendships. I will always remember the laughs we had, the crazy dinner parties and board game sessions!

Finally, a love-filled “Thank you!” to those most dear to my heart – my darling husband Daniel and my family in Romania. During my PhD Daniel has supported, encouraged, entertained, helped and loved me beyond measure, which has made these five years all the more enjoyable. I wouldn’t be here today without the love and support of my parents, who have always encouraged me to better myself. My wonderful mother, the person I always look up to, is the one who has first opened my eyes to the fascinating medical field and for this I will always be grateful.

TABLE OF CONTENTS

CONTRIBUTION OF AUTHORS

Chapter II: **Gene expression profiling distinguishes radiation-induced fibrosing alveolitis from alveolitis in mice**

A Paun, AM Lemay, CK Haston

A Paun performed the microarray analysis and the pathway analysis. AM Lemay irradiated and phenotyped the mice and measured the gene expression through RT-PCR. The manuscript was written by A Paun, AM Lemay and CK Haston.

Chapter III: **Genomic and genome-wide association of susceptibility to radiation-induced fibrotic lung disease in mice**

A Paun and CK Haston

A Paun performed the bioinformatics analyses. Mouse irradiation was done by A Paun and Jessica Fox. Mouse phenotyping was done by Jessica Fox. The manuscript was drafted by A Paun and CK Haston.

Chapter IV: Combined *Tlr2* and *Tlr4* deficiency increases radiation-induced pulmonary fibrosis in mice

A Paun, J Fox, V Balloy, M Chignard, ST Qureshi, CK Haston

A Paun irradiated and phenotyped the *Tlr2*-/- and *Tlr4*-/- mice, performed the statistical analyses and the RT-PCR for *Has2* and *Hyal2*. *Tlr2,4*-/- and C57Bl/6 mice were irradiated and phenotyped by Josée Paradis. J Fox performed the caspase 3 staining. The genetically altered mice were provided by ST Qureshi. The single knockout mice were generated by M Chignard and V Balloy. The manuscript was prepared by A Paun and CK Haston.

Chapter V: **The Th1/Th17 balance in the lung dictates a fibrosis response or sparing of radiation-induced lung disease in mice**

A Paun and CK Haston

A Paun planned and executed all experiments and data analysis. The manuscript was written by A Paun and CK Haston.

ORIGINAL CONTRIBUTION TO KNOWLEDGE

Chapter II: **Gene expression profiling distinguishes radiation-induced fibrosing alveolitis from alveolitis in mice**

I performed a lung transcriptome analysis of three mouse strains (A/J and C3H/HeJ prone to alveolitis at different timepoints after irradiation and C57Bl/6J succumbing to fibrosis) which revealed that alveolitis and fibrosis are dictated by distinct genetic profiles. These differences were reflected in the significantly altered pathways in the three strains uncovered by a Pathway Analysis – distinct immune, proliferation and remodeling pathways are altered in each phenotype.

Chapter III: **Genomic and genome-wide association of susceptibility to radiation-induced fibrotic lung disease in mice**

Using an online mouse SNP database and radiation-induced lung fibrosis phenotypes I performed a genome-wide association analysis of 27 inbred strains which I integrated with previous quantitative trait locus (QTL) and gene expression data. These studies revealed significant SNPs located in 10 loci across the genome as well as interactions between SNPs in previously-determined radiation-induced pulmonary fibrosis QTLs.

Chapter IV: Combined *Tlr2* and *Tlr4* deficiency increases radiation-induced pulmonary fibrosis in mice

Given the importance of the immune system in the pathology of radiation-induced lung disease and the fact that Toll-like receptors (Tlr) are key for both innate and acquired immune responses I studied the response of *Tlr2*-/-, *Tlr4*-/- and *Tlr2,4*-/- to thoracic irradiation in terms of the pulmonary histological aspects, survival time and gene expression and compared them to those of wildtype C57Bl/6J mice. Through the analysis of two hyaluronan-related genes, I determined a potential role for the degrading enzyme, hyaluronidase in the more severe radiation-induced disease of *Tlr2,4*-/- mice.

Chapter V: **The Th1/Th17 balance in the lung dictates a fibrosis response or sparing of radiation-induced lung disease in mice**

Using flow cytometry methods I studied the various lymphocyte populations infiltrating in the lungs of six strains of mice after irradiation (three strains prone to fibrosis and three prone to alveolitis) in order to find what lymphocytes distinguish between the two lung phenotypes. Based on the results obtained from this experiment, I also analyzed mice deficient in *Tlr2&4*, *Il17a* and invariant natural killer T cells in terms of lung histology, survival, T helper cell subsets and cytokine profiles in the lungs following thoracic radiation.\

LIST OF FIGURES

LIST OF TABLES

ABBREVIATIONS

Abl2	v-abl Abelson murine leukemia viral oncogene 2
ANOVA	Analysis of variance
ATM	Ataxia telagiectasia mutated gene
B6	C57Bl/6
BAL	Bronchoalveolar lavage
Btnl1	Butyrophilin-like 1
C3H	C3H/HeJ
Cadm1	Cell adhesion molecule 1
Cdkn1a	Cyclin-dependent kinase inhibitor 1A
CML	Chronic myeloid leukemia
DAMP	danger associated molecular patterns
Ddr1	Discoidin domain receptor family, member 1
EMMA	Efficient mixed model association
EOE	End of experiment
EST	Expressed sequence tag
FDR	False discovery rate
Gata3	GATA-binding protein 3
GO	Gene ontology
GOFFA	Gene ontology for functional analysis
Gp96	Heat shock protein 90, beta
GWAS	Genome-wide association study
Gy	Gray
H&E	Hematoxylin and eosin
HAM	Haplotype association mapping
Has2	Hyaluronan synthase 2
Hmgb1	High mobility group box 1
Hsp	Heat shock protein
Hyal2	Hyaluronidase
Ifnγ	Interferon gamma
Il	Interleukin
IPF	Idiopathic pulmonary fibrosis
LD	Linkage disequilibrium
LIMMA	Linear models for microarray analysis
MHC	Major histocompatibity complex
MMP	Metalloproteinase

mTOR	Mammalian target of rapamycin
MyD88	Myeloid differentiation primary response gene 88
NF-kB	Nuclear factor kappa B
NK cell	Natural killer
NKT cell	Natural killer T cell
p21	Cdkn1a, Cyclin-dependent kinase inhibitor 1A
PCR	Polymerase chain reaction
Pin1	protein (peptidyl-prolyl cis/trans isomerase) NIMA-interacting 1
PMN	Polymorphonuclear cells
QTL	Quantitative trait locus
QWAS	QTL-wide association study
Radpf	Radiation-induced pulmonary fibrosis locus
Rexo2	Rex2, RNA exononuclease 2 homolog (S. cerevisiae)
RT-PCR	Real-time PCR
SEM or SE	Standard error of mean
Shprh	SNF2 histone linker PHD RING helicase
Slamf6	SLAM-family member 6
SNP	Single nucleotide polymorphism
TCR	T cell receptor
Tgfβ	Transforming growth factor beta
Th	T helper
TIMP	Tissue inhibitors of metalloproteinases
Tlr	Toll-like receptor
Tnfα	Tumor necrosis factor alpha
XRCC	X-ray repair complementing defective repair in Chinese hamster cells
Xrn2	5'-3' exoribonuclease 2

CHAPTER I: GENERAL INTRODUCTION

Rationale and Approach

Thoracic tumor management through radiotherapy can lead to side-effects of excessive inflammation or uncontrolled deposition of collagen (fibrosis) in the lungs. A patient's response to thoracic radiotherapy is influenced by the dose of radiation, tissue volume treated and unknown genetic factors. Higher doses would ensure better tumor control however they are more detrimental to patients susceptible to develop lung disease. Prior knowledge, before radiotherapy administration, of the patients prone to develop side effects would allow physicians to increase the dose of radiation for resistant individuals and find more efficient treatment modalities for those whose genetic background predisposes them to pulmonary damage. The identification of causal variants associated with radiotherapy side-effects in patients is hampered by the difficulty of assembling a statistically relevant cohort for genetic screening as well as confounding environmental factors such as the presence of cancer, administration of chemotherapy or existing comorbidities. Studies in murine models can be replicated in sufficient numbers of genetically identical animals maintained in a controlled environment thus circumventing the difficulties of human association studies. In this thesis we used genetic, molecular and bioinformatic methods to identify the genetic variants and mechanisms contributing to radiation-induced pulmonary fibrosis in a murine model of the disease.

Given that pulmonary fibrosis is a complex phenotype, involving inflammatory, proliferative and remodeling processes, we undertook a multi-angle approach towards finding candidate genes. To determine the effects of lung irradiation on molecular pathways we studied gene expression profiles which we subsequently integrated with an association analysis of lung disease and genome variants between mouse strains. Also, based on the confirmed inflammatory contribution to pulmonary fibrosis, we analyzed lymphocyte populations

infiltrating in the lungs and the phenotype of mice lacking various immune genes in order to pinpoint how altering immune system components influences fibrosis development.

General principles of radiation damage

Thoracic radiotherapy is administered to patients with tumors in the thorax area (e.g. lung, breast, esophageal cancers and Hodgkin's lymphoma) [1-5] either with curative intent, as an adjuvant with chemotherapy or as a palliative treatment for symptomatic relief.

In this context the radiation dose is measured in Gray (Gy). 1Gy is the amount of energy imparted to a unit of matter (in this case tissue) and is equal to 1 Joule per kilogram [6]. In this thesis a Gamma Cell Cesium-137 instrument was used which produces radiation at the rate of 0.7Gy per minute.

Pulmonary tissue reactions to radiation involve DNA and cellular damage responses. High energy rays can break the hydrogen bonds in water molecules, immediately producing free radicals which lead to DNA strand breaks, base damage, DNA-DNA or DNA-protein crosslinks. Unrepaired chromosomal damage promotes mitotic cell death within the first few divisions after radiation [7, 8]. This initial cellular insult prompts a tissue response similar to wound healing, consisting of inflammatory cell migration to the site of damage, release of a cytokine cascade and collagen deposition in the later stages. Unlike normal wound healing which is self-limiting, these responses to radiation are perpetuated over months/years, increasing the amounts of free radicals and tissue damage, finally leading to excessive collagen production and destruction of tissue architecture [9]. Therefore the extent of damage following radiation is dictated by the ongoing tissue reaction to the initial insult as well as the ability to achieve homeostasis during the later stages by scavenging free radicals, compensating for cell loss, and balancing pro- and anti- inflammatory responses.

Radiation-induced lung damage

In the clinical context, the limiting side effects of thoracic radiotherapy occur in 20-40% of the patients [10-12] and increase to 40-60% when chemotherapy is also administered [13]. These adverse reactions limit the dose which can be given, preventing optimal tumor control [14, 15]. Indeed, lung cancer survival rates are significantly improved after treatment with higher doses of radiation [16] however a more aggressive treatment increases adverse side effects incidence. These side effects consist of two distinct but interconnected stages: the early inflammatory phase (pneumonitis or alveolitis) and the late fibrotic phase (fibrosing alveolitis) [12, 17].

Alveolitis occurs 2-3 months after treatment and its main characteristics are edema, alveolar cell death, inflammatory cell infiltration in the alveolar spaces and lung parenchyma, congestion and increased vascular permeability due to vascular system damage. Patients presenting with alveolitis display dyspnea, fever, cough and chest pain. Alveolitis responds to steroid treatment, although steroid use has both acute and long-term side-effects [18]. If alveolitis is not controlled, the release of cytokines and chemokines by immune cells, fibroblasts, epithelial and endothelial cells further exacerbates inflammation leading to fibroblast proliferation and ultimately lung fibrosis [19, 20].

Fibrosing alveolitis (fibrosis) develops insidiously between 6-24 months following radiation [21]. It is considered an irreversible condition characterized by fibroblast proliferation, deposition of extracellular matrix components and destruction of normal lung architecture. Symptomatically fibrosis manifests with progressive dyspnea, cough, cyanosis, and in late stages respiratory failure and cor pulmonale [22].

Cellular and molecular mediators of radiation-induced lung damage

Pulmonary fibrosis is considered a disease of impaired homeostasis. The non-resolving inflammation following pulmonary damage is due to an infiltration of inflammatory cells, impaired renewal of epithelial cells, impaired apoptosis of fibroblasts as well as aberrant remodeling and deposition of extracellular matrix in the alveoli, ultimately leading to destroyed lung architecture. Therefore assessing the functional significance of each cell type, immune cells in particular, can provide a better understanding of the pathways driving pulmonary fibrosis and aid in focusing the research to find genetic variants.

Pneumocytes, myofibroblasts, macrophages and neutrophils

There are two types of cells making up the alveolar wall: **type I and type II pneumocytes**. Upon radiation damage, sensitive type I cells undergo apoptosis. This prompts the proliferation of type II cells which have the capacity to differentiate into type I cells and repopulate the alveolar epithelium. Increased apoptosis of type II cells is a feature of idiopathic pulmonary fibrosis (IPF) [23] and targeted injury of these cells leads to fibrosis development [24, 25].

The cytokines and growth factors secreted by injured epithelial cells promote the differentiation of resident fibroblasts into **myofibroblasts** [25, 26] as well as increased collagen production [24]. Myofibroblasts are key effector cells in the fibrotic process due to the synthesis, deposition and degradation of extracellular matrix (ECM) through expression of matrix metalloproteinases (MMPs) and tissue inhibitors of metalloproteinases (TIMPs) [27].

Infiltration and proliferation of fibroblasts as well as production of ECM is driven by a network of resident and recruited inflammatory cells. Activated **macrophages** present at sites of inflammation are involved in removing tissue debris, cell killing and activation of myofibroblasts. In models of both lung and liver fibrosis [28, 29], during disease progression, macrophages promote the activation of

myofibroblasts through the release of pro-fibrotic mediators such as transforming growth factor beta (Tgfβ).

Once recruited from the blood at the site of inflammation, **neutrophils** degranulate, releasing proteolytic enzymes and reactive oxygen species [30] which can damage the lung parenchyma and cause degradation of ECM components. In several models of pulmonary fibrosis [31-34], including radiation-induced [35], a neutrophil influx in the bronchoalveolar lavage (BAL) of animals was observed.

Lymphocytes

Increased numbers of lymphocytes are observed in the BAL of patients who have undergone thoracic radiotherapy [36, 37] and a decreased incidence of pneumonitis was seen in patients undergoing a thymectomy prior to whole body irradiation [38]. Concerning the different T cell subtypes, in the BAL fluid of patients with radiation pneumonitis both higher and lower CD4/CD8 ratios have been reported [39, 40]. Animal models of radiation-induced lung damage also present high numbers of T cells in the lung parenchyma and BAL [20, 41-43]. In a rat model depleting CD4+ T cells led to significantly reduced radiation side-effects in the lung [44].

Perhaps more important than the numbers of CD4+ lymphocytes in the lungs after irradiation is their T helper Th1/Th2/Th17/Treg phenotype. Th2 cytokines are chemoattractants for fibroblasts [45], they promote fibroblast activation and proliferation [46] as well as Tgfβ and collagen production in these cells [47-49]. In the fibrosis-prone C57Bl/6 (B6) strain, lung irradiation leads to expression of *Gata3*, the transcription factor for Th2 differentiation as well as increased production of interleukin (Il)-13 [50]. Similarly, in rats radiation induces an elevated production of Il4 by infiltrating Th cells [44].

Th1 cells produce anti-fibrotic cytokines such as interferon gamma (Ifnγ), Il2, Il12 which inhibit the differentiation of the Th2 subset [51]. Moreover Ifnγ in particular directly inhibits collagen synthesis from lung fibroblasts [52],

antagonizes the effects of Tgfβ on fibroblasts [53] and has been assayed as a therapeutic in idiopathic pulmonary fibrosis [54, 55].

Following their recent discovery the Th17 subset has been associated with a variety of pulmonary phenotypes such as bleomycin-induced fibrosis [56, 57], hypersensitivity pneumonitis [58] and interstitial pneumonia [59]. The BAL of patients with IPF contains high amounts of this cytokine [56]. Il17 increases collagen production in cardiac fibroblasts [60] and is a potent neutrophil chemoattractant [61]. In fact neutrophil recruitment in the IPF lungs is an early mortality predictor [62] and blocking Il17 in a model of lung fibrosis leads to decreased collagen production [63]. Beside Th cells, other sources of Il17 include CD8+ T cells, natural killer (NK) cells, γδ T cells and a subset of natural killer T (NKT) cells [64-69].

Toll-like Receptors

Toll-like receptors (Tlr) are a class of proteins with a fundamental role in the innate immune system. Their role is to recognize and bind a series of structurally conserved microbial molecules (pathogen-associated molecular patterns or PAMPs) and to further activate downstream signaling pathways leading to the production of cytokines, chemokines and antimicrobial peptides by the immune cells.

Inflammation and immune responses can also occur in the absence of an infection when cells produce endogenous ligands called danger associated molecular patterns (DAMPs) which can trigger Tlr signaling. For example heat-shock proteins (Hsp)60, Hsp70 and Gp96 trigger nuclear factor kappa B (NF-kB) activation in neutrophils, macrophages and dendritic cells by binding Tlr2 and Tlr4 [70, 71]. The DNA-binding protein high mobility group box 1 (Hmgb1) is a potent inflammatory signal [72] as it induces production of tumor necrosis factor alpha (Tnfα), Il1β, Il10 and Il6 by monocytes, macrophages and neutrophils also through Tlr2 and Tlr4 [73, 74]. Fragmented ECM components such as fibronectin and heparan sulfate which signal through Tlr4 [75, 76] and induce dendritic cell maturation. Moreover

hyaluronan, a glycosaminoglycan acting as a biological lubricant binds Tlr2 and Tlr4 [77].

Tlrs in lung injury

The contribution of Tlrs, Tlr2&4 in particular, to various non-infectious inflammatory conditions of the lung has been intensely researched. Tlr4 recognizes diesel exhaust particles and triggers production of several inflammatory markers in mouse lungs [78], mediates ozone-induced lung hyperpermeability [79] and hemorrhage-induced acute lung injury [80]. Both Tlr2 and 4 contribute to cigarette smoke-induced cytokine production by macrophages, epithelial cells and lymphocytes [81-83]. These two receptors cross-talk in hemorrhage-induced lung injury [84] and exert similar functions in bleomycin-induced pulmonary fibrosis [77]. Radiation-induced danger signals activate both the innate and lymphocyte mediated immunity through Tlrs. For example, *Tlr4*-/- mice are protected from radiation-induced thymic lymphomas due to the inability of Hmgb1 to enhance pro-tumorigenic Il6 via Tlr4 [85]. Radiation directly affects the expression of several members of the Tlr family. For instance, small doses of radiation increase Tlr4 expression on macrophages as well as expression of a molecule downstream of Tlr2&4, myeloid differentiation primary response gene 88 (MyD88) [86]. Regarding the latter, a 2012 study [87] showed that MyD88 has a protective role against fibrosis by augmenting protective inflammatory responses.

Thus far, no reports exist on the function of Il17 and Tlr2&4 in radiation-induced pulmonary fibrosis and given their importance in inflammatory responses, in-depth understanding of their involvement in lung response to radiation is essential.

Factors influencing radiation response

The incidence and extent of the damage depends on treatment-specific factors such as the volume of the lung treated, the total dose received by the organ and the number of fractions forming the total dose. Predisposing patient-

related factors include advanced age, smoking, as well unknown genetic variants [88].

There are several lines of evidence for a genetic contribution to radiation-induced lung disease. Firstly, 20% of idiopathic pulmonary fibrosis cases, a disease of unknown etiology but with similar clinical manifestations as the fibrosis caused by radiation, are familial [89, 90]. Secondly, patients with genetic diseases such as Ataxia Telangiectasia and Nijmegen Breakage Syndrome have increased radio-sensitivity [91-93]. Moreover, several studies have shown association of radiotoxicity and changes in gene expression following treatment [94-97]. Lastly, the association studies through the candidate gene approach performed until recently have uncovered mutations in genes such as *TGFβ*, ataxia telangiectasia mutated (*ATM*), X-ray repair complementing defective repair in Chinese hamster cells (*XRCC*)1*&3* and antioxidant enzyme genes to be associated with normal tissue reactions to thoracic radiation [98-101].

Animal models of radiation-induced lung damage

The radiation responses of humans and mice results in similar lung disease both in terms of the underlying pathology and time course. The side effects of thoracic irradiation, alveolitis and pulmonary fibrosis, which occur 3 and 6 months post therapy, respectively, are also found in various inbred mouse strains, providing additional evidence for a genetic component to the phenotype [102-104]. Hence murine models of radiation-induced lung injury are valuable tools to investigate the disease mechanisms in vivo.

The most commonly used strains for the study of radiation-induced lung toxicity are C3H/HeJ (C3H) and B6 mice. B6 mice develop fibrosis approximately 6 months (23-26 weeks) post irradiation, whereas C3H mice succumb to a severe form of alveolitis 3 months (12-14 weeks) post irradiation [35, 105].

This phenotype difference between B6 and C3H mice has been used in linkage studies to map five quantitative trait loci (QTL) of pulmonary fibrosis: Radpf1-3 located on chromosomes 17 (27Mb - 37Mb), 1 (149Mb - 190Mb) and 6 (115Mb - 146Mb) as well as two additional loci on chromosomes 7 (0Mb - 47Mb) and 9 (32Mb – 65Mb) [35, 105].

As is the case with most complex phenotypes, the QTLs for pulmonary fibrosis are large and contain hundreds of genes, therefore different techniques are used to narrow down the region and number of candidate genes.

Congenic mice are used to confirm the existing QTL, and by creating subcongenic lines through additional crosses the donor region can be shortened until the number of candidate genes it contains are reduced to a more manageable number. Another popular bioinformatic method is based on single nucleotide polymorphisms (SNPs) between different strains of mice which can be tested in silico for association with a phenotype of interest. Performing a linkage as well as an association analysis can reduce the number of false positive loci [106] and the number of candidate genes within a QTL as shown in a study of lung cancer in mice [107].

Genome-wide association analysis

The principle behind genome-wide association studies (GWAS) is that given a biallelic SNP and a panel of inbred strains previously phenotyped for the trait of interest, the SNP is associated with the phenotype if one allele is present in susceptible strains and the other allele in resistant strains. Usually the analysis involves the regression of the phenotype on each SNP and from each test generating a p-value which reflects the degree of association of that SNP with the phenotype. Subsequently the SNPs are ranked based on their p-values and a significance threshold is set; all SNPs with p-values below the threshold are considered as significantly associated.

The polymorphism data source used in this thesis is the CGD1 database [108] encompassing 7.8 million SNPs in 49 inbred strains compiled from various existing databases. Missing genotypes for some SNPs were imputed with various levels of confidence based on linkage disequilibrium (LD) found in inbred strains.
The main drawbacks of GWAS stem from the genome architecture of laboratory mice. Their unique breeding history and small number of founder strains translates to population stratification, large LD blocks and a mosaic-like structure of the genome. This leads to diminished statistical power to detect associated SNPs, difficulty in fine-mapping loci past a certain resolution and spuriously associated SNPs. Recently Kang et al. [109] introduced a new algorithm which efficiently controls both the population stratification and the relatedness of the individuals in model organism studies. It does so by fitting a linear mixed model to the phenotypic data taking into account the effect of genetic relatedness through a kinship matrix calculated based on the degree of similarity between each two strains.

This algorithm has been used to detect murine loci controlling parasite growth and susceptibility to infection [110, 111], bone mineral density [112], depressive- and anxiety-like behavior [113], as well as novel candidate genes for pulmonary adenoma [114].

Haplotype association analysis

Given the drawbacks of single SNP association studies, mainly with respect to the power of statistical analyses, haplotype association mapping (HAM), also called in silico QTL mapping, is a powerful alternative which allows the identification of QTLs using a large number of strains. HAM requires a dense map of genotyped SNPs which are used to infer the limits of the haplotype blocks. As shown in Figure 1 for each of the haplotype blocks, the phenotype values are compared between the strains carrying different haplotypes and the association of the phenotype with the haplotype distribution is performed using a statistical test (e.g. analysis of variance [ANOVA]). This approach can be used to detect new

QTLs or to refine existing ones by finding, within the region, a block which segregates with the phenotype. Past studies have used HAM to identify novel susceptibility genes for malaria survival [115], cholesterol levels [116], hepatic fibrosis [117] and fatty liver disease [118].

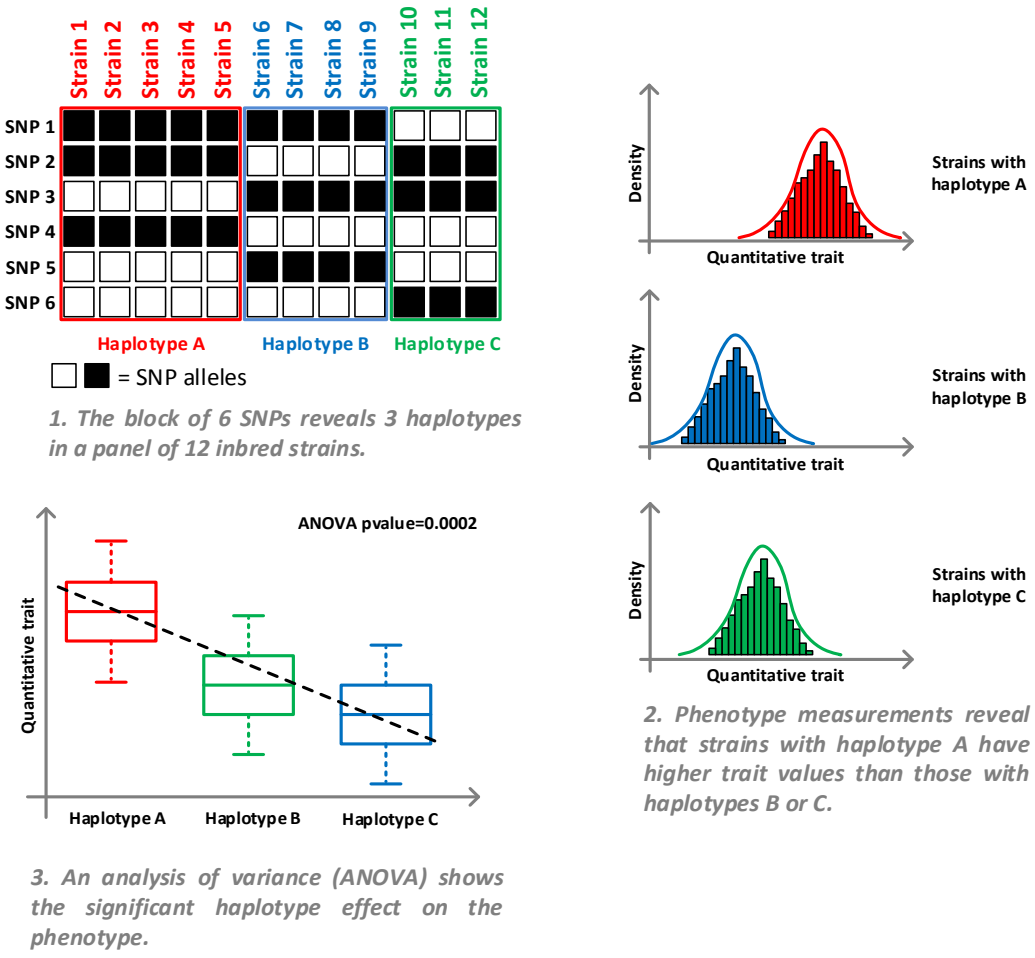

Figure 1. Principle of haplotype association mapping in inbred mice
Haplotypes are inferred *in silico* from SNP data, in a panel of inbred strains. The strains are then grouped according to their shared haplotype and the phenotype values are compared between groups of individuals sharing the same haplotype segment. A statistical test is performed, yielding the significance of the association. *Adapted with permission from Sterken R et al., Kidney International 2010.*

Gene expression profiling and pathway analysis

Genome-wide expression profiling through microarrays allows the simultaneous analysis of all genes in the genome. Used in combination with methods such as GWAS it provides additional support in further candidate gene discovery experiments (i.e the candidate gene list resulting from an association analysis can be refined by focusing solely on the genes expressed in the tissue where the disease manifests itself).

When analyzing the output of a microarray experiment the challenge is to gain insight into the biological mechanisms using the genetic profiles. It is more informative to analyze not individual differentially expressed genes but the pathways they belong to.

The microarray experiment used in this thesis compared gene expression profiles in the lungs of irradiated versus control mice of the three strains: A/J, B6 and C3H. These strains develop distinct phenotypes following thoracic irradiation (C3H and A/J succumb to alveolitis 12-14 and 24-26 weeks post irradiation whereas B6 mice develop fibrosis at the 23-26-week timepoint). For this study we applied the method developed by Draghici et al. [119] which generates an Impact Factor for each pathway, based on which it is decided whether a certain pathway is significantly altered. The Impact Factor statistic takes into account not only the number of pathway genes among those in the differentially expressed set, but also the fold changes of the genes and the topology of the pathway.

The same pathway analysis method has been used to study the effects of androgen on prostate fibroblasts [120], the transcriptional network during prostate cancer progression [121], changes in gastric epithelial cells after exposure to Helicobacter pylori [122] as well as transcriptome changes in hepatitis B-induced hepatic carcinoma [123].

Aims of the research project

The main question to be addressed in this thesis regards the genetic contribution to radiation-induced lung fibrosis in a mouse model. To answer this

we combined bioinformatic approaches of gene expression and SNP-phenotype association analyses with studies of mice deficient in various immune genes, aimed at determining the lymphocyte contribution to the disease.

Based on the hypothesis that thoracic radiation treatment alters the gene expression profile of the lung, we sought to find which genetic pathways differ between mice succumbing to alveolitis and those succumbing to fibrosis. For this we performed a microarray study on lung tissue in three strains of mice (two prone to alveolitis and one prone to fibrosis) and subsequently analyzed the differentially expressed genes in terms of the molecular pathways they belong to. Among these were immune-related pathways and Tlr signaling.

The second objective was to determine SNPs and haplotypes associated with pulmonary fibrosis. We hypothesized that the observed phenotype differences between inbred murine strains are due to genetic variations and performed association analyses in 27 strains of inbred mice whose lung phenotype following irradiation was also determined. Among the list of candidates, two genes involved in T lymphocyte activation, SLAM-family member 6, *Slamf6* and Butyrophilin-like 1, *Btnl1* were revealed to contain significant SNPs by this genome-wide analysis.

The third aim of the project was to determine the phenotype of mice lacking Tlr2 and/or Tlr4 receptors. The starting hypothesis was that these receptors, which act as a bridge between adaptive and innate immunity, mediate inflammation and fibrosis through their ability to bind self antigens from damaged tissues. To investigate this, *Tlr2-/-*, *Tlr4-/-*, *Tlr2,4-/-* and wildtype B6 mice received thoracic irradiation and their lung phenotype was assessed through inflammatory cell infiltration and histological evaluation, survival time and gene expression measurement.

The final objective was to assess how various lymphocyte subsets mediate radiation-induced lung disease. Given that inflammatory cells are important players in the response to radiation, we hypothesized that differences between

inbred strains in terms of lymphocyte subsets can partially explain their different pulmonary phenotypes after radiation. To test this hypothesis we studied the lymphocytes infiltrating the lungs in six inbred strains of mice and phenotyped three genetically-altered strains (lacking Tlr2,4 receptors or a functional *Il17a* gene) with varying degrees of fibrosis in terms of T helper cell subsets and cytokine production in the lungs.

CHAPTER II: GENE EXPRESSION PROFILING DISTINGUISHES RADIATION-INDUCED FIBROSING ALVEOLITIS FROM ALVEOLITIS IN MICE

A Paun, AM Lemay, CK Haston

Originally published in *Radiation Research, 2010, 173(4):512-21*

Abstract

Thoracic cavity radiotherapy is limited by the development of alveolitis and fibrosis in susceptible patients. To define the response to 18 Gy pulmonary irradiation in mice at the gene expression level and to identify pathways that may influence the alveolitis and fibrosis phenotypes, expression profiling was undertaken. Male mice of three strains, A/J (late alveolitis response), C3H/HeJ (C3H, early alveolitis response) and C57BL/6J (B6, fibrosis response), were exposed to thoracic radiation and euthanized when moribund, and lung tissue gene expression was assessed with microarrays. The responses of A/J and C3H mice were more similar to each other (60% of differentially expressed genes detected in both strains) than to that of B6 mice (17% overlap). Pathway analysis revealed the expression of complement and of B-cell proliferation and activation genes to distinguish fibrosis from the alveolitis response and cytokine interactions and intracellular signaling differed between A/J and C3H mice. A genomic approach was used to identify specific pathways that likely contribute to the lung response to radiation as fibrosis or alveolitis in mice.

Introduction

Radiotherapy delivered to the thoracic cavity can produce serious inflammatory (alveolitis) or fibrotic (fibrosing alveolitis) side effects in the lung [14, 124]. Pulmonary fibrosis is characterized by cellular proliferation and the progressive accumulation of extracellular constituents resulting in remodeling of the lung interstitium, while alveolitis is an inflammatory response associated with alveolar airspace cell infiltration and thickening of the alveolar walls [125]. Alveolitis usually occurs within weeks to months after the conclusion of treatment, while fibrosis can develop over years [126].

Both alveolitis and fibrosis occur in inbred mice after thoracic irradiation. The gene expression profiles for these responses in mice may be relevant to our understanding of this complication of radiation therapy. This approach was used

recently to distinguish mammary tumors induced by radiation from those induced by chemicals [127], to identify altered gene expression after brain irradiation in rats [128], and to uncover specific pathways that differentiate familial from sporadic idiopathic interstitial pneumonia [129] and mild from severe cystic fibrosis lung disease [130]. We [35, 102, 131] and others [103, 104] have reported mouse strain differences in lung response after high-dose whole thorax irradiation; C3H/HeJ (C3H) and A/J mice develop a diffuse lethal alveolitis while C57BL/6J (B6) mice respond to lung irradiation with alveolitis and with atelectatic regions of fibrosis. However, there is an important difference between C3H and A/J mice in the alveolitis response; C3H mice succumb with lung disease approximately 12–14 weeks after radiation treatment while A/J mice are in distress at 22–24 weeks after irradiation [35, 131]. The specific genes governing the alveolitis and fibrosis responses in mice have not been identified, but the phenotypic difference between the B6 and C3H strains has been used to map three loci of susceptibility to radiation-induced pulmonary fibrosis, named Radpf1, 2 and 3, [105] and loci of alveolitis that are distinct from the loci for fibrosis [35]. Strain specific changes in the expression levels of specific chemokine [130, 132], cytokine [41, 133] and extracellular matrix processing [134] genes after thoracic irradiation have also been reported.

In this study we used gene expression profiling with microarrays to investigate the hypothesis that distinct pathways lead to the development of alveolitis and of fibrosing alveolitis. To control for the fact that alveolitis classically occurs at an earlier time after irradiation than does fibrosis, the phenotype of the A/J strain, which develops alveolitis at the same time the B6 strain develops fibrosis, was assessed. The data reveal plausible affected pathways that may be implicated in the development of radiation-induced lung disease.

Materials and Methods

***Mice*:** Inbred strain mice (C57BL/6J, C3H/HeJ, A/J) were purchased from the Jackson Laboratory (Bar Harbor, ME) and housed in the animal facility of the Meakins-Christie Laboratories. All mice were handled according to guidelines and regulations of the Canadian Council on Animal Care.

***Radiation Treatment*:** Mice were treated at 8 weeks of age. Lung damage was elicited by whole-thorax radiation exposure (18 Gy) using a Gamma Cell Cesium-137 unit as described previously [102, 131]. The rest of the body was shielded with 3 cm of lead to reduce the beam strength to 3% in this area. The mice were weighed weekly from 8 weeks after irradiation and were euthanized when they exhibited loss of 20% body weight, distress through ruffled fur, accelerated breathing and hunched posture, as described previously [102, 131]. The control mice (five of each strain) were not treated and were killed at 15–26 weeks.

***Histology*:** At necropsy, the lungs were removed and the single left lobe of each mouse was perfused with 10% neutral buffered formalin and submitted for histological processing. Lung sections were stained with Masson's Trichrome to reveal fibrosis and alveolitis was assessed on hematoxylin and eosin-stained left lung sections.

***Gene Expression*:** The right lung of each of six B6, A/J and C3H male mice was immediately homogenized in 2 ml of Trizol reagent and placed in dry ice. The homogenates were stored at -80°C until RNA isolation. Total lung RNA was extracted according to the manufacturer's (Sigma) instructions. To define the set of expressed genes, the RNA from three mice euthanized after irradiation and three control mice was evaluated for each strain. RNA quality was assessed and confirmed using the Agilent Bioanalyzer (Agilent echnologies, Palo Alto, CA).
Microarray hybridization using the Mouse genome 430 2.0 GeneChip arrays containing 45101 probe sets was performed by the Affymetrix Gene Chip Core facility at the McGill University and Genome Quebec Innovation Centre. The probe

synthesis, hybridization and washing protocols followed the standardized Affymetrix protocol we used previously [35, 135-137].

***Microarray Data Analysis*:** Routines from Bioconductor version 2.0 (http://www.bioconductor.org/) within the R version 2.4.1 statistical language [138] were used for quality control, normalization and differential expression. In particular, the quality of the raw microarray data was assessed by inspecting similarities between the intensity distribution and RNA digestion plot for each array. Normalization was performed using the robust probe level model [139]. Lists of significantly differentially expressed genes ($P < 0.05$) were generated for radiation-treated mice compared to control mice and for interstrain differences among untreated and treated mice using the LIMMA package in Bioconductor. All analyses used standard false discovery rate (FDR) approaches with an FDR threshold of 5%. For the interstrain comparison of differential expression, genes for which the ratio of expression values in radiation-treated mice and that in untreated mice was lower than $2^{0.3}$ were considered as having a common strain dependent expression. Clustering of the samples according to their gene expression levels was completed using the Hierarchical Clustering method from TIGR Multi Experiment Viewer (http:// www.tm4.org/mev.html). The complete linkage method was used in which the cluster-to-cluster distance is the maximum distance between each member of one cluster and each member of the other cluster. The distance metric used was the Euclidean distance. Raw and normalized expression data are available from NCBI GEO (GSE 2250; http://www.ncbi.nlm.nih.gov/geo/).

The detection of significantly over-represented Gene Ontology (GO) categories was performed using the GOFFA library from the ArrayTrack microarray analysis tool v.3.4.0 [140]. Fisher's test of statistical significance, which considers the number of differentially expressed genes found in each category compared to the total number of genes in the category represented on the chip, was used. To compile the Gene Ontology results, the list of all significantly represented GO

identifiers was subsequently loaded into the GO Term Classifications Counter (http://www.animalgenome.org/cgi-bin/util/gotreei), and this tool was used to assign the GO terms to their corresponding parents (GO slim categories) in the ontology tree.

To identify pathways within the radiation response of each strain, an analysis was completed using Pathway-Express software (http://vortex.cs.wayne.edu/projects.htm) [119], as has been used by others [121, 141, 142], with the lists of differentially expressed genes. Genes that were differentially expressed in 3/3 replicates with a treated compared to control P value of 0.05 were analyzed. This software uses pathways present in the KEGG database and calculates significance, through hypergeometric distribution testing, based on the relative changes of the contained genes and the positions and interactions of the genes in the pathway. The significance threshold of pathways was set to 3 (derived by -log10 [P value], for P = 0.001).

***Quantitative Real-Time PCR*:** These experiments were performed as described previously [35, 136]. Briefly, 4–5 µg of total RNA from the right mouse lung was reverse transcribed with oligo(dT)12–18Primer using SuperscriptTM II RNase H2 Reverse Transcriptase (Invitrogen, Carlsbad, CA) to make cDNA. Quantitative real-time PCR assays were performed using the Applied Biosystems International Prism 7500 Sequence Detection System and assays on demand (cystic fibrosis conductance transmembrane regulator *Cftr*, Assay Mm00445197_m1, *Cd84* antigen, Assay Mm004488934_m1) or with SYBR Green and suitable primers. The reference gene used was Ataxin 10 (*Atxn10*, Assay Mm00450332_m1), because this gene was invariantly expressed across the gene expression arrays.

Results

Inbred Strain Radiation-Induced Lung Response Phenotype

The histological response to 18 Gy whole-thorax irradiation of A/J and C3H/HeJ mice was a diffuse lethal alveolitis, and that of C57BL/6J mice was a

fibrosing alveolitis (Figure 2). The time to respiratory distress after irradiation was 13.0 ± 1.2 weeks for C3H mice, which was significantly earlier than the times for either the B6 (23.5 ± 0.4 weeks, $P = 7.7 \times 10^{-11}$) or A/J mice (22.5 ± 3.1 weeks, $P < 0.01$), in agreement with previous studies [35, 102, 131].

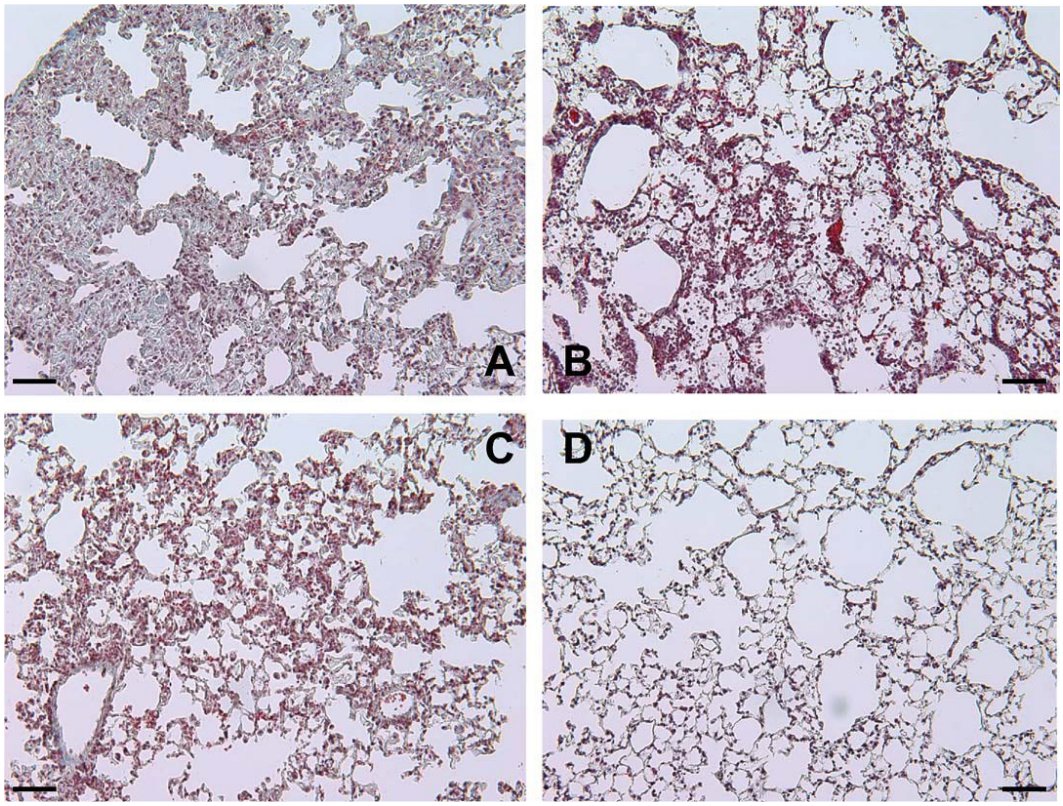

Figure 2. Radiation-induced lung disease phenotypes of C57BL/6J, C3H/HeJ and A/J mice.

Mice of each strain were exposed to 18 Gy whole thorax radiation and euthanized when they showed signs of severe lung injury. The average time postirradiation to respiratory distress was 13.0 ± 1.2 weeks for C3H mice, 23.5 ± 0.4 weeks for B6 mice, and 22.5 ± 3.1 weeks for A/J mice. Panel A: Subpleural regions of fibrosing alveolitis are evident in the lungs of C57BL/6J mice (blue streaks indicate collagen deposition) after irradiation, and the response of C3H/HeJ (panel B) and A/J (panel C) mice to treatment is alveolitis as indicated by the cellular influx to the airspace. Panel D: Control untreated C57BL/6J mouse. Masson's trichrome stain, original magnification 200x. The scale bar indicates 100 µm.

Gene Expression Profiling of Radiation-Induced Lung Disease

To identify genes with altered expression in the alveolitis and fibrosing alveolitis phenotypes, gene expression profiling of the radiation-induced lung responses of the A/J, B6 and C3H strains was completed. We used individual samples from mice in respiratory distress and from untreated controls to measure the expression profiles of lung disease in each strain. The numbers of unique genes/ESTs identified to be significantly differentially expressed ($P < 0.05$) in the lungs of treated mice compared to untreated controls for each strain are given in Figure 3.

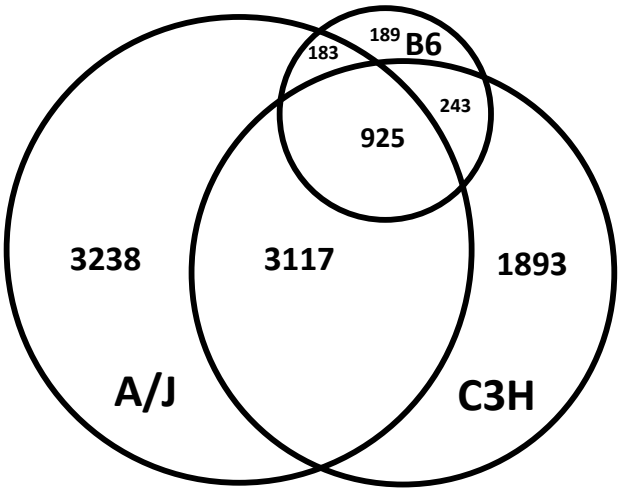

Figure 3. Numbers of strain-specific and common genes of response to thoracic irradiation.
Whole lung RNA was analyzed with microarrays. The numbers of pulmonary genes with differential expression ($P < 0.05$) between radiation-treated and control mice of each strain are displayed.

The detailed gene expression profiles for each strain after thoracic irradiation are available in Supplementary Tables 1–3 (see Appendix). As illustrated in Figure 3, the responses of A/J and C3H mice were more similar to each other than to B6 mice; 4042 genes (65% of the C3H response, 54% of AJ) were differentially expressed in treated mice compared to strain controls and were common to the response of these two strains, while the overlap of either strain with B6 was approximately 17% of differentially expressed genes.

The distinct gene expression profile of B6 mice was also evident after cluster analysis of the genes that differed in expression between strains. As shown in Figure 4, the samples from B6 mice formed a cluster separate from that of C3H and A/J mice for both irradiated and untreated mice. The effect of thoracic irradiation on gene expression was also evident in that the samples segregate by radiation treatment within each strain defined cluster.

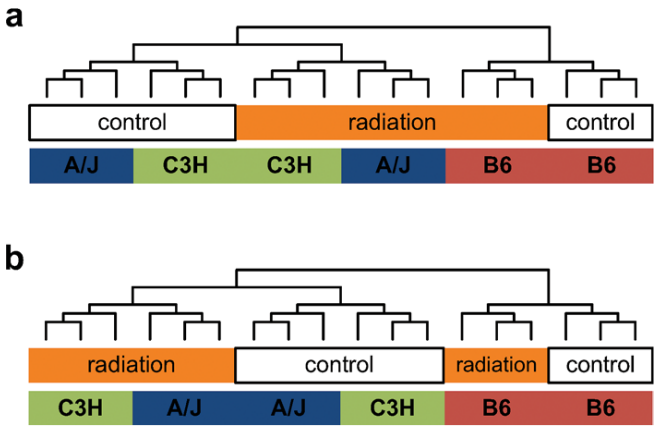

Figure 4. Cluster analysis of interstrain differences in the pulmonary gene expression.
Whole lung RNA was analyzed with microarrays, and genes with differential expression ($P < 0.05$) between strains for (panel a) untreated mice and (panel b) treated mice were used to generate dendograms. Mouse strain and radiation treatment are indicated by the boxes below the dendograms.

To determine the part of the response that could be attributed to the radiation treatment and the part that represented an inherent difference in pulmonary gene expression level, comparisons of the gene expression profiles were made. As shown in Table 1, on average 15% of the genes that differed in expression between strains after irradiation differed to a similar extent in untreated mice, with the greatest inherent difference occurring between B6 and C3H mice. The genes identified to differ in expression by strain are listed in Supplementary Table 4 (see Appendix).

Table 1. Interstrain Comparison of Numbers of Differentially Expressed Genes in the Lungs of Radiation-Treated and Control Mice

Interstrain comparison	Radiation-treated (18 Gy)	No treatment	Common[a]	Percentage of radiation response due to strain[b]
C57Bl/6J vs A/J	7308	3496	1207	16.5
C57Bl/6J vs C3H/HeJ	5680	2992	1173	20.7
C3H/HeJ vs A/J	6765	1493	610	9.0

[a] Number of genes that differed in expression by strain both in untreated lungs and after 18 Gy thoracic irradiation.

[b] Percentage of genes that differed in expression by strain after 18 Gy thoracic irradiation that also differed in untreated lungs.

To assess the validity of the gene expression differences identified by microarray analysis, the expression levels of seven genes that were identified as either changing significantly or not changing after irradiation were assessed with real-time PCR analysis. As shown in Figure 5, the differences in gene expression identified by microarray analysis were consistent with the results obtained with real-time PCR. In addition, RT-PCR revealed that the levels of interleukin 6 (Il6) were increased significantly in the lungs of C3H and A/J mice after thoracic irradiation (C3H mice relative to controls = 129 ± 14, $P = 4.8 \times 10^{-6}$; A/J = 20.0 ± 16; P = 0.04), but the expression of this cytokine postirradiation was not significantly different from control levels in the B6 mice ($P < 0.3$).

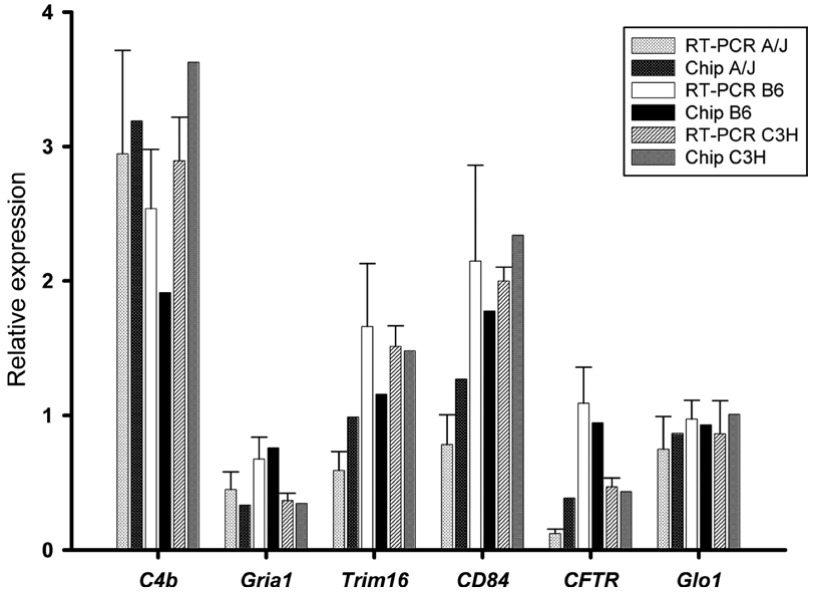

Figure 5. Comparison of microarray data with real-time PCR-derived expression values for selected genes.
The ratio of expression from the lungs of irradiated mice relative to control mice is shown with the SEM for each gene by mouse strain (n = 3 males per group). Expression values did not differ ($P > 0.05$) by measurement technique in a test comparing real-time PCR to microarray data. Each gene was significantly differentially expressed in lungs of radiation-treated mice compared to controls ($P < 0.05$) except for Glo1 and for Cftr in B6 mice and Cd84 in A/J mice.

To characterize the biological processes involved in each strain's response to radiation, the gene expression profiles were analyzed for Gene Ontology classification. GO analysis revealed that the differentially expressed genes in the AJ and C3H strains were found mostly in the cellular component of the cytoplasm (endoplasmic reticulum, vacuoles, lysosomes) while for the B6 strain the differentially expressed genes were identified as part of the extracellular region (Figure 6).

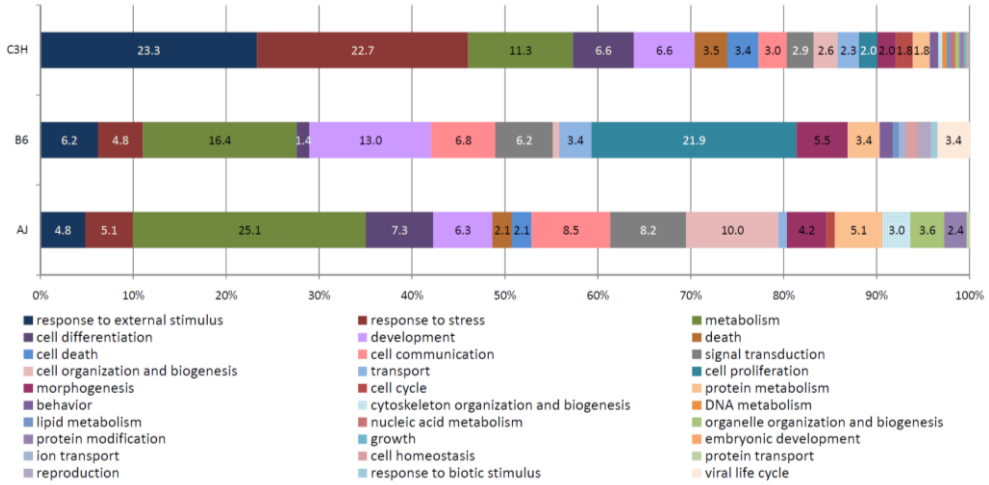

Figure 6. Gene ontology "cellular component" classification of the inbred strain response to radiation.
Male mice of each strain were exposed to 18 Gy whole thoracic irradiation and sacrificed when moribund. The most frequent cellular component Gene Ontology categories, of the genes of differential expression ($p<0.05$) between treated and control mice in each of the three strains, are displayed.

In further GO-based analyses, the categories of response to external stimulus and signal transduction were identified as among the processes most significantly enriched with differentially expressed genes in the C3H and A/J alveolitic strains, respectively (Table 2), while the category of cell proliferation, which features the term B-cell proliferation, was a significant part of the B6 mouse response to radiation only. A complete listing of the GO terms represented in each strain's response to thoracic irradiation is given in Supplementary Table 5 (see Appendix).

Table 2. Gene Ontology Biological Processes significantly represented in each strain response to 18Gy whole-thorax irradiation

GO Slim Category	A/J	C57Bl/6J	C3H/HeJ
Response to external stimulus	3.9[a]	9.3	13.6
Response to stress	4.5	7.2	11.7
Metabolism	11.8	6.2	NS[b]
Cell differentiation	4.5	2.1	6.8
Development	6.2	14.4	10.2
Death	2.2	NS	3.9
Cell death	2.2	NS	3.4
Cell communication	12.9	10.3	7.8
Signal transduction	12.4	9.3	7.3

Cell organization and Biogenesis	10.1	1.0	5.8
Transport	1.7	3.1	2.9
Cell proliferation	NS	13.4	1.9
Morphogenesis	4.5	6.2	5.3
Cell cycle	1.7	NS	4.4

[a] Percentage of significant GO terms in the radiation response of each strain, which are grouped in this GO Slim category.
[b] Not significantly represented in the strain response.

To illustrate the differences in gene expression that distinguish the alveolitis-responding strains from the fibrosis-responding strain, the genes with differential expression (radiation-treated compared to control) within the GO category of immune response (a subcategory of response to external stimulus) were assessed. As shown in Figure 7, cluster analysis of these genes grouped the samples first by radiation treatment and then within each cluster by the responses of the different strains, with the A/J and C3H strains separate from the B6 mice. The alveolitis genes included several chemokines, while immunoglobulin genes were represented in fibrosis. Similar analyses using genes from the GO categories cell communication and development also demonstrated the samples to cluster first by comparing to irradiated controls and then within these clusters by strain (data not shown). From this we infer that the GO categories listed as a significant part of the radiation response (Table 2) represent the postirradiation strain differences and not specifically genes with inherent differential expression.

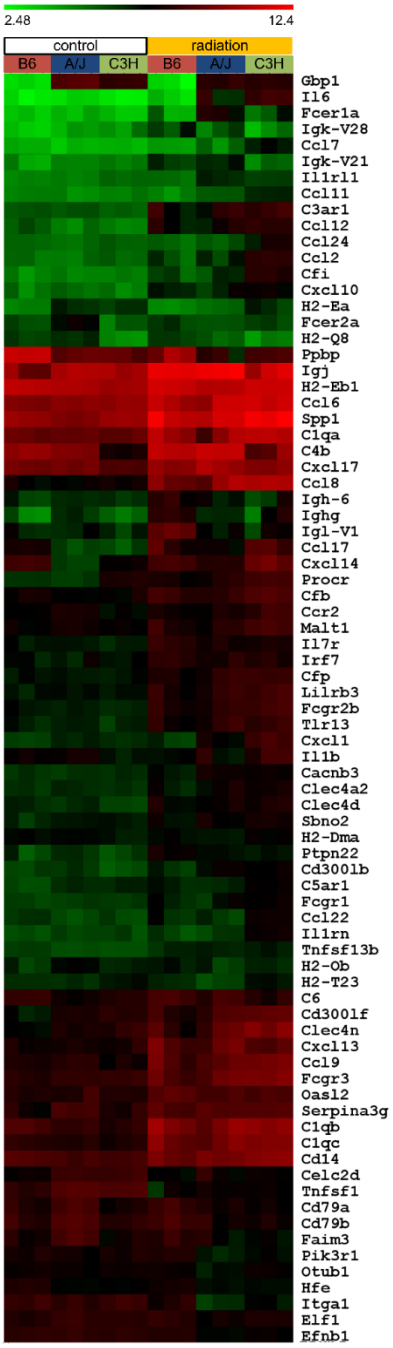

Figure 7. Gene expression profiling of the responses of mice to radiation for the Gene Ontology category of immune response.

Pulmonary genes with differential expression ($P < 0.01$) between treated and control mice in each of the three strains, which are part of the significantly overrepresented Gene Ontology category of immune response, are displayed. Mouse strain and radiation treatment are indicated by the boxes at the top of the figure. The color scale indicates the gene expression level after normalization; green indicates low expression and red indicates high expression.

Finally, to characterize the pathways involved in each strain's response to radiation, the gene expression profiles were analyzed with Pathway Express tools. This analysis revealed pathways of the pulmonary radiation gene expression profile that were common in all three strains (Figure 8) or were part of the response of only one or two strains. The early alveolitis response of C3H mice included cytokine-cytokine receptor interactions and natural killer cell-mediated cytotoxicity, while diverse signaling pathways, including Wnt, Insulin and Mapk, were significant in the A/J strain. The pathways that differentiated the alveolitis-responding strains from the B6 fibrosis strain included those related to the cell cycle; the complement and coagulation cascades and melanoma pathways were most prominent in the radiation response of B6 mice (Figure 8).

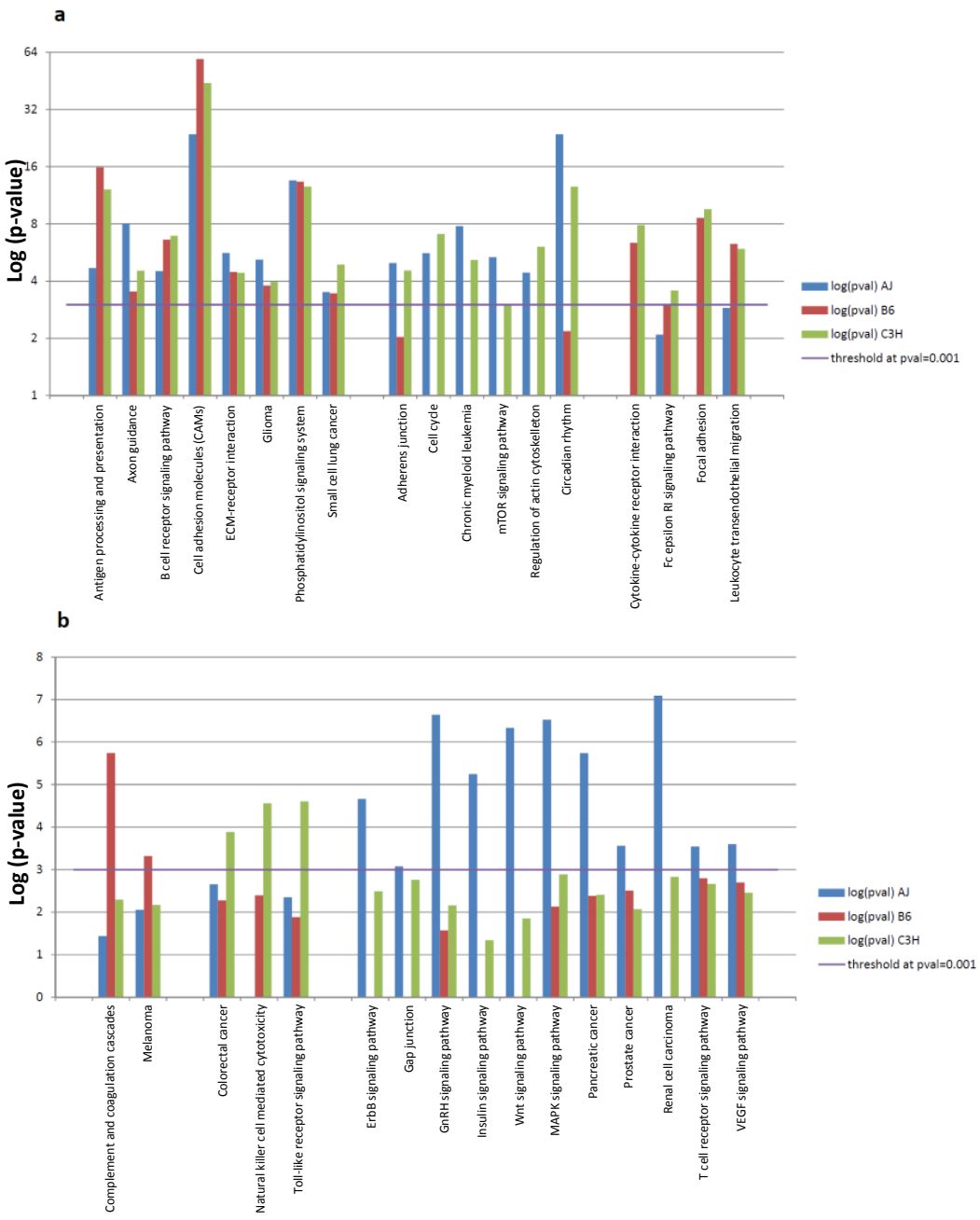

Figure 8. Biological pathways significantly represented in the responses of the three mouse strains to thoracic irradiation.

Pulmonary genes with differential expression ($P < 0.05$) in irradiated mice compared to controls were analyzed using Pathway Express software; all pathways shown to be significantly ($P < 0.001$) involved in the response of at least one strain are presented. Panel a: Pathways indicated in two or three strains. Panel b: Pathways prominent in one strain only.

Discussion

In this study we used microarrays to define the radiation responses of alveolitis and fibrosis at the gene expression level. The pulmonary fibrosis response of B6 mice featured genes of the complement pathway and of B-cell activation and proliferation; this was shown to be distinct from the alveolitis response of C3H and A/J mice. The evaluation of two alveolitis responding strains enabled us to show that time after treatment did not dictate the development of the gene expression phenotype after irradiation but that inherent inbred differences did, which is consistent with the findings in our previous evaluation of B6 x C3H backcross mice [35]. Finally, the responses of early and late alveolitis were differentiated; thus the same histological phenotype in C3H and A/J mice developed in part through different mechanistic pathways.

The pathways identified to differentiate alveolitis from fibrosis were those of higher significance in B6 mice (complement and melanoma) and those that were prominent in the response of C3H and A/J mice but were not significant in B6 mice (actin and cell cycle, CML and mTOR). Because the complement branch of innate immunity can be activated by antibody secretion [143], the contribution of this pathway to the B6 lung response is supported by GO data indicating that B-cell proliferation and activation genes are significantly represented in this strain. The complement and B-cell paths have been shown to be involved in fibrosis development in a related model, bleomycin response; Addis-Lieser et al. [144] reported that complement 5-deficient mice have reduced bleomycin-induced pulmonary fibrosis, and Komura et al. [145] showed that CD19-deficient mice developed less fibrosis after bleomycin exposure compared to wild-type mice, while the response was enhanced in CD19 transgenic mice. Second, within the melanoma pathway are phosphatidylinositol 3-kinase genes, which are from a pathway that has been shown to be activated in fibroblasts from idiopathic and systemic sclerosis-associated fibrosis patients [146, 147], and thus the increased

expression of these genes may contribute to fibrosis development. Finally, the genes that are part of the A/J and C3H but not the B6 mouse response to thoracic irradiation collectively include those encoding integrins and actin proteins that may function to facilitate the infiltration of inflammatory cells from the blood stream into the lung tissue [148], which is consistent with an alveolitis phenotype.

A comparison of the gene expression profiles of the pulmonary radiation response of C3H and A/J mice revealed pathways that differentiated the development of early and the late alveolitis. Pathways prominent in the response of C3H mice but not A/J mice response to radiation included cytokine-cytokine receptor interactions and natural killer cell-mediated toxicity, indicating an inflammatory response in moribund C3H mice that was not detected in the A/J strain. Among the cytokines more highly expressed in the irradiated treated C3H mouse lung were interleukin 6, chemokine (C-C motif) ligand 8, and chemokine (C-X-C motif) ligand 14; an increase in these genes at the tissue level in alveolitis is consistent with their involvement in lung inflammation [149] and natural killer cell migration [150]. Increased interleukin 6 levels in serum [151, 152] and lavage [153] have also been associated with acute lung disease after thoracic radiotherapy, indicating that this cytokine pathway may have important clinical relevance. The contribution of genes from the toll-like receptor signaling pathway to alveolitis in this strain, as indicated by Pathway Express analysis, agrees with the work of Bauer et al. [154], who showed that mice with functional Tlr4 had reduced pulmonary leukocyte inflammation in response to butylated hydroxytoluene injections compared to mice with mutated Tlr4 such as C3H/HeJ mice. In contrast, pathways more pronounced in the later alveolitis response of A/J mice included map kinase, insulin, and Wnt signaling, suggesting that alterations of these pathways can also affect alveolitis. The mechanism through which increased expression of signaling molecules or the increased number of cells within the inflamed lung expressing these genes contributes to alveolitis is not known, because these signaling

pathways are involved in diverse cell functions including proliferation, differentiation and apoptosis in both stem cells and immune cells [155, 156].

An evaluation of the microarray data revealed that the inbred strains differ in gene expression in the untreated lung and that this inherent variation contributed approximately 10–20% of the differences in expression between the strains after irradiation. Such strain variability in pulmonary gene expression has been documented [157, 158] and was assessed as contributing to lung cancer development [159], among other phenotypes. In this investigation part of the inherent variation was shown to be in immune genes, based on the clustering analysis shown in Figure 7; therefore, both induced and intrinsic levels of immune gene expression may contribute to the development of alveolitis or fibrosis after irradiation.

In this work we present the gene expression profiles that are associated with the radiation-induced lung diseases of alveolitis and fibrosis. In addition to the utility of these data in describing a complex phenotype [160, 161], such profiles are also applicable to investigations to identify genetic changes that predict for lung disease. For example, Marquis et al. [162] combined the results of linkage and gene expression experiments to identify genetic factors putatively involved in defense against tuberculosis. Similarly, the gene expression data reported here can be used to evaluate the genes within linkage intervals of radiation-induced pulmonary fibrosis susceptibility [35, 105] for those that potentially contribute to this trait. Such genes, when they are identified, may be found to have altered expression within hours of irradiation, as has been found in predictive studies [160], or may show changes in expression at the presentation of the phenotype. For example, Puthawala et al. [163] showed that a key TGFβ regulator, integrin α(v)β6, did not increase in expression until 20 weeks post irradiation, when the histological evidence of the radiation-induced fibrotic injury had appeared, and Westbury et al. [164] defined the gene expression in the late normal tissue radiation response of the breast using biopsies collected years after

treatment. The lung diseases characterized here are consistent with a tissue response to an injury, i.e. alveolitis or fibrosis, rather than the profiles being an evaluation of the primary radiation effect on the lung or the initial injury. In support of this, in addition to the assay time of weeks post irradiation, is the fact that the gene expression profile of the fibrosis-responding B6 mice has 25% overlap with the profile of the fibrosis response these mice develop after the lung injury induced by bleomycin [136].

In summary, we have defined gene expression profiles for radiation-induced pulmonary fibrosis and alveolitis. We found that a unique immune response occurred for both. Because the induction of alveolitis or fibrosis is a serious dose-limiting complication for thoracic irradiation, it is anticipated that the identification of genetic pathways contributing to these conditions could be useful in the treatment of lung disease.

Acknowledgements

This work was supported by funding from the McGill University Health Centre and Fonds de la Recherche en Santé Québec.

CHAPTER TRANSITION

The transcriptome analysis of Chapter II showed that alveolitis and fibrosis differ in terms of the molecular pathways activated after radiation and that there are more pathways activated in one or two versus all three strains which adds to the hypothesis that there is a genetic basis for lung disease susceptibility. This is confirmed by the fact that the similar phenotype of A/J and C3H mice occurs through different pathways in the two strains.

Therefore we set out to determine what genome variants are associated with pulmonary fibrosis in a larger number of inbred strains. For this we performed a Genome-Wide Association Analysis of 1.8 million SNPs in a panel of 27 strains with the fibrosis phenotype. The objective was to integrate gene variation and transcriptome data by filtering the candidate genes based on their expression in the lung and prioritizing those belonging to activated pathways.

CHAPTER III: GENOMIC AND GENOME-WIDE ASSOCIATION OF SUSCEPTIBILITY TO RADIATION-INDUCED FIBROTIC LUNG DISEASE IN MICE

A Paun and CK Haston

Originally published in *Radiotherapy and Oncology*, 2012, 105(3):350-7

Abstract

Background and Purpose: To identify genes which influence the fibrotic response to thoracic cavity radiotherapy, we combined a genome wide single nucleotide polymorphism (SNP) association evaluation of inbred strain response with prior linkage and gene expression data.

Material and Methods: Mice were exposed to 18 Gy whole thorax irradiation and survival, bronchoalveolar cell differential, and histological alveolitis and fibrosis phenotypes were determined. Association analyses were completed with 1.8 million SNPs in single markers and haplotypes.

Results: Nine strains developed significant fibrosis and 11 strains succumbed to alveolitis only or alveolitis with minimal fibrosis. Post irradiation survival time ($p<0.001$) and bronchoalveolar lavage neutrophil percent ($p = 0.055$) were correlated with extent of alveolitis and were not significantly correlated with fibrosis. Genome wide SNP analysis identified 10 loci as significantly associated with radiation-induced fibrotic lung disease ($p < 8.41 \times 10^{-6}$; by permutation test), with the most significant SNP within a conserved non-coding region downstream of cell adhesion molecule 1 (*Cadm1)*. Haplotype and SNP analyses performed within previously-identified loci revealed additional genes containing SNPs associated with fibrosis including *Slamf6* and *Cdkn1a*.

Conclusions: Combining genomic approaches identified variation within specific genes which function in the tissue response to injury as associated with fibrosis following thoracic irradiation in mice.

Introduction

The common cancer treatment modality of radiotherapy, when delivered to the thoracic cavity can produce serious inflammatory (alveolitis or pneumonitis) or fibrotic side effects in the lung [165]. Patients who are likely to develop fibrosis, an incurable normal tissue response to radiation, at present cannot be identified before therapy [165]. Efforts to isolate specific genetic variants which are

associated with clinical radiation response have focussed on candidate gene studies of small sample sized populations and have not produced consistent results [166]. In addition, the approach of using clinical data alone to identify causal genetic variations influencing susceptibility to radiation-induced lung disease can be confounded by the effects of multiple genes and their interactions on the phenotype, variability in the clinical description of the phenotype and by the cancer and other therapies.

To circumvent these limitations, inbred mouse strains which vary in their propensity to develop alveolitis and fibrosis after radiation exposure [104] can be evaluated to isolate candidate genetic variation contributing to the lung response phenotype. Indeed, the clinical outcomes of thoracic radiotherapy, with respect to adverse effects, of fibrosis and alveolitis, and the times at which they occur, are each represented in the radiation response of an inbred mouse strain. We [35, 131, 167, 168] and others [41, 104, 169] have reported murine strain differences in response to radiation wherein following high dose whole thorax irradiation, C3H/HeJ (C3H) mice develop a diffuse lethal alveolitis, characterized by an inflammatory infiltrate of alveoli, and C57BL/6J (B6) mice respond to lung irradiation with fibrosis. The phenotypic difference between B6 and C3H mice has been used in replicate studies [35, 105] to map loci of radiation-induced pulmonary fibrosis, named *Radpf1* on chromosome 17 and *Radpf2* on chromosome 1. Additional loci on chromosome 6 (ref [105]) and chromosomes 7, 9 (ref [35]) were detected in either one of the studies only, while the strain difference in alveolitis has been mapped to loci distinct from those of fibrosis [35].

The similarity to the clinical phenotype presented by the mouse models enables use of mouse genomic resources to investigate the genetic basis of radiation-induced lung disease. Among these is the mouse single nucleotide polymorphism or SNP map [108, 170] which has been used to complete genome-wide association studies (GWAS) in inbred mice for traits such as acetaminophen toxicity [171], acute lung disease [172] and lung cancer [114, 173, 174]. Mapping

of disease traits in mice through association data alone however can produce spurious results due to the relatedness of inbred strains created by their unique breeding history [109] and this approach may have reduced statistical power to detect associations given the limited number of inbred strains. To compensate, specific analyses incorporating inbred strain relatedness have been developed [109] and association data are often combined with quantitative trait loci determined through mapping or through the evaluation of specific congenic or consomic mice for the purpose of identifying causal genetic variation associated with the trait [106]. Association analysis limited to QTL regions has also been used to identify candidate quantitative trait genes [117, 175]. The second mouse genetics tool of chromosome substitution, or consomic mice, which are mice bred to contain one specific donor chromosome in a recipient inbred strain background [176], enables the assessment of a genomic interval contribution to a trait without the production of congenic mice.

In this study, we combine genomics approaches to identify specific genetic variants associated with predisposition to radiation-induced pulmonary fibrosis. Initially, to determine whether loci of lung response mapped in B6xC3H F2 [105] and backcross [35] mice might predict for response in another strain we made use of the difference in radiation response between B6 (fibrosis) and A/J (alveolitis) mice [131] and we evaluated the radiation response of available B6:A/J consomic mice. We next defined the radiation response of a panel of inbred strains and these data, combined with that from a high density SNP dataset were used to identify genes with allelic variants shared among alveolitis (only) responding mice which were distinct from those shared by fibrosis responding mice. Lastly we integrated data from a gene expression profiling experiment [167] and from an assessment of species sequence conservation to refine the list of associated genes.

Materials and Methods

***Mice*:** Mice of inbred (AKR/J, CBA/J, NOD/ShiLtJ, C3H/HeJ, LG/J, A/J, BTBR T+ tf/J, BALB/cJ, PL/J, CE/J, SM/J, LP/J, SJL/J, DBA/2J, I/LnJ, NON/ShiLtJ, BUB/BnJ, SWR/J, C57BL/6J, NZW/LacJ, MA/MyJ, 129S1/SvImJ, FVB/NJ, KK/HlJ, NZB/BlNJ, C57BLKS/J, C58/J) and consomic B6.A strains (C57BL/6J-Chr $1^{A/J}$/NaJ, C57BL/6J-Chr $4^{A/J}$/NaJ, C57BL/6J-Chr $14^{A/J}$/NaJ, C57BL/6J-Chr $17^{A/J}$/NaJ, C57BL/6J-Chr $X^{A/J}$/NaJ) were purchased from the Jackson Laboratory (Bar Harbor, USA) and housed in the animal facility of the Meakins-Christie Laboratories. All mice were handled according to guidelines and regulations of the Canadian Council on Animal Care.

***Radiation treatment*:** Mice were treated at 8 weeks of age. Lung damage was elicited by whole thorax radiation exposure (18 Gy; dose rate 0.7 Gy/minute) using a Gamma cell Cesium-137 unit as previously described [35, 102, 112, 131, 167]. The irradiated mice were sacrificed when moribund, or at 26 weeks after treatment. The mice were weighed weekly from eight weeks after radiation and mice losing > 20% body weight, and exhibiting distress through ruffled fur, accelerated breathing and hunched posture, were sacrificed as described previously [35]. The control mice (five of each of B6, C3H, FVB/NJ, & A/J strains, four NOD/ShiLtJ, seven BTBR T+ tf/J, four C57BL/6J-Chr $1^{A/J}$/NaJ and three C57BL/6J-Chr $4^{A/J}$/NaJ mice) were not treated and were euthanized at the 15-26 week time points.

***Histology*:** At necropsy, bronchoalveolar lavage (BAL) was performed by cannulating the trachea and retrieving cells from three 1-mL injections of phosphate buffered saline. The lungs were then removed and the single left lobe of each mouse was perfused with 10% neutral buffered formalin and submitted for histological processing. Lung sections were stained with Masson's Trichrome and the area of fibrosis in the left lung lobe was determined from a user drawn region surrounding the fibrosis (Image Pro Plus Software) compared to the area of the entire lobe to yield the percent of pulmonary fibrosis for individual mice [35, 131]. To assess alveolitis, hematoxylin and eosin (H&E) stained left lung sections

were evaluated through semi-quantitative histology [35, 131]. Mast cell numbers were determined by counting the positive cells present in 10 fields of a lung histological section stained with Toluidine blue, at a 400x magnification. All scoring was completed by a user blinded to mouse strain and treatment.

***Bronchoalveolar Lavage Fluid (BAL) Analysis*:** The BAL fluid was centrifuged (302g for 10 minutes @ 4°C) and the supernatant was removed and stored at -85°C. The cellular pellet was re-suspended in 0.25mL PBS. Inflammatory cell counts were performed (400x magnification) on cytocentrifuged cells (214.2g for three minutes), after staining with a hematoxylin-eosin kit (Hema-3 Stain Set by Protocol) and are reported as the percentage of 500 counted cells. To assess correlations among disease phenotypes pairwise Pearson's correlation coefficients and corresponding p-values were calculated using the rcor.test function in R (http://cran.r-project.org/).

***Genome-wide association studies (GWAS)*:** GWAS were completed using 236 mice from 27 inbred strains and the following phenotypes: percent fibrotic lung tissue, survival post irradiation, percent of lymphocytes & neutrophils in BAL and lung tissue mast cell count. The phenotype data include the response of one SWR/J mouse, which was included as the measured phenotype agrees with that previously reported for this strain [104]. Genotype data consisted of the CGD1 (http://cgd.jax.org/index.php) imputed dataset downloaded from the Mouse Phenome Database (Jackson Laboratory, Bar Harbor, ME). This dataset was filtered for SNPs imputed with confidence scores >0.9 as in [173], and SNPs with fewer than 20 strains typed/imputed or with a minor allele frequency <3/27 were removed as has been used by others [173, 174]. The 1,885,108 remaining SNPs span the mouse genome at an average of 1 per 1.8 kB and were assessed for association through single marker analysis and haplotype analysis.

In single marker analysis genotype-phenotype associations were evaluated for each individual SNP using efficient mixed model association (EMMA, ref [109]), a method which takes into account the relatedness between the inbred strains as

used by others [173, 177, 178]. For each SNP a two-sided p-value was obtained by testing the null hypothesis of no association between genotype and phenotype, using the R implementation of the EMMA package (http://mouse.cs.ucla.edu/emma). A locus was considered to be significantly associated with the phenotype if its SNP score (-log10(pvalue)) was above the genome-wide threshold and it contained at least two SNPs within 50 kB of each other [179]. The significance thresholds were determined through permutation testing as in [174, 178]. In detail, for each of 1000 permutations, phenotype values were randomly shuffled, genotype-phenotype associations tested and the minimal nominal p-value retained. The resulting 1000 minimal p-values were sorted in ascending order and the 5% quantile of the distribution was taken as the genome-wide significance threshold (global p-value of 0.05) as used by Lu *et al.* [174].

***QTL-wide association studies (QWAS)*:** To specifically assess the SNP variation within the previously identified linkage intervals [35, 105] for association with radiation-induced lung disease we performed QWAS. For this SNPs located in linkage regions on chromosomes 1,6,7,9 & 17 and the percent fibrosis phenotype data of the GWAS were re-analysed with the single marker method. We added the condition that the A/J and C3H alleles be different from the B6 allele for the regions on chromosomes 1 & 17; and that the C3H allele be different from the B6 allele for the regions on chromosomes 6, 7 & 9. The significance level for association was determined through permutation testing with the QTL region SNPs and the 5^{th} percentile of the resultant distribution was taken as the QTL-wide significance threshold.

Linkage interval genotypes were also tested for association with the fibrosis phenotype using haplotype blocks derived from the SNP data through a build-and-step-back approach, based on the method developed by Cahan *et al.* [180]. Our algorithm iteratively joins consecutive SNPs into haplotype blocks by clustering strains based on their genotypes. A consensus haplotype (a vector

composed of the most frequent genotypes at each string position) was derived for each cluster of strains and we allowed an overall error rate of 10% of the block length between the genotypes of each individual strain and the consensus haplotype (e.g in a haplotype block of 100 SNPs shared among 4 strains, we allowed a total of 10 SNPs to be different among the 4 individual strain genotypes and the consensus haplotype). At each step in the algorithm the haplotype was "built" by adding the consecutive SNP, if the above condition was met. When this condition was not met our algorithm "stepped back" and re-analyzed the shorter block obtained by iteratively subtracting the first SNP in the current block until a valid haplotype was obtained. Thus the method generated larger, overlapping haplotypes, and not adjacent blocks, as in Cahan *et al.* To ensure a maximum number of polymorphisms were evaluated in this approach we used the complete SNP dataset without applying the minor allele frequency and genotyping rate filters and thus only SNPs with a minor allele frequency of zero in the 27 strains were removed. The "step-back" approach greatly increased the computational time, therefore the analysis was restricted to the QTL level.

In this analysis each haplotype block was represented by a string of "labels" for each strain indicating the haplotype belonging to each strain. The association of the phenotype (percent fibrosis) with the haplotype "labels" was assessed using an analysis of variance (ANOVA). The weighted bootstrap significance threshold was too stringent ($<10^{-32}$) and yielded no significant results. We therefore present the ten most significant haplotypes in each QTL as in [179], for which the lowest nominal p-values ranged from 10^{-12} for chr 7 to 10^{-19} for chr 9.

***SNP-SNP interaction between Radpf1 and Radpf2*:** To determine whether an interaction of genotypes within the linkage intervals *Radpf1* on chromosome 17 and *Radpf2* on chromosome 1 contributes to the fibrosis phenotype, as suggested in [105], we tested the association between the phenotype and all possible pairwise sets of SNPs as predictors through a linear model including a SNP-SNP interaction term. The significance of the interaction term was

determined using an F test by comparing a full model including the interaction term with the partial model that excludes the interaction variable. Approximately 8 million tests were performed and the results were corrected for multiple testing using the Benjamini-Hochberg FDR approach.

***Candidate Gene Identification*:** Genes with SNP variation meeting the GWAS/QWAS significance criteria were initially defined using BioMart feature of Ensembl which incorporated NCBI build 37 (http://www.ensembl.org).

These genes were next filtered to reveal those that are expressed in lung, which was defined as genes having a "Present" call as obtained using the MAS5.0 algorithm, in a prior microarray study of radiation induced lung disease [167]. The lung expression of the "Present" genes was confirmed using data from two additional microarray experiments (GEO database - GDS1492 (ref [136]) and GDS1649 (ref [181]). Similarly, genes not expressed in the lung were deemed to be absent in the two other microarray studies. The only exception was *Kcnip4* which shows lung expression in the majority of assays in the GEO database, including GDS1492, and was therefore retained in the list of candidates. Of the genes filtered for pulmonary expression, further evaluation revealed those harbouring SNPs which create a non synonymous mutation, or interrupt a splice site as in [171, 173, 182].

SNPs of significant association were retained in the candidate list if determined to map to conserved non coding regions (CNS) of the genome. In this analysis, for each SNP region an alignment was performed between the mouse sequence and all vertebrate genomes available in the database Genome Browser (http:// genome.ucsc.edu) using the MULTIZ method [183]. The most conserved elements were identified and scored by PhastCons [184] and were considered as potential regulatory sequences if they were not located in gene exons, their length >100 bp and the PhastCons LOD score was higher than 70, as defined by others [185, 186].

The QWAS-derived candidate genes with significantly associated SNPs in potential regulatory regions (intronic, 5' or 3' UTR, CNS) were further filtered for those with strain dependent pulmonary differential expression (in the untreated condition or post thoracic radiation), using our gene expression profiles [167] as in [173, 177].

Results

B6.A consomic strain response to thoracic irradiation

To determine whether loci linked to the radiation-induced pulmonary fibrosis response in B6 mice relative to C3H mice also predict for the radiation response of the B6 relative to A/J strain studies of B6.A consomic mice were completed. As shown in Figure 9a, consomic B6 mice with A/J alleles for chromosomes 1 or 17 developed minimal fibrosis, which was not significantly different from that of the A/J strain ($p > 0.11$) following radiation treatment, while mice consomic for chromosomes 4, 14, or X, selected to be distinct from the *Radpf* loci, were not spared fibrosis, thus the previously mapped *Radpf* loci are also relevant to the B6:A/J strain comparison for this phenotype. Further phenotyping showed the mice of the B6.17A consomic strain to be resistant to the development of radiation-induced alveolitis, compared to the parental strains (Figure 9b,c).

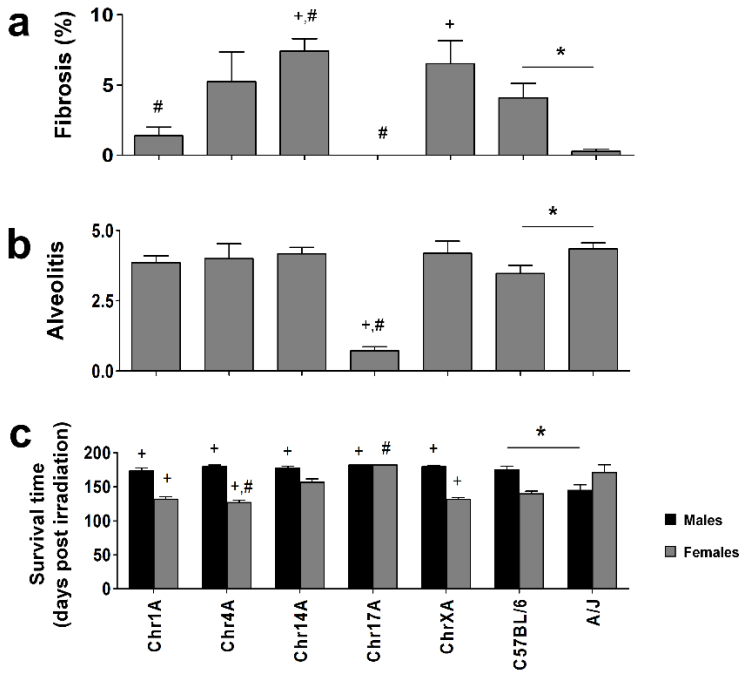

Figure 9. Radiation-induced lung phenotype of consomic B6.A mice.
Mice of each strain were exposed to 18 Gy whole thorax irradiation and euthanized when moribund or at 26 weeks post treatment. (a) percent fibrotic lung tissue in Trichrome stained histological sections (b) alveolitis score derived from semi quantitative evaluation of histological sections and (c) time post treatment to develop respiratory distress. Phenotypes are presented as the mean ± std error of groups of 7-15 mice. The average phenotypes of untreated control mice were an alveolitis score of 1.8 and 0% fibrosis. *indicates a significant difference in phenotype between the parental strains, $p < 0.05$; + indicates a significant difference in phenotype compared to the A/J strain, $p < 0.05$; # indicates a significant difference in phenotype compared to the B6 strain, $p < 0.05$.

Inbred strain response to thoracic irradiation

To enable the use of a mouse SNP map for evaluating genetic susceptibility to radiation-induced fibrosis, the radiation response to 18 Gy whole thorax irradiation of a panel of 27 inbred strains was determined. The majority of mice suffered from alveolitis in response to thoracic irradiation, evident through increased average histological scores compared to those of untreated mice, as shown in Figure 2. Only male mice of the BTBRt+ tf/J strain did not exhibit respiratory distress and thus were euthanized at the experimental endpoint of 26

weeks. Nine mouse strains also developed fibrosis wherein fibrotic scars covered greater than 4.5% of the lung (Figure 10).

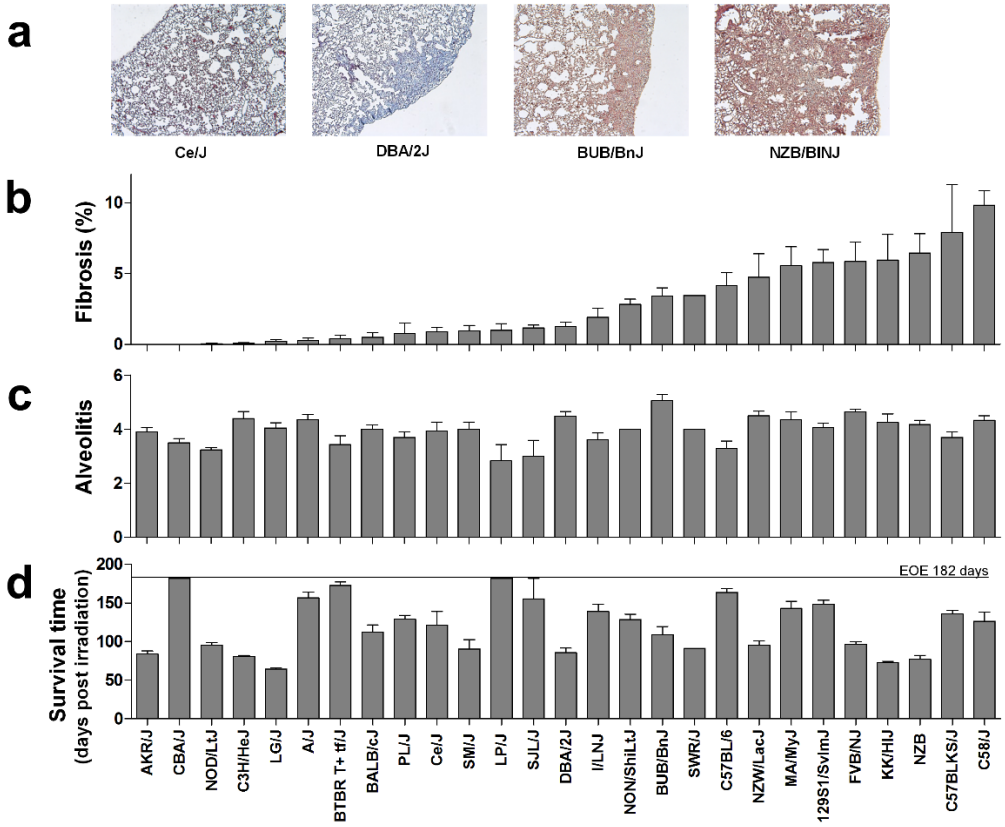

Figure 10. Murine strain difference in lung response to radiation.
Mice of each strain were exposed to 18 Gy whole thorax irradiation and euthanized when moribund, or at 26 weeks post treatment which was the end of experiment (EOE). (a) images of Masson's trichrome-stained lung sections from strains indicating different fibrosis responses to whole thorax irradiation; magnification = 200X. (b) percent fibrotic lung tissue in Trichrome stained histological sections (c) alveolitis score derived from semi quantitative evaluation of histological sections and (d) time post treatment to develop respiratory distress. Phenotypes are presented as the mean ± std error of groups of 9-20 mice. The average phenotypes of untreated control mice were an alveolitis score of 1.6 and 0% fibrosis.

The inflammatory response to irradiation was assessed by quantifying mast cell counts in lung tissue and bronchoalveolar cell differentials in mice euthanized in distress or at the end of the experiment. Neither measure was significantly correlated with the development of fibrosis in the inbred strain panel (Figure 11 and Figure 12).

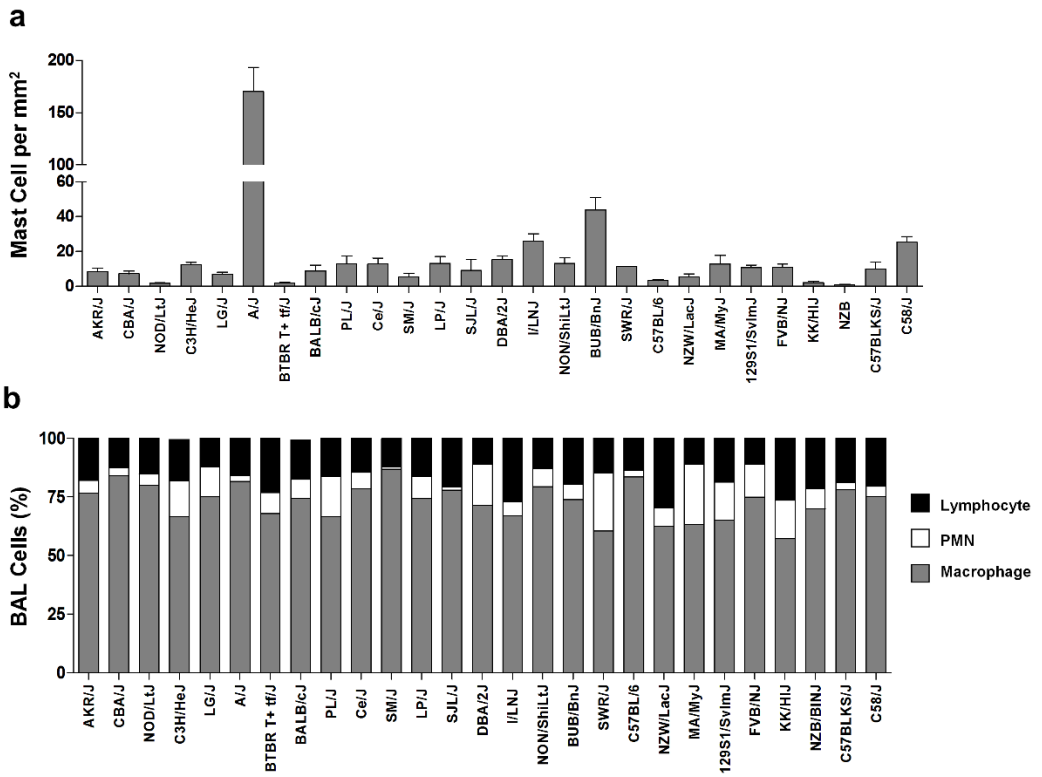

Figure 11. Murine strain difference in inflammatory lung response to radiation. Mice of each strain were exposed to 18 Gy whole thorax irradiation and euthanized when moribund. (a) mast cell count from Toluidine blue stained lung sections post radiation treatment. Mast cell counts in control mice were 0.07±0.05 cells/mm^2 and (b) cell types in bronchoalveolar lavage (BAL). Phenotypes are presented as the mean ± SEM of groups of 9-20 mice.

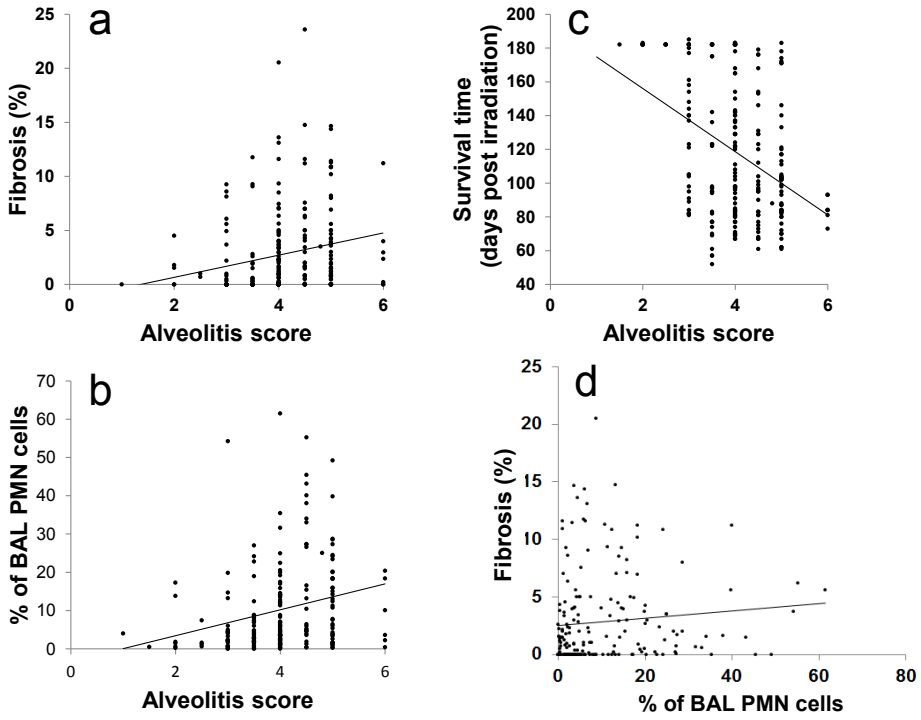

Figure 12. Correlations between radiation-induced lung response phenotypes in the panel of inbred strains.
Mice were exposed to 18 Gy whole thorax irradiation and euthanized when moribund or at 26 weeks post treatment. Phenotypes as presented in Figure 2. Correlations of alveolitis score and (a) fibrosis score, (b) bronchoalveolar lavage neutrophil percent (c) survival time post radiation treatment; and of (d) the fibrosis score to bronchoalveolar lavage neutrophil percent.

GWAS analysis of inbred strain radiation response

To determine whether specific polymorphisms are significantly associated with the lung response phenotypes single marker association analyses were completed with a genome wide SNP map. Regions on ten chromosomes were identified as associated with the development of the radiation-induced fibrosis lung response in the 27 inbred strains, $p < 0.05$, as shown in Figure 13a. Significant associations were also detected for time to onset of respiratory distress (survival), mast cell count and lavage lymphocyte percent & neutrophil percent (Figure 14).

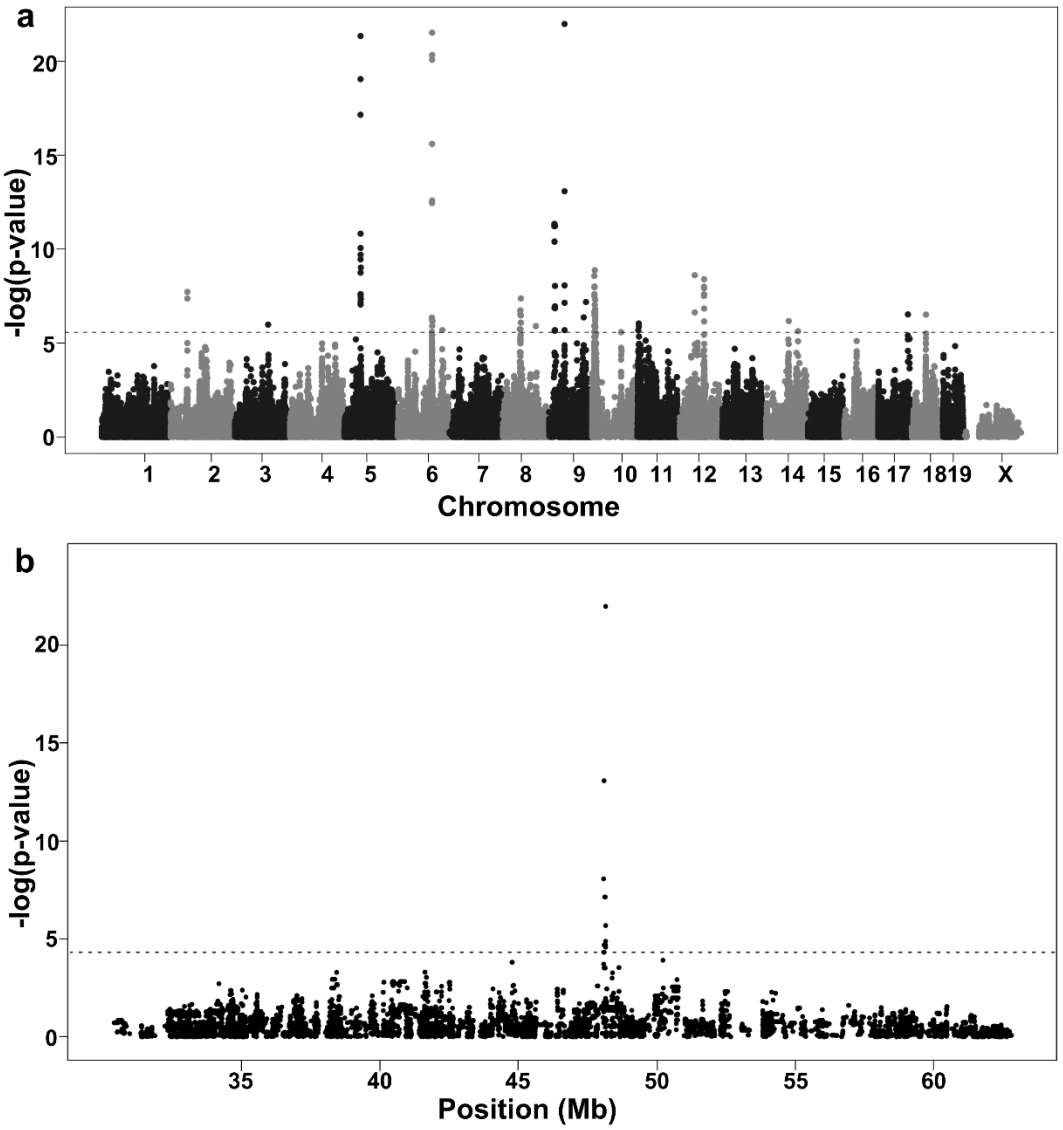

Figure 13. GWA and QWA of radiation-induced pulmonary fibrosis in mice.
The fibrosis phenotype data of Figure 2 were analysed with (a) genome-wide and (b) chromosome 9 QTL SNP genotypes and p values for association computed using EMMA. The dashed grey line indicates the 0.05 significance threshold which for the genome-wide dataset corresponds to a point-wise p-value of 2.68×10^{-6}.

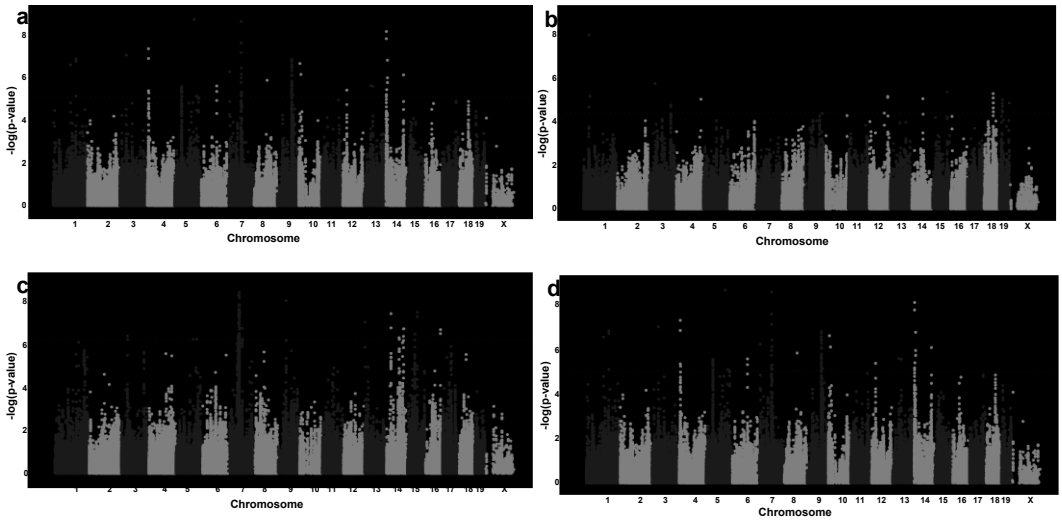

Figure 14. GWA of radiation-induced lung phenotypes in mice.
The survival phenotype data of Figure 1 and the inflammatory response data of Supplementary Figure 2 were analysed with genome-wide SNP genotypes and p values for association computed using EMMA. (a) Lavage PMN percent, (b) Survival time post radiation, (c) lavage lymphocyte percent, (d) mast cell counts. The horizontal lines indicate the 0.05 genome-wide significance thresholds.

QWAS analysis of inbred strain radiation response

To investigate variation within previously identified linkage intervals as associated with fibrosis susceptibility we performed an association analysis limited to five QTL intervals [35, 105]. Using the single marker method the most significant associations were found for SNPs in the chromosome 9 locus (Figure 13b), followed by those on chromosomes 6 and 7.

Within the chromosome 1 (*Radpf2*) & 17 (*Radpf1*) linkage intervals no SNPs reached the QTL-wide threshold for significance. Given the previously suggested genetic interaction between variation within *Radpf1* & *Radpf2* on fibrosis susceptibility [105], we tested for a significant interaction of SNP genotypes at these loci and the phenotype of fibrosis. Assessing the interaction term between all pairs of SNPs in the two loci produced 10 significant SNP-SNP interactions (Supplementary Table 6 [see Appendix]).

To enable an evaluation of strain haplotypes within the linkage intervals as associated with fibrosis we developed an algorithm which iteratively “steps-back” to produce large, overlapping blocks of shared haplotypes among strains with a

minimal error rate. The significantly fewer haplotype blocks in each QTL, compared to the numbers of SNPs, resulted in a 5-10 fold reduction in the number of association tests performed for each QTL. An analysis of variance was used to reveal linkage interval haplotype blocks most significantly associated with radiation-induced pulmonary fibrosis. Since none of the blocks passed the stringent weighted bootstrap significance threshold, the 10 unique most significant p-values in each QTL were retained for candidate gene analysis. The most significant unique p-values correspond to an average of 21 blocks per QTL, and these overlap with a total of 8 genes, including 3 common to the single SNP QWAS set.

Candidate genes for susceptibility to radiation-induced pulmonary fibrosis

A summary of the candidate genes revealed by each analysis, filtered for expression in lung tissue, together with information of the nature of the polymorphisms and of the differential expression status of the genes, is given in Table 3. Based on the genome wide analyses ten candidate genes for radiation-induced pulmonary fibrosis were revealed while from the QTL level eight additional genes were identified as having variation which could influence the trait. Figure 15 shows the effect of genotype on the pulmonary fibrosis phenotype for four of these significant associations presented in Table 3.

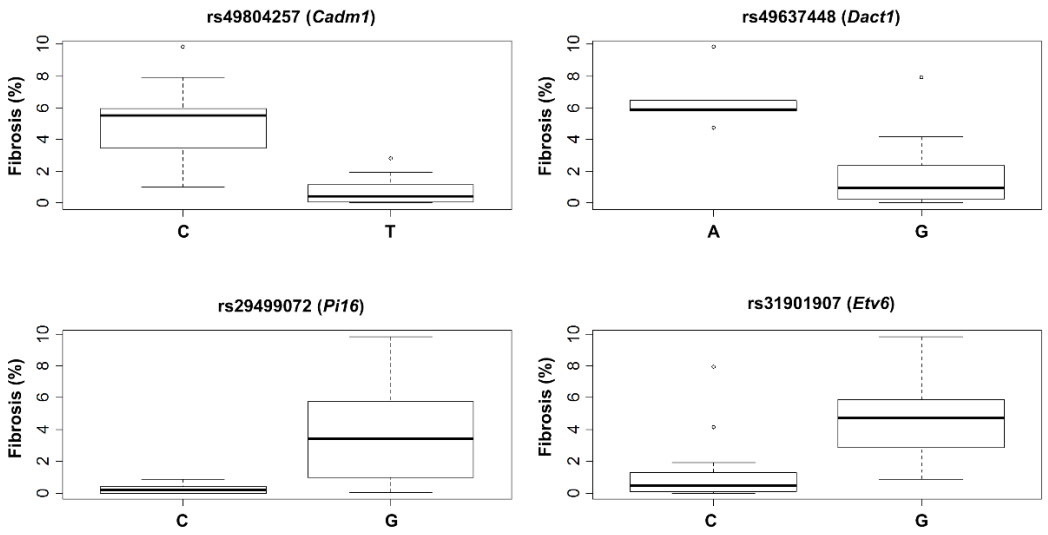

Figure 15. Genotype-phenotype associations of radiation-induced pulmonary fibrosis in mice.
Each boxplot shows the median, lower and upper quartiles and extreme values of the fibrosis levels of the inbred strains, as presented in Figure 2, according to their genotype at a particular SNP of significant association. The polymorphism as well as the gene it is located in is indicated in the title of each plot.

In addition, the *Radpf1-Radpf2* interaction evaluation revealed potential epistasis between two genes on chromosome 1 and six genes on chromosome 17 as affecting fibrosis and these are included as candidates in Table 3. As an example of the detected interaction, inbred strains with an allele "A" at SNP rs31529220, within *Slamf6* on chromosome 1, developed an average of 4% fibrosis in their lungs post irradiation, but, when the responses of these strains are segregated by genotypes at SNP rs31528128, near *Btnl1* on chromosome 17, average fibrosis scores of approximately 2% and 7%, depending on *Btnl1* SNP genotype, are revealed, as illustrated in Figure 16.

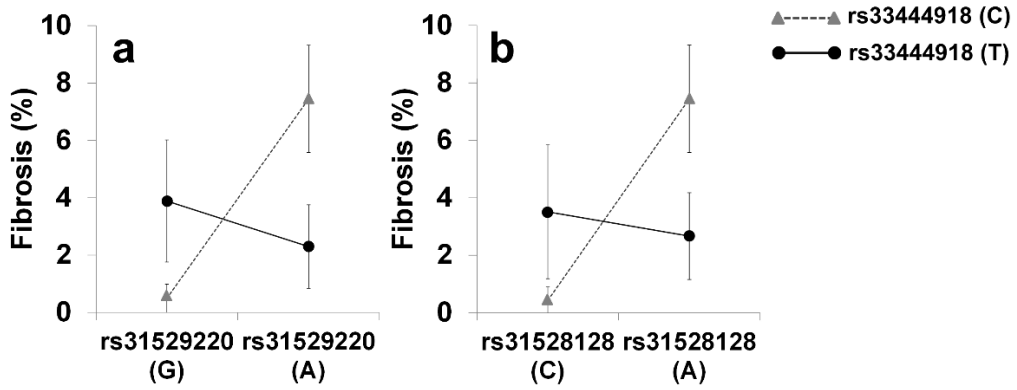

Figure 16. Epistatic interaction between SNPs in *Radpf1* and *Radpf2* influences radiation-induced pulmonary fibrosis in mice.

Linear models were adjusted for the phenotype of radiation-induced pulmonary fibrosis in 27 inbred strains using the two SNPs as covariates. The significance of the interaction term was obtained by comparing the complete model (with interaction) versus the simple additive model (no interaction). The x axis shows the genotypes for A) rs31529220 B) rs31528128 on chromosome 1. The genotypes for the interacting SNP, rs33444918 on chromosome 17, are shown in the legend. Phenotype values on the y axis are presented as mean ± stdev for each genotype group.

Table 3. Candidate genes revealed by association analyses

Gene	Chromosome	SM GWAS[1]	SM QWAS[2]	HAPLO QWAS[3]	Interaction	Differential expression (treated vs. control)[4]	Differential expression (controls)[5]	SNP location[6]
Cadm1 / Rexo2	9	x	x	x		a, b, c / a, b, c	ba / ba, bc, ca	CNS
Zfp426	9	x				a		3'utr, 5'utr, Cn, i 3, 4, 5, 6
Utrn	10	x				a, c	ba, bc	i 61
Dact1	12	x				c	ca, ba	Cn
5730601F06 Rik	9	x				a, b, c		i 2,3,6
Pin1	9	x						i 1, 2
Ubl5	9	x						i 3
Shprh	10	x				a		i 17, 21
Arid4a	12	x						i 23
Kcnip4	5	x						i 1
Prg4	1		x	x				i 1, 4
Tpr	1		x	x	x	a	ba	Cn, i 9
Pi16	17		x			a, c		Cn, i 9, 14
BC003331	1			x				Cn, 3'utr, i 1
Etv6	6			x		a, c		i 1
Zfp30	7			x		a	ba	Cn
Zfp84	7			x		a		3'utr, 5'utr, i 1
Cdkn1a	17			x		a, b, c		Cn, 3'utr, i 1
Abl2	1				x		ba, bc	3'utr
Slamf6	1				x	b, c	ba, bc	i 1
Myo1f	17				x	c	ba, bc	i 1, downstream
Btnl1	17				x			downstream
Notch4	17				x	a, b, c		i 17, upstream
Ddr1	17				x	c		i 7
Btbd9	17				x	a, c	ca, ba, bc	i 4
Mrps18b	17				x	a, c		i 1

[1] Single Marker Genome Wide Association Analysis

[2] Single Marker QTL Wide Association Analysis

[3] Haplotype Analysis QTL Wide

[4] a = differentially expressed in A/J Treated vs A/J Control; b = differentially expressed in C57BL6/J Treated vs C57BL6/J Control; b = differentially expressed in C3H/HeJ Treated vs C3H/HeJ Control. Treated is defined as irradiated with a single dose of 18Gy to the thorax (ref 6).

[5] ab = differentially expressed in A/J vs C57BL6/J; bc = differentially expressed in C57BL6/J vs C3H/HeJ; ca = differentially expressed in C3H/HeJ vs A/J

[6] CNS=Conserved Noncoding Sequence, Cn=Coding nonsynonymous SNP, i=intron

Discussion

Recent evidence indicates that interpatient variation in the development of side effects after cancer radiotherapy cannot be explained, to a clinically relevant effect, by polymorphisms in individual candidate genes [187], therefore alternative approaches to investigating the genetic basis of radiotherapy side effects are needed. One approach involves evaluating the whole genome, which allows the discovery of a priori unknown variants as associated with the trait, in the controlled environment of a model system.

In this study we made use of a mouse model which presents a phenotype similar (in time of onset and histologically) to the clinical radiotherapy late effect of pulmonary fibrosis and report the first genome-wide evaluation of radiation-induced side effects; a prevalent clinical problem. Through association and linkage-based studies novel genetic variants which influence susceptibility to radiation-induced lung disease, including in genes which function in immune pathways, were revealed.

Using chromosome substitution (consomic) mice we have shown the *Radpf* loci, previously mapped in a B6 x C3H mouse cross [35, 105], to be relevant to the B6 strain response to radiation, relative to A/J, as A/J alleles on chromosomes 1 or 17 protected against fibrosis development. In addition, for chromosome 17, the presence of A/J alleles reduced the extent of radiation-induced alveolitis in consomic mice compared to B6 mice. This result is similar to that reported for the radiation response of congenic B6.AKR-H2^{k} mice [105] where the presence of AKR alleles in a genomic region of chromosome 17 enabled the post treatment survival of the congenic B6 mice to the end of the experiment with minimal lung disease. These studies indicate that B6 alleles on chromosome 17 are necessary for the development of fibrosis, in B6 mice, and also contribute to the alveolitis response as the consomic B6.17A and congenic B6.AKR-H2^{k} mice did not develop the alveolitis presented by the inbred B6 mice.

From the 27 strains of mice we observed a clear phenotype separation in propensity to develop fibrosis following thoracic radiotherapy which supports the use of inbred mice as a tool to dissect this complex clinical trait. Our results showed the lung disease phenotype of B6, C3H, A/J, BALB/c, KK/HIJ, AKR/J, SWR and CBA mice to agree with responses presented in prior reports on these mice [103, 104, 168, 169], while to our knowledge, the response of the 20 remaining strains to pulmonary irradiation has not been previously reported. In addition to the fibrosis phenotype, strain dependent inflammatory responses to thoracic irradiation have also been documented [41, 43] including mast cell numbers and bronchoalveolar lavage cell differential [35]. The survey of radiation response in inbred mice indicates that the inflammatory phenotypes evaluated, bronchoalveolar lavage cell profile and mast cell counts, did not, however, correlate with the development of fibrosis, suggesting the inflammatory contributions to the trait, if any, are not the same in every inbred strain. Finally, consistent with prior datasets [35, 131] is the observation that time to respiratory distress was not predictive of the phenotype of fibrosis in the inbred strain panel.

Using the phenotype data of the inbred strain panel we performed GWA studies and identified novel genetic variants associated with susceptibility to radiation-induced pulmonary fibrosis. Our results are derived from the phenotypes of 27 inbred strains, a number which is reasonable for such studies [114, 173, 188] but includes limitations. For example, as with all association studies, a larger sample size would increase the statistical power to detect polymorphisms with small effects. Secondly, our source for sequence polymorphism was the CGD1 dataset which contains both experimentally-derived SNPs and imputed SNPs and is, to our knowledge, the most dense genotype dataset available, pending the delivery of complete genomic sequence, which has been reported for a subset of our evaluated inbred strains [189]. Finally, the phenotypes and genotypes were analysed with EMMA, an algorithm which

addresses strain relatedness, but does not permit genotypes to be evaluated in haplotypes.

We extended the linkage region association analysis, or QWAS, to include an assessment of haplotypes for association with the trait, given the limited genetic information of single marker analysis which can not reveal linked, interacting SNPs within disease loci. To facilitate this analysis haplotypes of a specified minimal error rate were generated. Tests for associations of fibrosis with extended haplotypes, however, produced no results exceeding the stringent threshold for significance, as we were unable to adequately account for strain relatedness in this analysis. Nevertheless by focusing on most significant associations, we identified the haplotype of several QTL genes which were found, through the single marker analysis, to be significantly associated with fibrosis and identified additional candidates for the trait.

Our investigation identified 26 genes as potential candidates for the lung response phenotype. The majority of the genes have been demonstrated to be differentially expressed in lung tissue following whole thorax irradiation [167], but, as is the case with most GWAS, many of significant SNPs found by our analysis reside in introns which makes the mechanism of their genetic contribution to disease difficult to interpret [190]. For example, on chr 9, highly significant SNPs and haplotypes were found in a conserved noncoding sequence of an intergenic region, between *Cadm1* and *Rexo2* closest to a cluster of *Fam55* genes and predicted genes/pseudogenes. Whether such variation could act in gene regulation, which is possible for long-range cis-acting SNPs of gene targets [174, 191], and if so which of the nearby genes it acts upon however are uncertain. *Cadm1* is cell adhesion molecule 1 and as our previous study [167] demonstrated cell adhesion molecule signalling to be the pathway most altered in the lungs of mice following thoracic irradiation, variation in cell adhesion mediated by *Cadm1* could alter the lung response to radiation injury. Indeed, Hallahan *et al.* [192] showed intercellular adhesion molecule-1 deficient mice to develop less

pulmonary fibrosis following thoracic irradiation than that measured in wild type controls. Secondly, *Rexo2* is an RNA exonuclease and recently another similar enzyme, *Xrn2* has been associated with murine lung cancer [174] through its involvement in epithelial cell proliferation. Impaired restoration of the alveolar epithelium following the initial stimulus is a potential trigger for pulmonary fibrosis [193], therefore variation in a gene implicated in alveolar cell proliferation could contribute to radiation-induced lung damage.

Additional candidate genes revealed here by genomic investigation are also physiologically plausible for affecting the phenotype. For example, pulmonary fibrosis can occur as a result of increased extracellular matrix deposition and genes involved in this process such as *Abl2* and *Ddr1* [194, 195] were identified to have variation significantly associated with the trait. Supporting this, *Ddr1* -/- mice have been shown to develop a reduced amount of pulmonary fibrosis in response to a related challenge, that of bleomycin-induced lung injury [196], and in separate work [197], to be protected from renal fibrosis. An inflammatory contribution to the tissue response of fibrosis has also been suggested [198] and polymorphisms within particular candidate genes which function to alter the inflammatory response (*Slamf6*, *Btnl1*) could thus affect susceptibility to radiation-induced lung disease [199, 200]. Further, increased levels of the cytokine transforming growth factor beta (Tgf-β) in lung tissue have been implicated in the development of fibrosis in animal models [201], including in response to irradiation [202] and specific candidate genes identified in our analysis (*Cdkn1a* or *p21*, *Pin1*) have been demonstrated to influence fibrosis development by altering Tgf-β levels [203, 204]. Finally, among the identified candidate genes *Shprh* is known to function in DNA repair [205], therefore variation in cellular radiation sensitivity such as reported by others [179, 206], in addition to strain specific tissue responses to radiation injury, may contribute to the development of the fibrosis phenotype.

The radiotherapy-associated side effect of pulmonary fibrosis is a genetically complex trait, whose development is most likely dictated by several

genes which each contribute a small effect to the disease phenotype. Our investigation of the genetic basis of this trait therefore encompassed genome-wide and QTL-specific association analyses, both at the single marker and haplotype level, to increase the power of identifying true candidates for this trait. These data, combined with strain dependent and post thoracic irradiation gene expression profiling, have revealed variants in genes including cell adhesion molecules and those which function in adaptive immune responses to be associated with radiation-induced pulmonary fibrosis in mice.

Acknowledgements

These studies were funded by the Canadian Institutes of Health Research (#MOP62846) and Fonds de la Recherche en Sante Quebec, to CKH. The study sponsors did not contribute to the study design, the collection, analysis and interpretation of data; the writing of the manuscript; nor in the decision to submit the manuscript for publication.

Conflict of Interest Statement: None to disclose.

CHAPTER TRANSITION

The transcriptome analysis of Chapter II identified a series of immune pathways activated in at least one of the three strains. Toll-like receptors are considered a bridge between adaptive and innate immunity and are activated not only by microbial peptides, but also by self antigens during sterile inflammation as in the case of radiation-induced damage. Therefore we wanted to determine whether disrupting the Tlr pathway influences the response to radiation. For this we analyzed the phenotype of *Tlr2*-/-, *Tlr4*-/- and *Tlr2,4*-/- after thoracic irradiation and compared it to that of wildtype B6 mice in terms of histological traits, survival time and expression of specific genes.

CHAPTER IV: COMBINED TLR2 AND TLR4 DEFICIENCY INCREASES RADIATION-INDUCED PULMONARY FIBROSIS IN MICE

A Paun, J Fox, V Balloy, M Chignard, ST Qureshi and CK Haston

Originally published in the *International Journal of Radiation Oncology Biology Physics*, 2010, 77(4):1198-205

Abstract

Purpose: To determine whether Toll-like receptor 2 or 4 genotype alters the lung response to irradiation in C57BL/6 mice using a model developing a phenotype that resembles radiotherapy-induced fibrosis in both histological characteristics and onset post-treatment.

Methods and Materials: The pulmonary phenotype of C57BL/6 mice deficient in each or both of these genes was assessed after an 18-Gy single dose to the thoracic cavity by survival time postirradiation, bronchoalveolar lavage cell differential, histological evidence of alveolitis and fibrosis, and gene expression levels, and compared with that of wild-type mice.

Results: The lung phenotype of *Tlr4*-deficient and *Tlr2*-deficient mice did not differ from that of wild-type mice in terms of survival time postirradiation, or by histological evidence of alveolitis or fibrosis. In contrast, mice deficient in both receptors developed respiratory distress at an earlier time than did wild-type mice and presented an enhanced fibrotic response (13.5% vs. 5.8% of the lung by image analysis of histological sections, $p < 0.001$). No differences in bronchoalveolar cell differential counts, nor in numbers of apoptotic cells in the lung as detected through active caspase-3 staining, were evident among the irradiated mice grouped by *Tlr* genotype. Gene expression analysis of lung tissue revealed that *Tlr2,4*-deficient mice have increased levels of hyaluronidase 2 compared with both wild-type mice and mice lacking either *Tlr2* or *Tlr4*.

Conclusion: We conclude that a combined deficiency in both *Tlr2* and *Tlr4*, but not *Tlr2* or *Tlr4* alone, leads to enhanced radiation-induced fibrosis in the C57BL/6 mouse model.

Introduction

Thoracic cavity radiotherapy can produce serious inflammatory (alveolitis) or fibrotic (fibrosing alveolitis) side effects in the lung [14, 124]. Pulmonary fibrosis is characterized by cellular proliferation and the progressive accumulation of

extracellular constituents that result in remodeling of the lung interstitium [125]. Alveolitis, or pneumonitis, is an inflammatory response associated with cellular infiltration of the airspace and thickening of the alveolar walls [125]. Measures of the bronchoalveolar lavage of patients after radiotherapy reveal increased numbers of mast cells and neutrophils [40] to be present in this fluid, indicating a contribution of innate immunity to this treatment-induced lung response. Animal models which exhibit radiation-induced alveolitis and fibrosis phenotypes with similar temporal and histological patterns to the clinical response [14, 124] also show an increase in lavage neutrophils [20, 41, 133] and tissue mast cell levels [35]. Specifically, we [35, 102, 131] and others [103, 104] have reported that C57BL/6J (B6) mice respond to high-dose whole-thorax irradiation by developing alveolitis and atelectatic regions of fibrosis at approximately 6 months after radiation treatment.

An important trigger of the innate immune response is the engagement of Toll-like receptors (Tlr), which recognize both pathogen-associated molecular patterns that are unique to microbes [207] and endogenous ligands, or damage associated molecular patterns, which are usually generated through tissue injury. The latter group includes stimuli such as heat shock proteins, hyaluronan, fibronectin, heparin and surfactant protein A, which have been reported to activate Tlr2 and Tlr4 [208, 209]. As the development of fibrotic lung disease can involve the excessive deposition of fibronectin [210] or can occur through mutations in surfactant protein A [211], it is possible that altered signaling through Tlrs may be a component of radiation-induced fibrotic lung disease. In support of this hypothesis, we recently used gene expression microarray analysis to document the pathways involved in radiation-induced alveolitis and fibrosis [167] and identified Tlr signaling to be a significant component of the pulmonary response. In addition, as Tlr2 and Tlr4 are expressed on cell types putatively involved in the radiation response, including epithelial cells that respond to tissue

damage through cytokine secretion [212], defective Tlr2 and/or Tlr4 signaling could alter the tissue capacity to heal from radiation induced injury.

In this study we phenotyped *Tlr2*, *Tlr4*, and *Tlr2,4* knockout mice for their responses to whole-thorax irradiation to determine whether a deficiency in these Toll-like receptors would alter the development of radiation-induced lung disease.

Materials and Methods

Mice**:** *Tlr2* and *Tlr4* knockout mice were obtained from S. Akira, Osaka University, Japan, and were backcrossed eight times with C57BL/6J to ensure similar genetic backgrounds. C57BL/6-*Tlr2,4*-/- mice were generated by breeding C57BL/6-*Tlr2*-/- mice and C57BL/6J-*Tlr4*-/- mice. Inbred C57BL/6 mice and knockout strains (C57BL/6-*Tlr2*, C57BL/6-*Tlr4*, C57BL/6-*Tlr2,4*) were bred at the Montreal General Hospital and housed in the animal facility of the Meakins-Christie Laboratories. All mice were handled according to guidelines and regulations of the Canadian Council on Animal Care, as approved by McGill University.

Radiation treatment**:** Mice were treated at 8 weeks of age. Lung damage was elicited by whole-thorax radiation exposure using a Gamma cell Cesium-137 unit as previously described [35, 131]. A dose of 18 Gy delivered at 0.6 Gy/min was given to elicit a lung disease response in the majority of the animals based on the known response of the background strain [20, 35, 102-105, 131, 167, 213]. The rest of the body was shielded with 3 cm of lead to reduce the beam strength to 3% in this area. The irradiated mice were killed when moribund or at 26 weeks after treatment. The mice were weighed weekly beginning 8 weeks after radiation; animals that lost >20% of their body weight and exhibited distress through ruffled fur, accelerated breathing, and hunched posture were killed, as described previously [35]. Differences in survival between strains of mice grouped by *Tlr* genotype were assessed by the log-rank test. The control mice were not treated and were killed at the 15- to 26-week time points.

***Histology*:** At necropsy, bronchoalveolar lavage was performed as previously described [35, 131]. The lungs were then removed, and the single left lobe of each mouse was perfused with 10% neutral buffered formalin and submitted for histological processing. Lung sections were stained with Masson's Trichrome; the area of fibrosis in the left lung lobe was determined from a user drawn region (Image Pro Plus Software) and compared with the area of the entire lobe to yield the percent of pulmonary fibrosis for individual mice [105, 135, 213]. To assess alveolitis, hematoxylin and eosin (H&E)–stained left lung sections were evaluated through semiquantitative histology [35]. Alveolitis was scored subjectively on a scale of 0 to 6, with 0 representing no alveolitis and 6 representing extreme alveolitis characterized by excessive thickening of the alveolar walls, with cellular infiltration and diffuse exudates throughout the alveolar spaces. Mast cell numbers were determined by counting the positive cells present in 10 fields of a Toluidine Blue–stained lung section at x400 magnification. All scoring was completed by a user blinded to mouse strain and treatment. Differences in lung phenotype between mice grouped by genotype were assessed with Student's t test or analysis of variance.

***Immunohistochemistry*:** Staining for active caspase-3 was completed as described previously [102], using the cleaved caspase-3 rabbit monoclonal antibody (dilution 1:100; catalogue no. 9664, Cell Signaling Technology, Beverly, MA) and the biotinylated swine anti-rabbit secondary antibody (dilution 1:100; DakoCytomation, Mississauga, ON).

***Apoptosis scoring*:** Apoptotic cells were identified by positive active caspase-3 staining and by characteristics including cell shape and apparent nuclear density. The percentage of apoptotic cells was determined from counts of positive cells and of total cells within 10 fields of the subpleural alveolar space, as in a prior study [102]. Cells were counted using a 0.1 mm^2 grid, at x400 magnification. The types of cells undergoing apoptosis were determined by morphology. The lungs

were scored by an investigator blinded to sample identity, and differences between groups were assessed by Student's t test.

***Bronchoalveolar lavage fluid analysis*:** Bronchoalveolar lavage (BAL) fluid was centrifuged (302 g for 10 min at 4°C), and the supernatant was removed and stored at -85°C. The cellular pellet was resuspended in 0.25 ml of PBS. Inflammatory cell counts were performed (x400 magnification) on cytocentrifuged cells (214.2 g for 3 min), after staining with a hematoxylin-and-eosin kit (Hema-3 Stain Set by Protocol) as previously described [35, 131].

***Quantitative real-time polymerase chain reaction*:** After sacrifice, the right lung of each mouse was immediately homogenized in 2 ml of Trizol reagent and placed on dry ice. The homogenates were stored at -85°C until RNA isolation was completed according to the instructions of the manufacturer (Sigma, St. Louis, MO). For gene expression analysis, 4 to 5 mg of total RNA from the right mouse lung was reverse transcribed to cDNA with oligo(dT)12-18Primer using Superscript II RNase H– Reverse Transcriptase (Invitrogen, Carlsbad, CA). Quantitative real-time polymerase chain reaction assays were performed using the Applied Biosystems International Prism 7500 Sequence Detection System using the TaqMan Gene expression assays Mm00477731_m1 for Hyal2 and Mm00515089_m1 for Has2. Ataxin 10 (Atxn10, Assay Mm00450332_m1) was used as the reference gene as in a prior study [167].

Results

Survival time and histological phenotype

To determine whether mice deficient in *Tlr2* and/or *Tlr4* differ from wild-type mice in their response to whole lung irradiation, mice of each genotype were exposed to18 Gy irradiation and killed upon presentation of respiratory distress. As shown in Figure 17, *Tlr2,4*-/- mice developed distress significantly earlier than wild-type mice, whereas the survival time for either *Tlr2*-/- or *Tlr4*-/- mice did not differ from that in wild-type mice. Histological evaluation of the lungs, which was completed after euthanasia at the times indicated in Figure 17 revealed the

respiratory distress of the irradiated mice to be caused by fibrosis, as shown in Figure 18, in agreement with previous reports of the wild-type strain [35, 102, 104, 135, 214]. Image analysis of histological sections demonstrated that *Tlr2,4*-/- mice had developed significantly more fibrosis after thoracic irradiation than had wild-type mice, whereas the fibrosis levels in *Tlr2*-/- and *Tlr4*-/- mice did not differ from that of the background strain (Figure 18b). The extent of alveolitis, assessed through semiquantitative scoring of histological sections, did not differ among groups of mice segregated by genotype (Figure 18c).

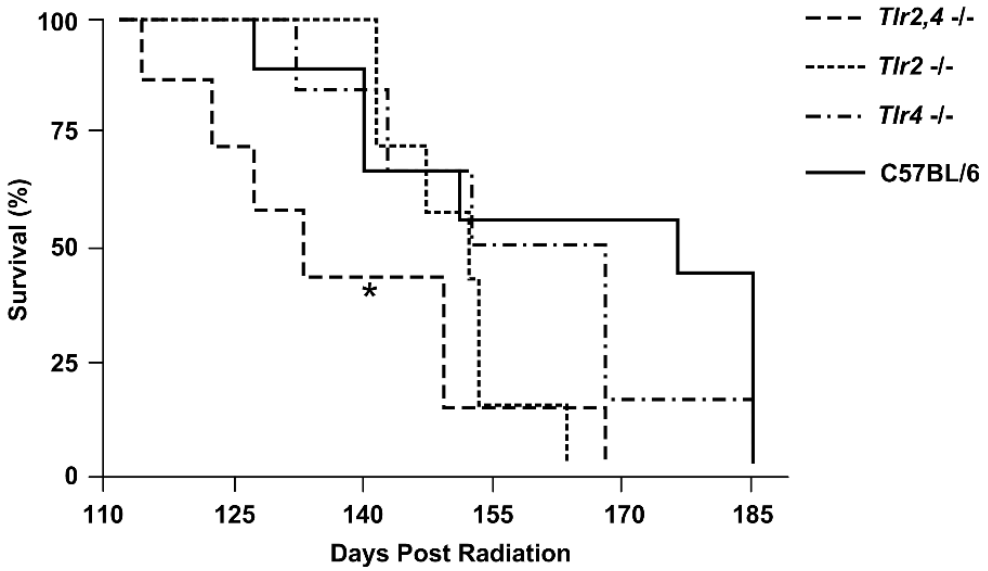

Figure 17. Post-irradiation survival time of wild-type, *Tlr2*-, *Tlr4*-, and *Tlr2,4*-deficient mice.

Mice (n = 6–9 per strain) were exposed to a single dose of 18-Gy whole thorax irradiation and euthanized when in respiratory distress or at 185 days postirradiation. *Significantly different from wild-type survival ($p < 0.05$).

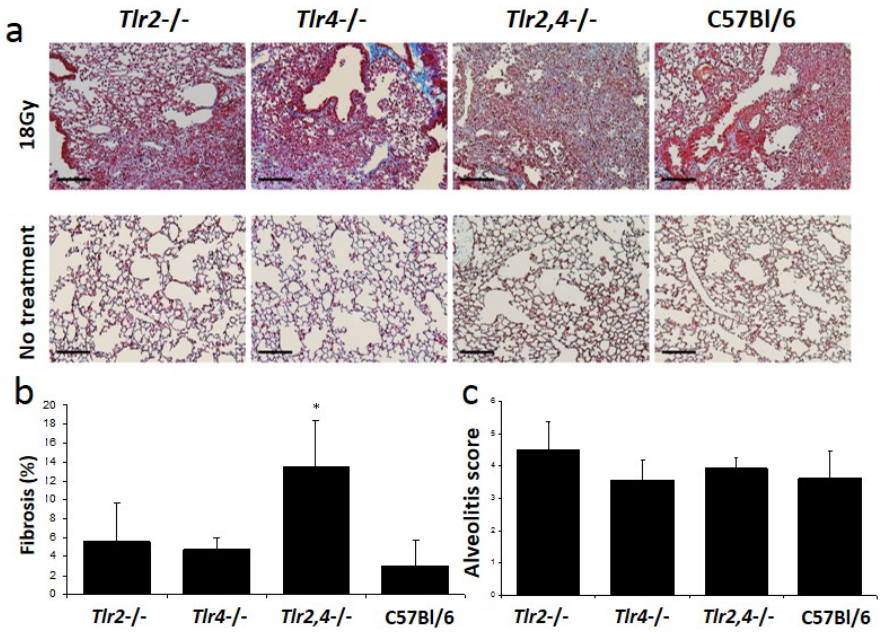

Figure 18. Radiation-induced lung disease phenotype of wild-type, Tlr2-, Tlr4-, and Tlr2,4-deficient mice.

Mice of each strain were exposed to 18-Gy whole thorax irradiation and euthanized when in respiratory distress or at 185 days postirradiation. (a) Histological sections illustrate subpleural regions of fibrosing alveolitis (blue streaks indicate collagen deposition) in radiation-treated but not control mice. Masson's trichrome stain, magnification x200; bar = 200 mm. (b) Average (±SD) percent fibrosis based on image analysis of histological sections (n = 6–9 mice per group). (c) Average alveolitis score derived from semiquantitative evaluation of histological sections. The average fibrosis in untreated control mice was 0% for all strains, and the average alveolitis score of 1.6 in untreated mice was not altered by *Tlr2* or *Tlr4* genotype. *Significantly different from wild-type level ($p < 0.05$).

Apoptosis

Tlr2,4-deficient mice have been reported to develop greater fibrosis in response to bleomycin treatment than do wild-type B6 mice, in association with higher levels of epithelial cell apoptosis [77]. To investigate an alteration in apoptotic cell numbers as a potential mechanism leading to the enhanced radiation-induced fibrotic response of *Tlr2,4*-/- mice, we stained the lung tissue for active caspase 3 and counted the number of positive cells. The lungs of irradiated mice had a higher percentage of caspase 3–positive cells in the subpleura compared with levels in untreated control mice (23.3±8.1 vs. 2.5±4.5, p

= 7.1 x 10^{-6}) in agreement with a previous report [102], but this increase did not depend on *Tlr2,4* genotype, as shown in Figure 19. In addition, the apoptotic cells were morphologically consistent with macrophages, and very few epithelial cells were positive for caspase 3 staining in this experiment.

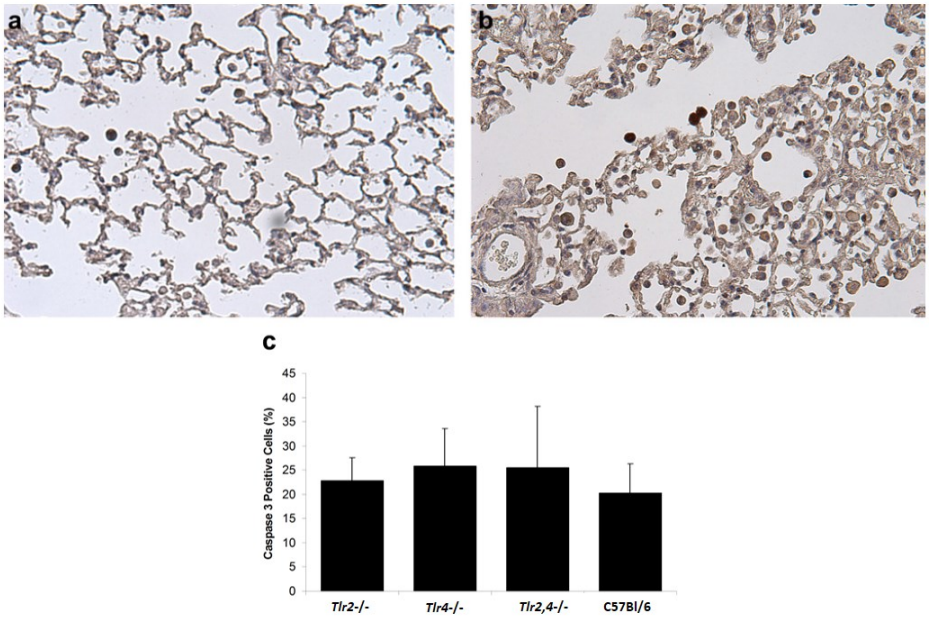

Figure 19. Apoptosis levels in radiation-induced lung disease of wild-type and Tlr-deficient mice.
Mice of each strain were exposed to a single dose of 18-Gy whole-thorax irradiation and euthanized when in respiratory distress or at 185 days postirradiation. Expression of active caspase-3 was assessed with immunohistochemistry, and positively stained cells were counted in five subpleural fields per mouse lung. Sections from C57BL/6 mice (a) and *Tlr2,4-/-* mice (b) are shown; magnification x400. (c) Mean percentage (±SD) of caspase 3–positive cells in mice grouped by *Tlr* genotype (n = 6–9 mice per group). There was no significant difference in numbers of caspase 3–positive cells among these strains (p = 0.52).

Inflammatory cell count

To determine whether the inflammatory response to whole thorax irradiation is altered by a *Tlr2* and/or *Tlr4* deficiency, we quantified the mast cell influx and assessed the bronchoalveolar cell types. There were radiation-induced increases in total bronchoalveolar lavage cell counts for all strains (data not shown) in agreement with previous reports of the wild type strain [35, 131], but as shown in Figure 20, there was no difference in lavage cell differential by *Tlr2,4*

genotype in radiation-treated mice. Quantification of mast cell influx revealed an increased number of these cells in all strains postirradiation, as previously reported for B6 mice [35, 131], with a significantly greater influx in *Tlr4*-/- mice, as shown in Figure 21.

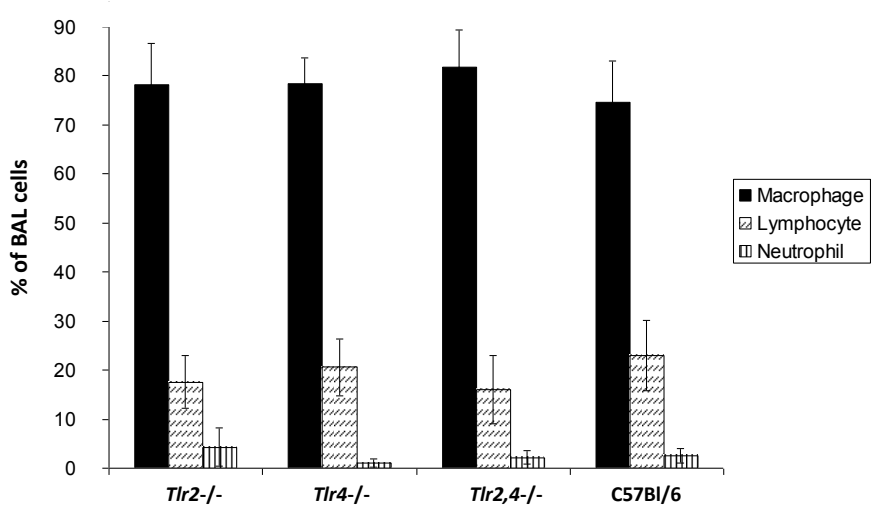

Figure 20. Bronchoalveolar lavage cell differential of wild-type, *Tlr2*-, *Tlr4*-, and *Tlr2,4*-deficient mice after whole-thorax radiotherapy.

Mice of each strain were treated with 18 Gy to the lung and killed upon presentation of respiratory distress or at 185 days postirradiation. Bronchoalveolar lavage samples were collected at necropsy, and cells were morphologically identified from cytospin preparations. The average percentage of each cell type (± SD, n = 5–7 mice per group) is presented. There were no significant differences among the strains in lavage cell differential ($p > 0.52$).

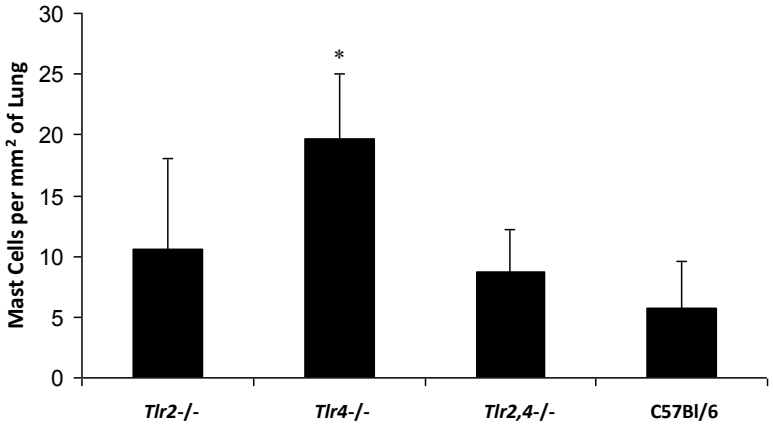

Figure 21. Effect of *Tlr2*, *Tlr4*, and *Tlr2,4* deficiency on radiation-induced pulmonary mast cell influx.

Mice of each strain were exposed to a single dose of 18-Gy whole-thorax irradiation and euthanized upon presentation of respiratory distress or at 185 days postirradiation. The average mast cell numbers (± SD) in the left lungs of mice (n

= 6–9 per group) from Toluidine Blue–stained histological sections is shown. The average mast cell number (0.2 per mm^2) in untreated mice was not altered by *Tlr2* or *Tlr4* genotype. *Significant difference between knockout mice and wild-type controls ($p < 0.05$).

Hyaluronan-associated gene expression

As radiation-induced changes in expression of hyaluronan synthase 2 (Has2) and hyaluronidase 2 (*Hyal2*) genes have been documented in a lung disease model [215], and hyaluronan is an endogenous ligand for Tlr2 and Tlr4 [77], we measured the expression of these genes in the wild-type and knockout mice. As shown in Figure 22, *Tlr2,4* knockout mice had greater levels of *Hyal2* postirradiation than did wildtype, *Tlr2*-/-, or *Tlr4*-/- mice, whereas no differences in the expression of *Has2* among mice by Tlr genotype were detected.

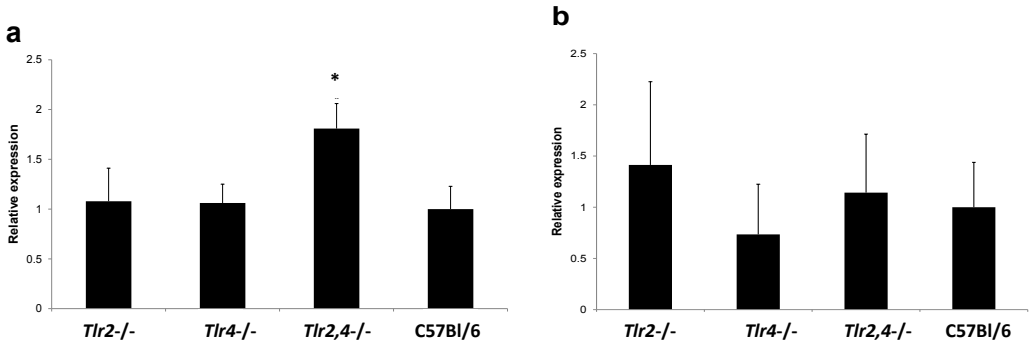

Figure 22. Relative expression of hyaluronan synthase 2 (*Has2*) and hyaluronidase 2 (*Hyal2*) genes in the lungs of wild-type, *Tlr2*-, *Tlr4*-, and *Tlr2,4*-deficient mice.
Mice were exposed to a single dose of 18-Gy whole thorax irradiation and euthanized upon presentation of respiratory distress or at 185 days postirradiation, whereas control mice were not irradiated. The fold change in expression of each gene (a. *Hyal2* b. *Has2*) in the right lung, relative to the level in control mice, and normalized to this ratio in B6 mice, is shown (± SD, n = 3–8 mice per group). *Significant difference between knockout mice and wild type controls ($p < 0.05$).

Discussion

In this study, we demonstrate that a combined *Tlr2,4* deficiency, but not defects in *Tlr2* alone or *Tlr4* alone, accelerates the onset of respiratory distress and

the amount of fibrosis in mice exposed to whole-thorax irradiation. Given the established functions of both *Tlr2* and *Tlr4* in innate immunity, these data implicate one or more components of these two signaling pathways in sparing the lung tissue response to radiation-induced pulmonary fibrosis. We further show a unique increase of hyaluronidase 2 transcript levels in the radiation response of *Tlr2,4* deficient mice, suggesting that an associated increase in hyaluronan fragments may have contributed to enhanced radiotherapy-induced fibrosis in this model. The finding of increased radiation-induced fibrosis in *Tlr2,4* knockout mice compared with wild-type mice is consistent with data reported by Jiang et al. [77], which characterized the response of these mice to bleomycin. We did not detect a difference in epithelial apoptosis in the present work, however, whereas Jiang et al. implicated epithelial cell apoptosis in the fibrotic response of bleomycin-treated *Tlr2,4* knockout mice. Evaluation of the apoptotic pathway in this study revealed that macrophages were the active caspase 3–positive cells in the irradiated lung, as previously described [102], and no differential increase in lung cell apoptosis was evident in *Tlr2,4* knockout mice compared with the wild-type strain. The difference between the two investigations may be attributable to the fact the bleomycin was delivered intratracheally in the work of Jiang et al. [77], and this mode of administration may be more directly injurious to the epithelium than external beam irradiation.

The enhanced fibrotic response of *Tlr2,4* knockout mice in the bleomycin model may also be dose dependent, as Gasse et al. [216] showed that intranasal delivery of bleomycin resulted in the same level of pulmonary fibrosis in both *Tlr2,4* knockout and wild-type mice. In addition to apoptosis, Jiang et al. reported fewer bronchoalveolar lavage neutrophils in *Tlr2,4* knockout mice before the development of bleomycin-induced fibrosis, while we did not detect a difference in the lavage cell differential in the radiation response of mice with established fibrosis when grouped by *Tlr* genotype. Our data thus indicate that the enhanced fibrotic response of *Tlr2,4* knockout mice after thoracic radiotherapy may be

mediated by separate mechanisms from those that regulate the bleomycin response.

The molecular pathways and cellular mechanisms that contribute to the earlier onset and enhanced radiation-induced pulmonary fibrosis in *Tlr2,4*-deficient mice are not clear. Tlr signaling can influence innate and adaptive immune responses [217-219], both of which are implicated in the development of radiation-induced lung disease. For example, innate immunity promotes the differentiation of naive T cells to effector lymphocytes [220, 221], and bronchoalveolar lavage measures of patients after chest radiotherapy [153, 222] as well as animal models of radiation- induced lung disease [103, 105, 153, 192, 223-225] indicate increased numbers of lymphocytes to be a component of the response. Therefore an alteration in specific T-cell numbers or phenotypes resulting from defective Tlr2,4 signaling and impaired MyD88-dependent nuclear translocation of the proinflammatory transcription factor nuclear factor–kB (13), could influence the development of fibrosis. The plausibility of a unique effect of combined *Tlr2,4* mutations on T lymphocyte populations was recently demonstrated by Martin et al. [226], who showed contact hypersensitivity, a T-cell–mediated inflammatory skin disease, to be abolished in *Tlr2,4*-/- but not *Tlr4*-/- mice. In addition, the enhanced lung disease in the *Tlr2,4* knockout could involve altered Tlr signaling in B lymphocytes [227, 228], a hypothesis supported by our gene expression data, which implicate B cell proliferation and the associated complement response as significant pathways in the radiation-induced pulmonary fibrosis response of B6 mice [167]. Furthermore, as Tlr2 and Tlr4 receptors are also expressed on neutrophils [229], and as we have previously shown the numbers of lavage neutrophils to be positively correlated with fibrotic lung disease in a population of genetically mixed mice [35], it is conceivable that defective Tlr signaling in this cell type could affect the level of pulmonary fibrosis. Such an effect could occur through, for example, radiation-induced necrotic cells signaling through Tlrs to induce the expression of tissue repair genes [230] or of cytokine

secretion [229] by neutrophils. Finally, the activation of the Tlr2 and/or Tlr4 pathways has been shown to cause changes in adhesion molecule expression [231], which can influence radiation-induced lung disease [192].

The enhanced radiation-induced pulmonary fibrosis in *Tlr2,4* knockout mice may have developed through an increased inflammatory response to hyaluronan fragments, which are known to induce the recruitment of specific T-lymphocyte types [232, 233], as we have shown these mutant mice to have higher expression levels of hyaluronidase 2 in the lungs. In particular, accumulation of the extracellular matrix glycosaminoglycan hyaluronan has been documented to be part of the radiation response of the lung, both clinically [234] and in animal models [134, 235, 236], and this phenotype coupled with increased *Hyal2* expression would be expected to produce high levels of low-molecular weight hyaluronan. Short hyaluronan fragments have been demonstrated to be inflammatory to the lung [237] and this stimulus, signaling through Cd44 or other known pathways [238], in the fibrotic prone B6 mouse background [35, 105], may have contributed to the enhanced fibrosis in *Tlr2,4* knockout mice. Supporting this conjecture is the report of Li et al. [215], who demonstrated hyaluronan fragments to increase collagen gene expression by fibroblasts.

In this work, deletion of *Tlr2* alone or *Tlr4* alone did not influence the amount of alveolitis or fibrosis presented by B6 mice in respiratory distress, but the *Tlr4*-/- mutant mouse lung phenotype did include more mast cells than that of the wild-type strain. This finding suggests that a deficiency in signaling through *Tlr4* may alter mast cell survival, which has not, to our knowledge, been reported, although it has been demonstrated that increased signaling through Tlr4 reduces the apoptotic cell death of bone marrow–derived mast cells [239, 240]. The increased number of mast cells in the lungs of *Tlr4*-/- mice, without a change in the extent of alveolitis or fibrosis is in agreement with results from our previous study wherein mast cell depletion did not alter the radiation-induced alveolitis or fibrosis phenotypes in mice (unpublished observations).

Conclusion

In summary, this study has evaluated the effect of *Tlr2* and/or *Tlr4* deficiency in a murine model of radiation-induced lung disease, and has shown that the combined deficiency of these receptors decreases survival time and enhances the development of fibrosis. These results therefore implicate an innate immune response and/or its influence on the adaptive immune response in the wound repair phenotype of lung fibrosis.

CHAPTER TRANSITION

The GWAS in Chapter III revealed an interaction between SNPs in genes *Slamf6* and *Btnl1*, both involved in lymphocyte activation. Previous studies in humans and mice have pointed to the role of lymphocytes in radiation-induced lung disease, therefore in Chapter 5 we asked what populations specifically are associated with either alveolitis or fibrosis in six strains of mice (three prone to alveolitis and three prone to fibrosis). Based on the observed results, we also studied T helper cells and various cytokines in mice deficient in Il17 and Tlr2&4 in order to see how these deficiencies influence the development of lung disease.

CHAPTER V: THE TH1/TH17 BALANCE IN THE LUNG DICTATES A FIBROSIS RESPONSE OR SPARING OF RADIATION-INDUCED LUNG DISEASE IN MICE

A Paun and CK Haston

Manuscript in preparation

Abstract

The specific pathways through which radiation produces the lung injuries of alveolitis (pneumonitis) and fibrosis are unknown. Herein we initially characterize the fibrosis and pneumonitis lung disease phenotypes in 6 inbred strains of mice, in terms of lymphocyte populations present, and specifically show fibrosis-responding mouse strains have greater numbers of T helper type 17 in their lungs than do pneumonitis responding strains which presented with increased T helper type 1 cell numbers. Next, we investigated the hypothesis that the radiation induced lung phenotype of *Il17*-/- mice (which lack Th17 cells) is altered relative to that of C57BL/6J genetic background strain and to toll-like receptor 2&4 deficient mice which served as a positive control for enhanced fibrosis. Following 18 Gy whole thorax irradiation C57BL/6J mice succumbed to respiratory distress at 24 weeks post irradiation and developed a fibrotic lung disease with increased numbers of pulmonary Th1 and Th17 cells, and augmented lavage neutrophil percentage, while the enhanced fibrotic response in *Tlr2,4* -/- mice included increased levels of Th17, but not Th1, cells. In mice developing respiratory distress the percentage of neutrophils in the lavage was positively correlated with the extent of pulmonary fibrosis. Irradiated *Il17*-/- mice developed significantly increased levels of pulmonary Th1 cells, only, and were spared both pneumonitis and fibrosis, surviving to the end of the experiment. We conclude that an increased Th17 cell count enhances and a Th1 response spares radiation-induced pulmonary fibrosis in mice.

Introduction

Cancers affecting organs in the thoracic region are commonly treated with radiation, although side-effects of pulmonary fibrosis and pneumonitis, which occur in almost 30% of treated patients [124], can limit the effectiveness of this modality. The mechanisms leading to the pathologies of excessive inflammation,

characteristic of pneumonitis, or deposition of extracellular matrix in the lung interstitium (fibrosis) as a consequence of radiotherapy are incompletely understood but likely include a primary response of cell injury or death and reactive oxidative species generation, induced by radiation [241, 242] and a tissue response to this primary injury [214, 243, 244]. This tissue response can include the rapid production of cytokines, such as Tnfα, Tgfβ and interleukins Il1α&β and Il6, which, as they serve to promote the pulmonary infiltration and activation of innate and adaptive immune cells, can contribute to disease [153, 245-249]. Indeed, there is clinical evidence for a lymphocyte contribution to the tissue response to radiation injury in that patients who had undergone a thymectomy prior to receiving total body irradiation for bone marrow transplantation showed a decreased incidence of radiation pneumonitis [38] and from reports of increased numbers of bronchoalveolar lavage lymphocytes in patients following chest radiotherapy [36, 37, 40]. The specific lymphocytes and their involvement in the development of radiation-induced lung injuries has yet, however, to be elucidated.

The pneumonitis and fibrosis responses evident clinically have been modelled in mice, which show strain dependent presentations of these traits [104, 250]. Specifically we [131, 168, 250] and others [104] have documented certain inbred strains to develop pneumonitis, including C3H/HeJ, AKR/J and A/J mice, while others are prone to fibrosis (C57BL/6J, KK/HIJ and 129/SvMIJ mice). Animal models of radiation-induced lung disease also present the increased lymphocyte numbers evident clinically [20, 41, 43, 134].

Phenotyping of animal models with clinical relevance permits the evaluation of genetically altered mice for a contributory effect on the trait. For example we showed combined toll-like receptor 2 (*Tlr2*) and *Tlr4* deficient mice to develop an enhanced fibrotic response, of earlier onset, relative to that of wild type C57BL/6J mice, in response to thoracic irradiation [251]. The contributions of specific cytokines or lymphocyte classes to radiation induced lung disease has

not been investigated in genetically altered mice, although in a related model interleukin-17 (Il17) deficient mice have been used to reveal the cytokine's contribution to hypersensitivity pneumonitis [252] and bleomycin-induced pulmonary fibrosis [56].

Herein we investigated the radiation-induced responses of specific inbred and genetically altered mice to define the lymphocyte populations and thus specific pathways contributing to the development of pneumonitis and fibrosis as a consequence of radiotherapy.

Materials and methods

***Mice**:* Mice of inbred strains, A/J, AKR/J, C3H/HeJ, C57BL/6J, 129S1/SvImJ, and KK/HIJ, were purchased from the Jackson Laboratory (Bar Harbor, USA) and housed in the Meakins-Christie Laboratories. Mice of other strains were obtained through collaboration (*Tlr2,4*-/- mice from Dr. Qureshi of McGill University) or through material transfer agreements (*Il17*-/- mice from Dr. Iwakura of the University of Tokyo) and experimental mice bred in house. All mice were handled according to guidelines and regulations of the Canadian Council on Animal Care.

Thoracic irradiation and experimental groups: At the age of 8-10 weeks, mice were exposed to a single dose of 18 Gy to the thorax using a Gamma Cell Cesium-137 source as previously described [35, 102, 131]. Inbred strain mice were weighed weekly from 8 weeks after irradiation and euthanized when they showed signs of distress (ruffled fur, accelerated breathing, hunched posture, weight loss >15% of body weight). Groups of genetically altered mice were euthanized when they showed signs of distress and at specific timepoints (16, 20, 26 and 35 weeks) post irradiation. The genetically altered mice were divided into 2 experiments: one group of mice was assayed by flow cytometry and the second group evaluated by survival, BAL analysis, and histologically. Control mice were not irradiated and were euthanized at matching timepoints.

***Lung histopathology and bronchoalveolar lavage (BAL) fluid analysis*:** Bronchoalveolar lavage collection was performed by cannulating the trachea and

instilling the lungs with 1 mL phosphate buffered saline. The lungs were then removed and the single left lobe was perfused with 10% buffered formalin and processed histologically. 5µm lung sections were stained with Masson's Trichrome and the fibrosis score was calculated as the lung surface covered by fibrosis relative to the total lung surface using the Image Pro Plus software [250, 251, 253].To determine the degree of pneumonitis, lung sections were stained with hematoxylin and eosin and evaluated semi-quantitatively through subjective blind scoring. A score of 0-6 was given, 0 being no pneumonitis and 6 being severe pneumonitis, as in previous studies [35, 131].

The BAL fluid was centrifuged (300g for 10 minutes at 4 degrees C) and the supernatant was stored at -80°C. The cellular pellet was re-suspended in 125µL PBS. Inflammatory cell counts were performed at 400X magnification on centrifuged cells (214.2g for 3 minutes) following staining with hematoxylin-eosin (Hema-3 Stain Set) and are reported as percentage of 500 counted cells. The correlation tests between BAL cell differentials and other disease phenotypes were performed using the cor.test function in R (http://cran.r-project.org).

Lymphocyte profiling: At necropsy both lungs were cut into small pieces and placed in PBS containing 1mg/mL collagenase (Roche) and 1mg/mL DNase (Roche) at 37°C for 45 minutes. The tissue was further disrupted using a Cell Dissociation Kit (Sigma-Aldrich) and the total number of cells retrieved was determined using a Hemacytometer. Cells were stained using the following antibody combinations: T cells (CD3+), B cells (CD19+), Th cells (CD3+ CD4+), cytotoxic T cells (CD3+ CD8+), NK cells (CD3- Cd49b+). For detection of intracellular cytokines (Th1 cells (CD4+ Ifnγ+), Th2 cells (CD4+ IL13+), Th17 cells (CD4+ IL17+)), the cells were incubated at $1x10^6$ cells/mL in complete media (37 degrees C, 4 hours) in the presence of 50ng/mL PMA (Sigma-Aldrich), 1µg/mL ionomycin (Sigma-Aldrich) and 1µl/mL Golgi Stop (BD Biosciences). After activation, the cells were washed and stained with the corresponding surface antibodies and then fixed and permeabilized using Cytofix/Cytoperm (BD Biosciences). Subsequently

the intracellular staining was performed and the cells were acquired using FACSCalibur or LSR II cytometers. The lymphocyte population was identified based on size and granularity on a forward scatter / side scatter plot and the analysis of cell counts was completed using the FACS Diva and FlowJo software.

Cytokine profiling: BAL supernatants were profiled using a custom 8-plex Bioplex Pro Cytokine kit (BioRad) containing the following cytokines: Ifnγ, Tnfα, Il1β, Il4, Il10, Il6, Il17, Il13. Tgfβ levels were measured by ELISA, using a Tgfβ platinum ELISA kit (eBioscience) after performing a 1:1.5 dilution of the sample with the assay buffer provided by the manufacturer.

Data analysis: Differences in survival between genetically modified strains and inbred C57BL/6J mice were assessed with log-rank tests using GraphPad Prism software (www.graphpad.com). Phenotypic differences among groups were evaluated using T tests, or ANOVA's, which were performed using R (http://cran.r-project.org) or Microsoft Excel software.

Results

Radiation-induced pulmonary lymphocyte populations in inbred mice

To investigate whether distinct lymphocyte populations could contribute to the phenotypes of pneumonitis and fibrosis, following whole thorax irradiation, we measured the lymphocyte numbers in the lungs of 3 strains of mice we had previously determined to develop the pneumonitis phenotype (C3H/HeJ; A/J; AKR/J) and compared these data to that of three strains which we showed to develop fibrosis (C57BL/6J; 129S1/SvImJ; KK/HIJ) [35, 102, 131, 167, 168, 250, 251, 254]. Mice were irradiated with 18 Gy to the thorax, euthanized upon presentation of respiratory distress and lymphocyte populations of the lung assessed with fluorescence activated cell sorting. The onset of distress, which varied from 8 weeks in KK/HIJ mice to 25 weeks in A/J mice, differed among the strains (Figure 23) and was not indicative of a pneumonitis or fibrosis response, in agreement with previous studies [167, 168, 250].

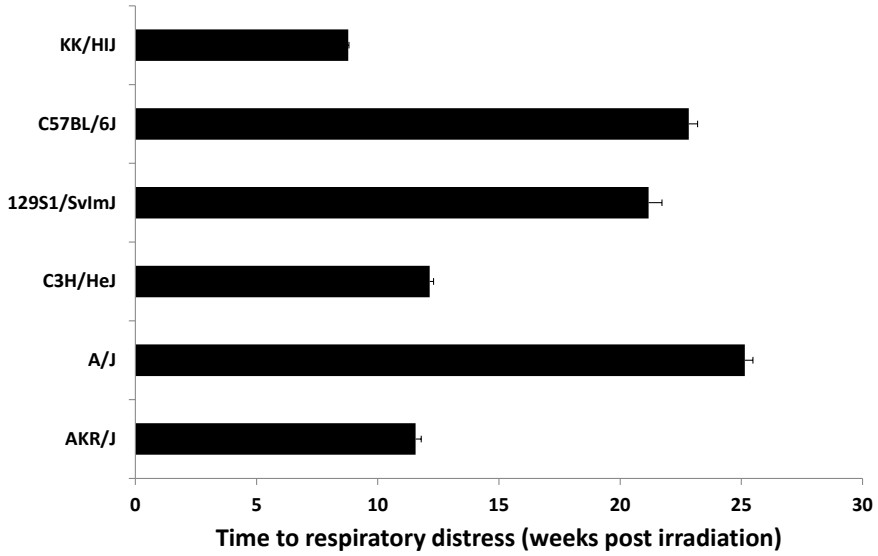

Figure 23. Onset of respiratory distress in inbred mice following whole thorax irradiation

Mice of 6 inbred strains received 18 Gy of whole thorax irradiation and were euthanized when in respiratory distress. Survival times are shown for each strain as mean±SE for groups of 5-10 mice.

Of the 9 lymphocyte populations surveyed, radiation-induced increases in Th17 cell numbers, where responses significantly exceeded control levels for fibrosis prone strains, only, were detected, as shown in Figure 24.

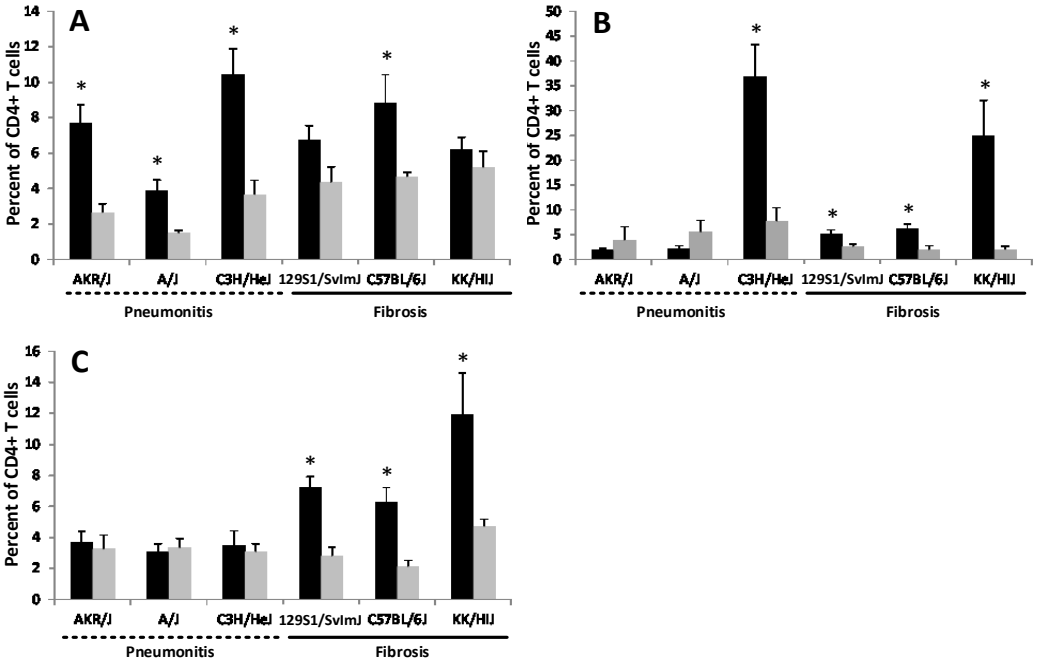

Figure 24. Pulmonary T helper cells in inbred mouse strains following thoracic irradiation

Mice of 6 inbred strains received 18 Gy of whole thorax irradiation and were euthanized when in respiratory distress. Shown are percentages of A) Th1 (CD4+Ifnγ+), B) Th2 (CD4+IL13+) and C) Th17 (CD4+IL17+) cells of total lung lymphocytes in distressed (black bars) and control (grey bars) mice. Results are mean±SE for n=5-10 mice per group. * indicates a significant difference compared to unirradiated control (T test pvalue<0.05).

In addition, significant increases in numbers of Th2 cells were evident in three fibrosis-prone and in one pneumonitis prone strain while Th1 cells were of greater numbers in the three strains developing pneumonitis, and in one fibrosis prone line. Regarding the remaining cell types, a radiation-induced decrease in NK cells was evident for all strains, except 129S1/SvImJ mice, while no consistent differences in numbers of T, B, CD4 or CD8 cells in the lung were evident between pneumonitis prone and fibrosis prone strains (Figure 25).

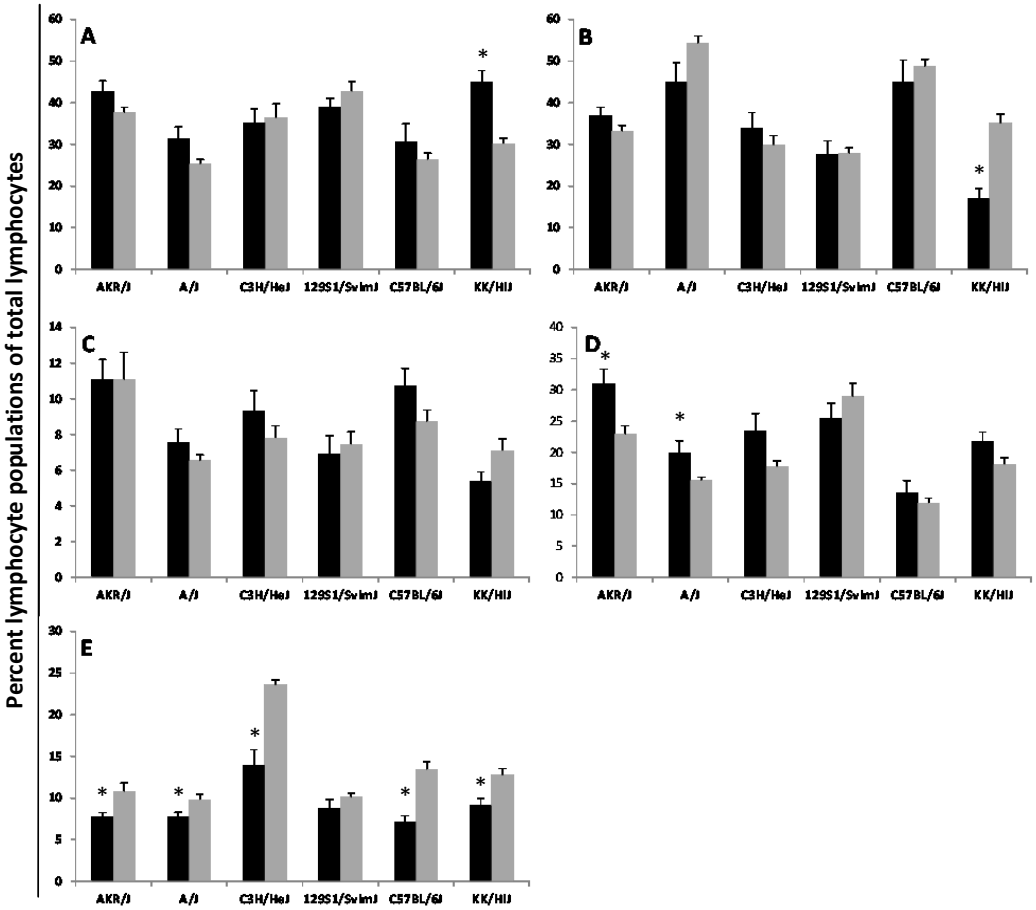

Figure 25. Lymphocyte populations in the lungs of inbred mice following whole thorax irradiation

Mice of 6 inbred strains received 18 Gy of whole thorax irradiation and were euthanized when in respiratory distress. Through flow cytometry different lymphocyte populations were analyzed in the lung tissue from treated mice (black bars) and unirradiated controls (grey bars): A) CD3+; B) CD19+ C) CD3+CD8+; D) CD3+CD4+; E) CD49b+CD3- cells. The results are percentages of total lymphocytes and are shown as mean±SE for groups of 5-10 mice. * denotes a significant difference compared to unirradiated control (T test pvalue<0.05).

Survival and lung disease phenotypes of genetically altered mice

To determine whether a deficiency in interleukin-17 (Il17) cells affects the development of radiation induced lung disease, groups of mice (C57BL/6J, *Tlr2,4-/-* and *Il17-/-*) were irradiated and their survival to the onset of respiratory distress, or to 35 weeks post irradiation, was recorded. As shown in Figure 26A, mice of the inbred C57BL/6J (B6) strain developed respiratory distress at 24-26 weeks post irradiation and of the *Tlr2,4-/-* strain significantly earlier than B6 as in a prior study

[251]. *Il17*-/- mice survived significantly longer than B6 mice (p<0.0001) with all mice euthanized at the experimental endpoint of 35 weeks post irradiation, as shown in Figure 26A. For each strain, all mice presenting respiratory distress were confirmed to have developed significant pneumonitis (average score of all groups = 4.5, for B6 and *Tlr2,4*-/- mice euthanized in respiratory distress; ANOVA p=0.11). The average pneumonitis score of *Il17*-/- mice, euthanized at the experimental endpoint of 35 weeks post irradiation, was 1.25 ± 0.41; and significantly lower than that of B6 mice (p=0.006). The extent of fibrosis, evident histologically, also depended on strain with levels in irradiated *Tlr2,4*-/- mice exceeding those of B6 mice (Figure 26B,C). No fibrosis was evident in the lungs of 7/8 *Il17*-/- mice; while one *Il17*-/- mouse developed fibrosis of 0.9% of its lung tissue.

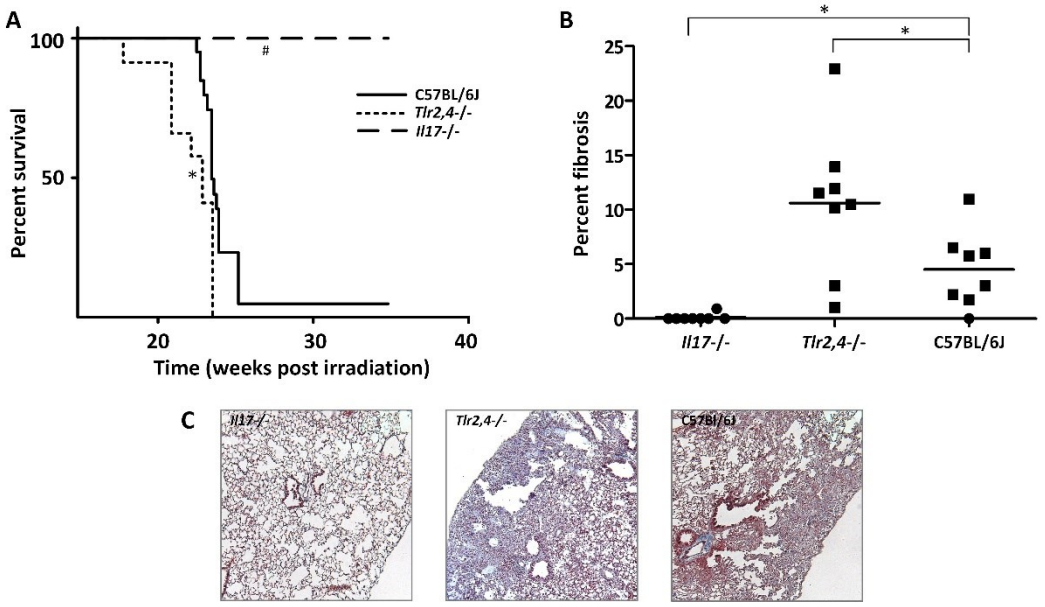

Figure 26. Radiation-induced pulmonary phenotype of genetically altered mice
Following a single dose of 18 Gy of thoracic irradiation, B6 WT, Tlr2,4-/- and Il17-/- mice were euthanized when in respiratory distress or at 35 weeks post irradiation which was the end of experiment (EOE). A) Survival following treatment. *, # indicate a significant difference in survival compared to B6 WT mice (logrank test p-value<0.05); n=13-44 mice per strain. B) Fibrosis scores calculated as the percent of fibrotic lung tissue in Trichrome stained histological sections. Squares indicate mice that were euthanized due to respiratory distress and circles indicate mice that survived to the EOE. * indicates a significant difference in fibrosis compared to B6 WT mice (T test p-value<0.05). C) Images of

Masson's trichrome-stained lung sections from strains indicating different fibrosis responses to whole thorax irradiation; magnification = 200X.

To monitor the development of the lung response phenotype groups of *Il17* and *Tlr2,4*-deficient mice, and B6 genetic background control mice, were exposed to 18 Gy whole thorax irradiation and their lung responses assayed in mice surviving to 16, 20, 26 and 35 weeks post irradiation. As shown in Figure 27, minimal lung disease was evident, histologically, at the early time point of 16 weeks post irradiation in all strains. The pneumonitis and fibrosis scores increased in mice of the *Tlr2,4*-/- strain at 20 weeks and no mice of this strain survived to the later timepoints. In B6 mice the significant fibrosis phenotype increase occurred at 26 weeks post irradiation in agreement with the survival data of Figure 26. The fibrosis phenotype of *Il17*-/- mice did not differ from that of control (unirradiated) mice at any of the time points ($p>0.37$), but a significant, although minimal, increase in pneumonitis was evident in these mice at 16 weeks post irradiation ($p<0.05$).

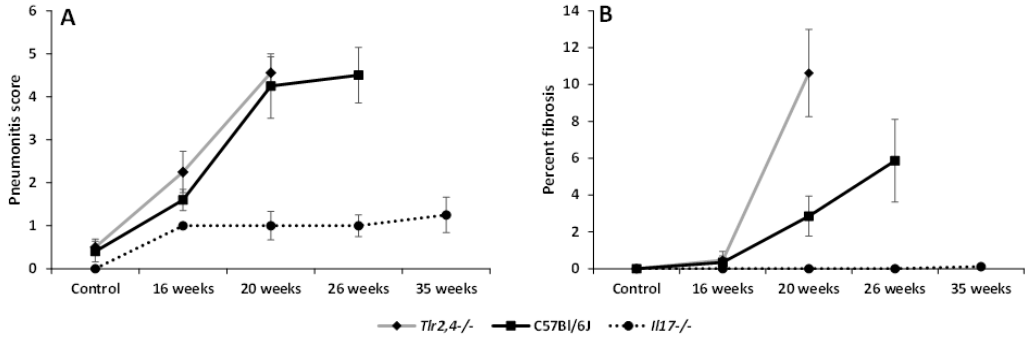

Figure 27. Radiation-induced lung phenotype development in genetically altered mice

Following a single dose of 18 Gy of thoracic irradiation, surviving B6 WT, *Tlr2,4*-/- and *Il17*-/- mice were euthanized at 16, 20, 26 or 35 weeks post irradiation. A) Pneumonitis scores derived from semi quantitative evaluation of histological sections. B) Percent of fibrotic lung tissue in Trichrome stained histological sections. Control values are from unirradiated mice. Phenotypes are presented as mean±SE for groups of 5-10 mice.

Bronchoalveolar lavage cells were counted in tissue from mice euthanized in the time course experiment to document the inflammatory response in the development of radiation-induced lung disease. Thoracic irradiation resulted in a ten fold increase in the total number of cells infiltrating the lungs of the strains of mice succumbing to fibrosis (C57BL/6J and *Tlr2/4*-/-mice) with the influx evident at 20 and 26 weeks post irradiation, (Table 4). In *Il17*-/- animals, however, the total cell count at 16, 20, 26 and 35 weeks post irradiation was not different from control levels (T test $p>0.08$) and was, consistently, significantly lower than that measured in distressed B6 mice ($p<0.05$).

Table 4. Total bronchoalveolar lavage cell count (x10^4/ml) in genetically altered mice.

	C57Bl/6J	***Il17-/-***	***Tlr2,4-/-***
Control	2.15 ± 0.50	4.95 ± 0.75	3.02 ± 0.69
16 weeks	2.95 ± 0.49	6.93 ± 0.44	10.59 ± 2.42*†
20 weeks	40.29 ± 11.27*	4.18 ± 0.46†	24.35 ± 5.39*
26 weeks	34.18 ± 10.12*	3.17 ± 1.24†	
35 weeks		4.96 ± 0.63	

Data are presented as mean±SE. * indicates significant differences compared to control and † indicates significant differences compared to B6 cell numbers at the corresponding time point.

As shown in Figure 28A, the lavage of *Tlr2,4*-/- mice contained significantly more neutrophils than B6 mice at 16 and 20 weeks post irradiation ($p<0.04$) while the lavage neutrophil % did not differ between these strains in mice euthanized due to distress ($p=0.26$). The lavage PMN percent of irradiated *Il17*-/- mice over the time course was not different from control levels ($p>0.09$), and was significantly reduced compared to B6 levels at 26 weeks post irradiation ($p<0.04$) which corresponds to the time of distress in the inbred strain. As significantly increased numbers of neutrophils were detected in the lavage of mice presenting significant pulmonary fibrosis (*Tlr2,4*-/- mice at 20 weeks post irradiation and B6 mice at 26 weeks) we investigated the association of these traits. These analyses revealed the number of PMN cells in lavage at the time of distress to be

significantly correlated with extent of fibrotic lung disease (correlation coefficient=0.72, p value=0.00024, Figure 28B).

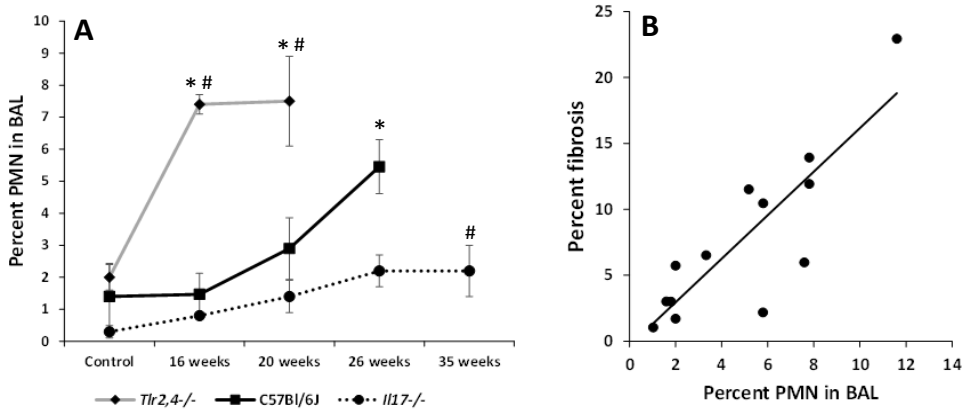

Figure 28. Radiation-induced pulmonary inflammatory response of genetically altered mice

Following a single dose of 18 Gy of thoracic irradiation, surviving B6 WT, *Tlr2,4*-/- and *Il17*-/- mice were euthanized at 16, 20, 26 or 35 weeks post irradiation. Bronchoalveolar lavage (BAL) samples were collected at necropsy and cells were morphologically identified from cytospin preparations. A. PMN percentages (mean±SE) for groups of 5-10 mice. * indicates a significant difference compared to corresponding control values, # indicates a significant difference compared to B6 values at the same time point (T test p-value<0.05). B. Correlation of BAL PMN percentages and fibrosis scores in animals euthanized due to respiratory distress. Pearson test p-value<0.001.

The lymphocyte percentage of the lavage was also increased in irradiated mice compared to control levels, in all strains ($p<0.05$; Figure 29). The increase preceded the distress response in B6 and *Tlr2,4*-/- mice which resulted in the lymphocyte percentages differing significantly among the strains at 16 weeks post irradiation (ANOVA $p=0.03$) but not at the 20 or 26 week timepoints (ANOVA $p>0.24$). In *Il17*-/- mice the radiation-induced increase in lavage lymphocyte percentage was evident at 16 – 26 weeks post irradiation, as shown in Figure 29, but decreased significantly ($p=0.013$), reaching control levels at 35 weeks post irradiation.

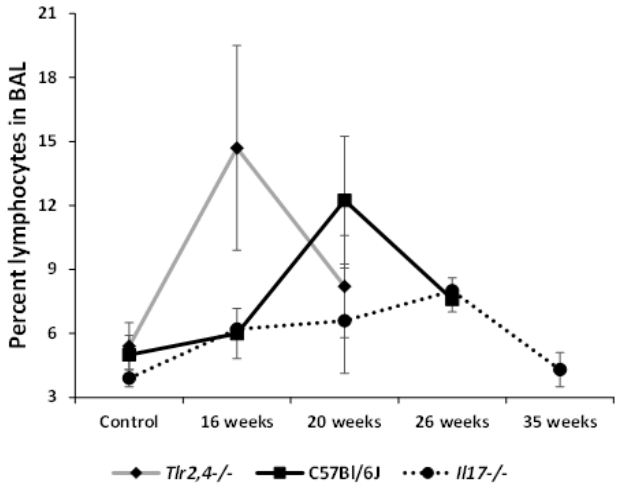

Figure 29. Lymphocytes in the bronchoalveolar lavage of genetically altered mice following whole thorax irradiation
Following a single dose of 18 Gy of thoracic irradiation, surviving B6 WT, *Tlr2,4*-/- and *Il17*-/- mice were euthanized at 16, 20, 26 or 35 weeks post irradiation. Bronchoalveolar lavage (BAL) samples were collected at necropsy and cells were morphologically identified from cytospin preparations. Control values are from unirradiated mice. The lymphocyte percentages (mean±SE) for groups of 5-10 mice are shown.

Lymphocyte populations and cytokine levels in genetically altered mice

To elucidate the mechanisms producing the immune response associated with radiation-induced pulmonary fibrosis we typed the pulmonary lymphocyte populations present during the development of the phenotype. Groups of Il17- and Tlr2,4-deficient mice, and B6 genetic background control mice, were exposed to 18 Gy whole thorax irradiation and lymphocyte populations were assayed in mice surviving to 16, 20, 26 and 35 weeks post irradiation. As shown in Figure 30 and Figure 31, B6 mice presented with radiation-induced increases in Th17 (CD4+Il17+), Th2 (CD4+Il13+) and Th1 (CD4+Ifnγ+) cells during the development of the phenotype, while the most prominent change in Tlr2,4 deficient mice was a significant increase in Th17 cells in irradiated mice. Indeed, a significant increase in the numbers of pulmonary Th17 cells was associated with fibrosis in B6 and Tlr2,4-/- mice in that all animals succumbing to the disease displayed increasing numbers of Th17 cells, peaking at the time of distress, and a significant increase in

these cells. Distressed Tlr2,4-/- mice, further, presented significantly lower numbers of Th1 cells compared to distressed B6 mice (p=0.001) despite similar values in control animals (p>0.16). In contrast, the lymphocyte phenotype of Il17-/- mice included radiation-induced increases in Th1 cells, only, which were evident at 20-35 weeks post irradiation and exceeded the response of B6 mice at the 20-week time point (p=0.001).

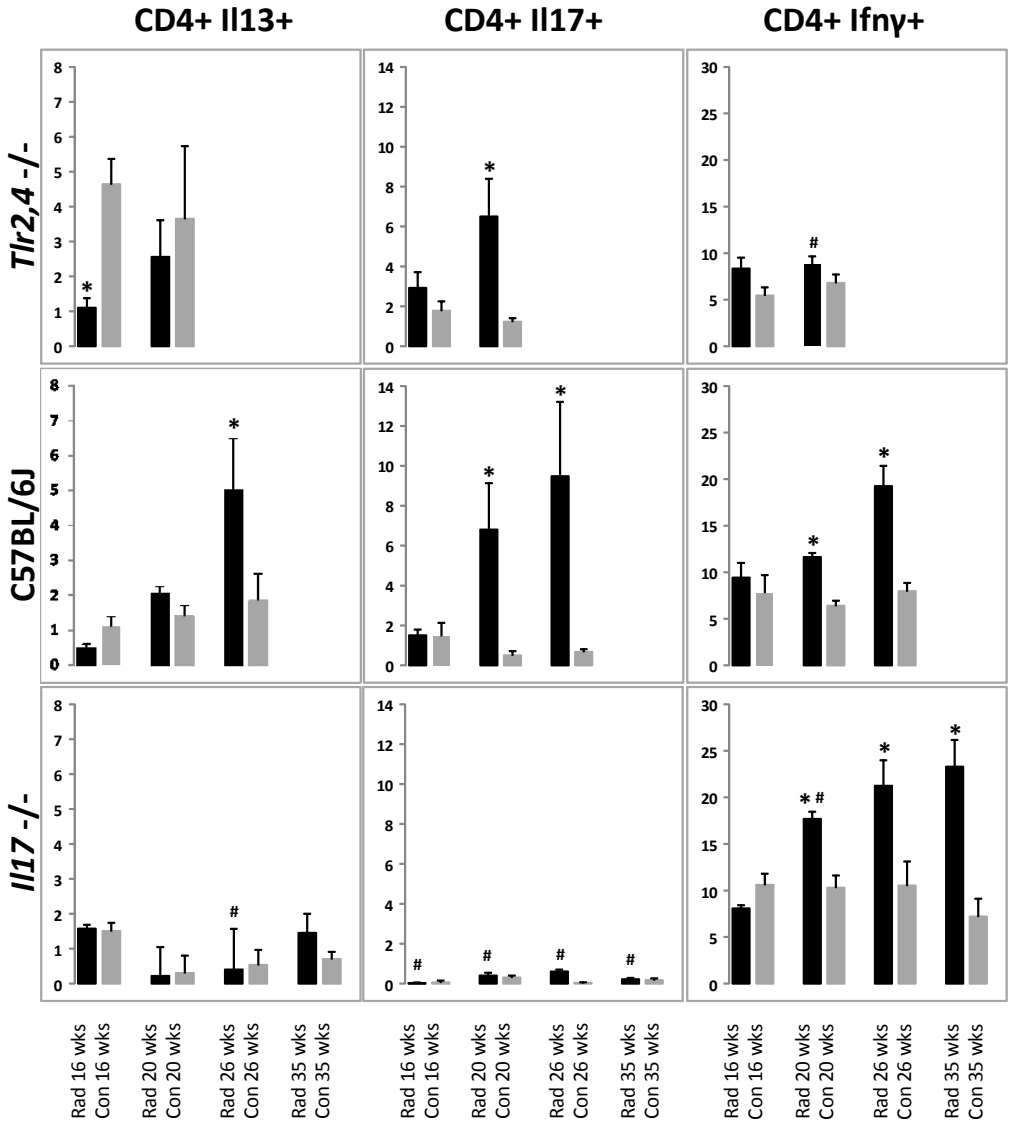

Figure 30. Radiation-induced pulmonary T helper cell populations in genetically altered mice

Mice of B6 WT, *Tlr2,4*-/- and *Il17*-/- strains were exposed to 18 Gy of thorax irradiation and survivors euthanized at 16, 20, 26 and 35 weeks post treatment.

Th1 (CD4+Ifnγ+), Th2 (CD4+Il13+) and Th17 (CD4+Il17+) cell counts were measured through flow cytometry of total lung tissue. Results are percentages of total CD4+ lymphocytes and are shown as mean±SE for groups of 5-8 mice. * indicates a significant difference compared to corresponding control values, # indicates a significant difference compared to B6 values at the same time point (T test pvalue<0.05).

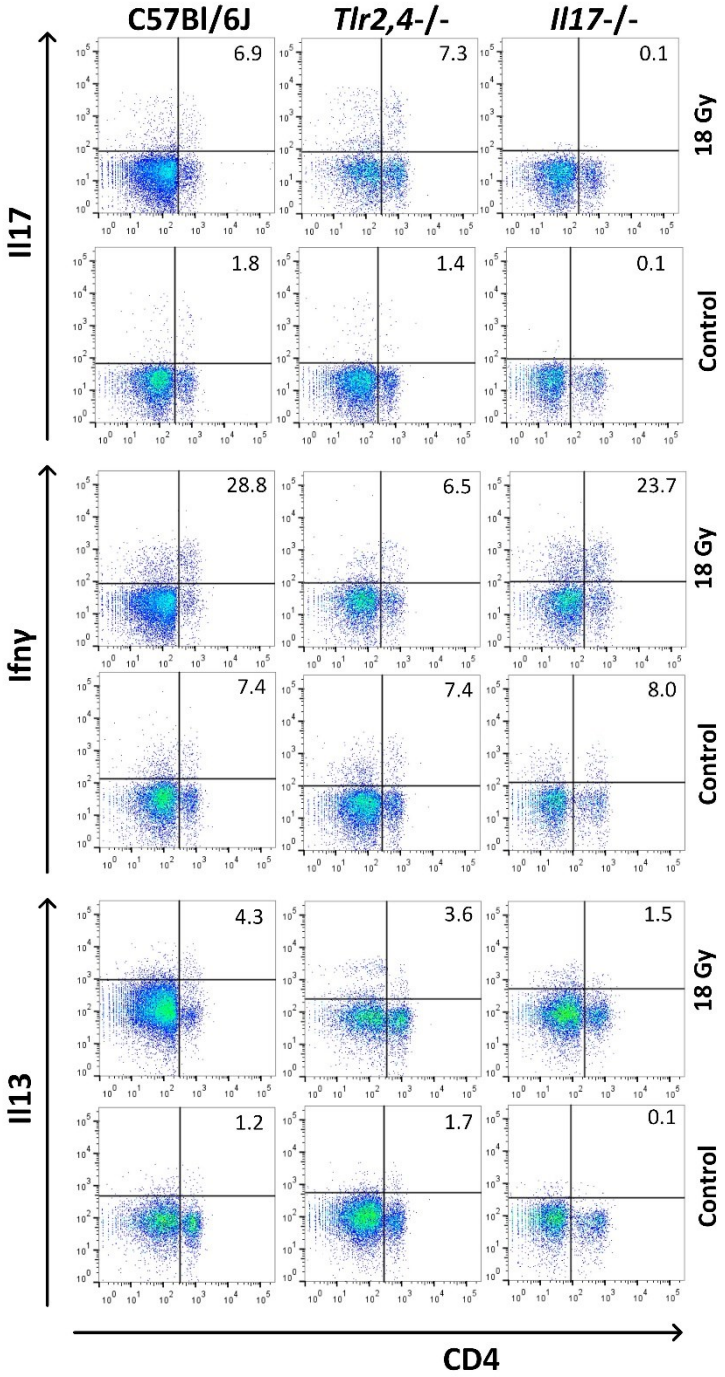

Figure 31. Representative scatter plots of pulmonary tissue from genetically altered mice

Mice received 18 Gy of whole thorax irradiation and were euthanized when in respiratory distress. Through flow cytometry different T helper cell subsets were analyzed in lung tissue from treated mice and unirradiated controls. Shown are representative scatter plots of gated lymphocytes, in control and treated mice at the latest time point after irradiation (20 weeks for *Tlr2,4-/-*, 26 weeks for B6 and 35 weeks for *Il17-/-* mice). The numbers in the top right-hand corner represent percentages of Th17, Th1 and Th2 cells of total CD4+ cells.

A radiation-induced increase in Il17-producing lymphocytes, apart from the CD4+ population, was also observed in all fibrosis-prone strains euthanized at the time of distress, compared to levels in control animals ($p<0.04$), as shown in Figure 32. The proportion of CD4-Ifnγ+ cells among lung lymphocytes was also increased in all strains after irradiation ($p<0.02$), with levels in *Il17-/-* animals exceeding the response of B6 mice.

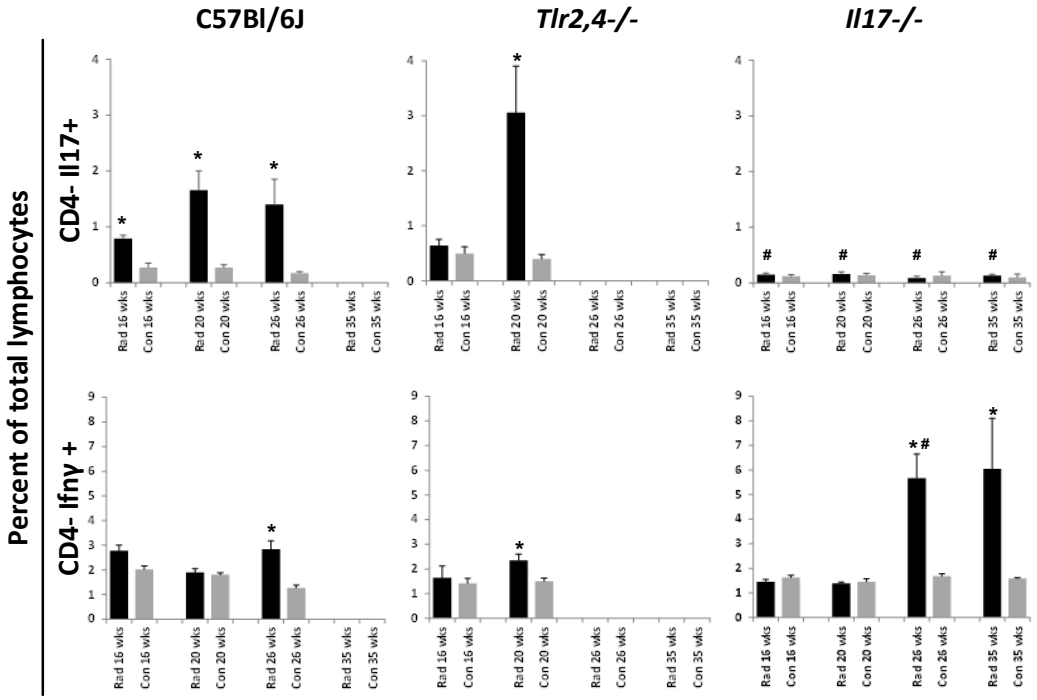

Figure 32. CD4-Il17+ and CD4-Ifnγ+ lymphocytes in genetically altered mice following whole thorax irradiation

Following a single dose of 18 Gy of thoracic irradiation, surviving B6 WT, *Tlr2,4-/-* and *Il17-/-* mice were euthanized at 16, 20, 26 or 35 weeks post irradiation. CD4-Il17+ and CD4-Ifnγ+ cells were counted through flow cytometry on total lung tissue of irradiated (black bars) and control (grey bars) mice. Results are percentages

among total lymphocytes shown as mean±SE for groups of 5-10 mice. * indicates a significant difference compared to corresponding control values, # indicates a significant difference compared to B6 values at the same time point (T test pvalue<0.05).

To support the observations made by lymphocyte profiling, we analysed the levels of 8 cytokines in the bronchoalveolar lavage of *Tlr2,4*-/- and B6 mice at a presymptomatic timepoint and from mice in respiratory distress and compared these data to profiling from *Il17*-/- mice at similar timepoints. As shown in Figure 33, the cytokine measurements from presymptomatic mice differed only minimally from those of untreated mice, with a significant increase in Tnfα in B6 mice, Il6, Il13 and Ifnγ in Tlr2,4-/- mice and decrease in Il13 and Tnfα in Il17-/- animals ($p<0.05$). Upon presentation of distress in *Tlr2,4*-/- and B6 mice, however, the lavage levels of all 8 cytokines exceeded that of controls and showed strain dependent increases. In particular, the lavage of *Tlr2,4*-/- mice contained significantly greater amounts of Il6 and Il17 compared to that of B6 mice ($p<0.05$), similar amounts of Tgfβ, and reduced levels of Ifnγ, Tnfα Il10, Il1β and Il13. The cytokine levels in the lavage of *Il17*-/- mice did not differ from the levels in untreated controls at either of early (16 and 20 weeks post irradiation) or later time points (26, 35 weeks post irradiation), $p>0.08$, with the exceptions of a later increase in Il10 ($p=0.01$) and of Tgfβ, which was decreased post irradiation in *Il17*-/- mice ($p<0.002$).

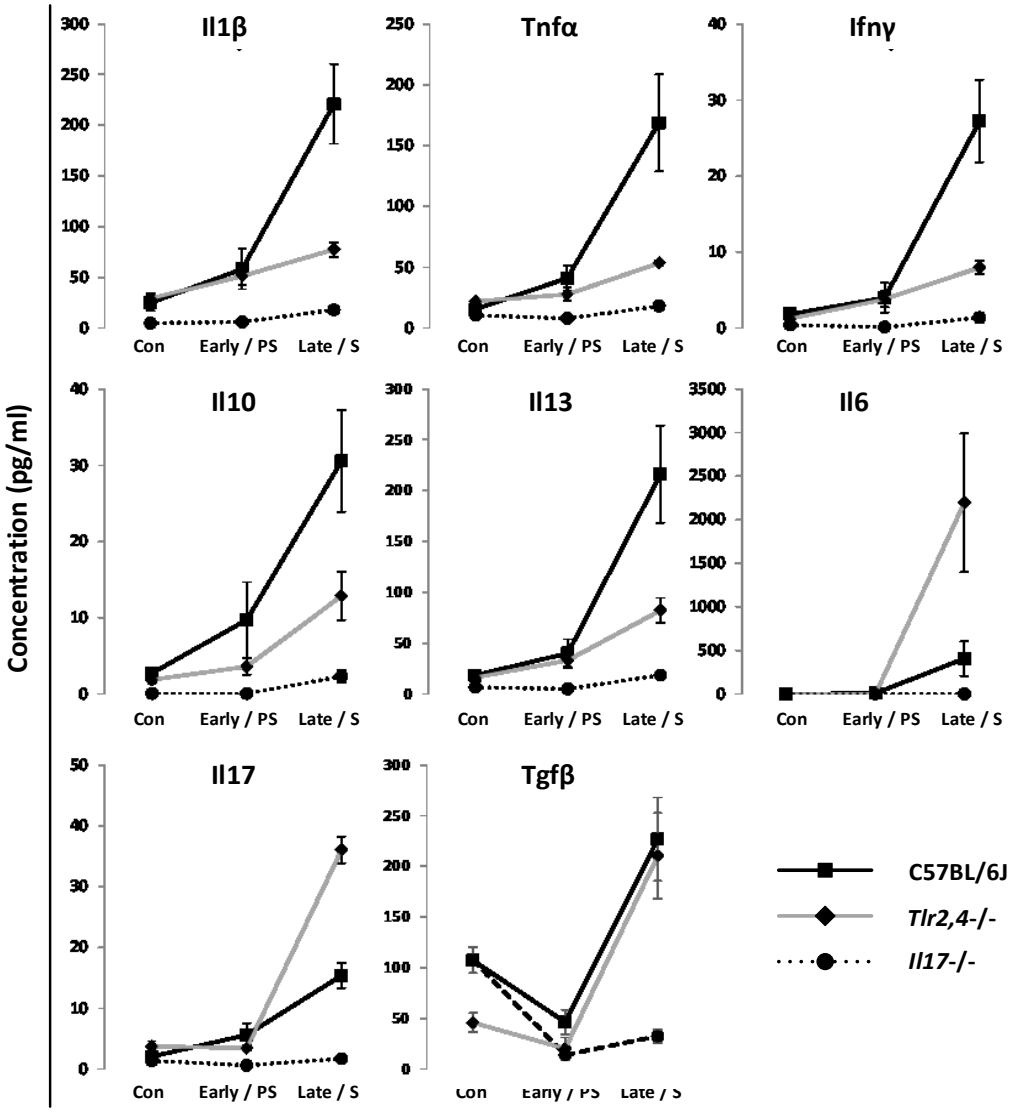

Figure 33. Radiation-induced bronchoalveolar lavage cytokine levels in genetically altered mice

Mice of B6 WT, *Tlr2,4-/-*, and *Il17-/-* strains were exposed to 18 Gy of thorax irradiation and survivors euthanized at 16, 20, 26 and 35 weeks post treatment. Bronchoalveolar lavage (BAL) samples were collected at necropsy and cytokine levels measured using the Multiplex (Il1β, Ifnγ, Tnfα, Il10, Il13, Il17, Il6) and ELISA (Tgfβ) assays. Results are presented as mean±SE for 5-8 mice.

On the x axis, Early/PS (Early/Pre-symptomatic) indicates early timepoints or when the animals are not showing signs of lung damage (*Tlr2,4 -/-*: 16 weeks; B6 WT: 16&20 weeks; *Il17-/-*: 16&20 weeks) and Late/S (Late/Symptomatic) indicates late timepoints or when the mice are in respiratory distress (*Tlr2,4 -/-*: 20 weeks; B6 WT: 26 weeks; *Il17-/-*: 26&35 weeks).

In summary, we found that, compared to wildtype B6 mice, decreased numbers of Th1 cells combined with high amounts of Il6 and Il17 promoted severe fibrosis in *Tlr2,4*-/- mice, whereas in the absence of Il17, a prominent Th1 lymphocytic response and minimal inflammatory cytokine production were associated with sparing from fibrosis.

Discussion

Our studies to characterise the phenotypes of pneumonitis and fibrosis in terms of inflammatory responses have shown an association of Th17 cells with the presence of radiation-induced pulmonary fibrosis in inbred mice. Moreover, the study of knockout mice revealed severe fibrosis to be induced through the activation of the Il6-Tgfβ-Il17 pathway, infiltration of PMN to the lung and downregulation of Th1 responses.

Radiation-induced pulmonary fibrosis was associated with both increased numbers of Th17 cells, and of their main effector population, PMN, in the lungs of mice. Indeed, of the six inbred strains, only fibrosis-prone but not pneumonitis-prone mice showed an increase in pulmonary Th17 cells upon the presentation of radiation-induced lung disease. This effect was not due to the onset of respiratory distress in pneumonitis-prone strains preceding that of fibrosis-prone strains as KK/HIJ mice had the earliest onset of distress, and increased Th17 cells while A/J mice survived to 25 weeks post irradiation with no increase in Th17 cells. Secondly, the investigation of genetically altered mice (*Tlr2,4*-/-) revealed Th17 cells to peak in number upon presentation of fibrosis and for fibrosis to be absent in *Il17*-/- mice, a model with undetectable levels of these lymphocytes. Thirdly, a limited cytokine survey revealed Il17, Il6 and Tgfβ to be the only cytokines produced by distressed *Tlr2,4*-/- mice in higher or equal amounts to those of B6 mice. As it has been reported that Il17 can induce Il6 production, which, through a positive feedback loop, together with Tgfβ, can promote Th17 differentiation [255-258], this pathway may have led to increased fibrosis in *Tlr2,4*-/- mice. Further, Il1b,

Il10, Il13, Tnfα and Ifnγ production was significantly lower in the lavage of distressed *Tlr2,4*-/- mice compared to their wildtype counterparts, reflecting an impaired inflammatory response in the absence of Tlr2,4 signaling, similar to the findings of Jiang et al. [77]. In addition to increased Il17, Il6 and Tgfβ, low amounts of Il10 might have contributed to the severe phenotype of *Tlr2,4*-/- mice since this cytokine inhibits the activation of Tgfβ [259] and limits the production of Th17 and Il17-secreting γδ T cells [56] in bleomycin models of fibrosis. Finally, distressed mice had fibrosis scores proportional to the percentage of infiltrating PMN, a known effect of Th17 signaling [260], established in other lung disease models [261-263]. Th17 cell recruitment of PMN has been shown to contribute to asthma [264], hypersensitivity pneumonitis [252] and bleomycin-induced pulmonary fibrosis where *Il17a*-/- mice developed less disease with fewer PMN [56]. The correlation of fibrosis with lavage neutrophil level is supported by our similar findings in populations of genetically mixed mice [35, 131], and is clinically relevant as increased lavage PMN are a known radiation pathology [40].

The lymphocyte profiles of inbred and genetically altered mice indicated that while Th17 cells dictated the development of fibrosis, Th1 cells influenced the onset and/or severity of the fibrosis. Specifically, in addition to a prominent Th17 response, distressed *Tlr2,4*-/- mice had lower numbers of CD4+Ifnγ+ cells, decreased Ifnγ amounts in lavage and succumbed with more severe fibrosis compared to wildtype mice. Similarly, KK mice had the earliest onset of distress, among the strains surveyed, and displayed no increase in Th1 cells after radiation. Thus lack of a Th1 response in the presence of a Th17 profile equated to severe or early onset disease as in the KK and *Tlr2,4*-/- mice whereas in the wildtype strain an increase in both cell types resulted in less severe and delayed disease. The fibrotic response of B6 mice post radiation is similar to that which develops after a bleomycin challenge, which also includes pulmonary increases in Th1,2&17 cells [56, 265] in this strain. Of further similarity, the T helper cell balance in the lung has been associated with extent of fibrosis in this related model of bleomycin-

induced fibrosis. Yoshizaki et al. [265] showed mice deficient in certain cell adhesion molecules (L-selectin and ICAM) to have reduced levels of bleomycin-induced pulmonary fibrosis, and this response to be associated with increased levels of Th1 cells in the lavage and decreased Th2 & Th17 levels. They showed, further, that deficiencies in P- or E-selectin or in PSGL-1 were associated with increased bleomycin-induced pulmonary fibrosis, associated with augmented Th2 and Th17 levels and decreased Th1. In a model of pulmonary fungal infection Rivera et al. [266] demonstrated that dectin-1-/- mice present a diminished Th17 response to fungal challenge which is accompanied by an increased Th1 response in the lavage. A direct interaction of lymphocyte populations may be occurring as O'Connor et al. [267] reported that *in vitro* Il17 treatment of naïve CD4+ T cells cultured in Th1 polarizing conditions has a suppressive effect on Tbet expression and Th1 development.

The Th1 response in B6 mice dampened the fibrotic response to radiation, but its increased presence in both inbred strains which developed pneumonitis, and *Il17*-/- mice, which were spared an overt lung injury, suggests Th1 cells spare the fibrosis response and may permit pneumonitis development. Mechanistically, increased levels of the Th1 cytokine Ifnγ, in conjunction with other cytokines such as Tnfα, are known to lead to the activation of M1 macrophages [268] which, unlike the fibrosis-promoting M2, might contribute to pneumonitis development through their pro-inflammatory profile [269-271]. As the response of *Il17*-/- mice included a prominent Th1 profile only, and minimal pneumonitis, the Th1 profile alone is not sufficient for the presence of pneumonitis. Indeed as discussed by Lo Re et al. [272] the functions of CD4+ lymphocytes differ depending on various factors, including the immune environment, suggesting that, despite high Th1 cell numbers, the minimal cytokine production in *Il17*-/- mice, in contrast to the high amounts of Il1β [273], and Tnfα [41] produced by pneumonitis-prone C3H mice may render the *Il17*-/- mice pneumonitis-resistant. Supporting these findings are data of Kirby et al. [274] who reported an association between increased *Ifng* gene

expression and reduced lung inflammation and fibrosis, and prolonged survival, in B6.*Ccr1*-/- mice following thoracic irradiation [275]. In addition, the increase in Th1 phenotype in the absence of Il17 is in agreement with the finding of Mi S et al. [63] that blocking Il17 signaling reduces the degree of bleomycin-induced fibrosis partially through augmentation of the Th1 environment and in a model of fibrosis, and further, in a model of graft versus host disease, the absence of Th17 translates to an enhanced Th1 response [276].

As we observed an increase in Il17-producing CD4- lymphocytes in mice prone to fibrosis, there are thus other sources of this cytokine apart from Th17 cells. Previous findings in hypersensitivity pneumonitis [58] experimental silicosis [277] and bleomycin-induced fibrosis [56, 278] suggest these CD4-Il17+ cells to be γδ T cells, a population of innate immune cells capable of rapidly producing Il17 upon stimulation. Other lymphocyte sources of both Ifnγ and Il17 include NKT [279-282] or CD8+ cells [68, 283, 284], therefore this aspect of the disease pathology remains to be elucidated. Despite the more severe phenotype of the *Tlr2,4*-/- strain, we did not observe a difference compared to B6 mice in terms of Il17-secreting CD4- lymphocytes, suggesting this population, similar to Th17, is associated with the presence rather than severity of fibrosis. In addition, radiation prompted an increase in Ifnγ-secreting CD4- lymphocytes in all mice, but at significantly higher levels in *Il17*-/- animals, confirming the opposing effects of Il17 and Ifnγ in lung fibrosis. We did not, however, observe a difference between wildtype and *Tlr2,4*-/- mice in terms of the CD4+Ifnγ- population, suggesting that lack of Th1 cells specifically contributes to more severe disease in the double knockouts.

Following the same stimulus (i.e. thoracic radiation), different mouse strains responded with distinct Th1/2/17 lymphocyte profiles, which ultimately dictated the presence or absence, and extent, of fibrosis. Treatment options for fibrosis are limited, therefore an improved mechanistic understanding of disease in a preclinical model could be the base for subsequent assessments in patients.

These studies revealed that lung tissue responds to the primary radiation injury through an altered Th cell profile which further defines pulmonary disease development. Specifically, we found the presence of Th17 cells to predict for fibrosis development whereas Th1 cells have a protective effect. We also identified the levels of Il17, Il6 and Tgfβ in the the bronchoalveolar lavage, a clinically accessible tissue, to be associated with severe lung disease. Our analysis points towards the Il17 pathway as a therapeutic target for radiation-induced pulmonary fibrosis, which could eventually permit pre-treatment identification of radiation-sensitive or resistant patients thus assisting in defining patient specific radiotherapy. The phenotypes of the six inbred strains studied are consistent with those of our prior study [250] and are representative of the clinical phenotype range suggesting that these disease markers would be relevant for further investigation in patients.

CHAPTER VI: GENERAL DISCUSSION

The ultimate goal of radiogenomics is to develop genetic profiles of at-risk patients in order to maximize tumor control while minimizing side effects in susceptible individuals. In this thesis we used the similarities between human and mouse responses to irradiation and studied the response of various strains of mice to thoracic irradiation to reveal the immune and genetic components of alveolitis and pulmonary fibrosis. We described for the first time the pulmonary phenotype after thoracic irradiation in *Il17*-/- and *Tlr2,4*-/- as well as 27 inbred strains of mice, 20 of which had not been previously reported. Gene expression profiling together with association analysis uncovered novel immune pathways and candidate genes for pulmonary fibrosis. These are paralleled in the lymphocyte study which revealed for the first time the involvement of Il17 in the lung response to radiation. Our approach was based on the advantages of mouse models compared to clinical research. Human studies of radiation response are encumbered by confounding factors related to the dose and irradiation site, additional chemotherapy, as well as patient-related variables such as age, smoking status and existing comorbidities. Given the similarities in radiation response between mouse and man, it is anticipated that murine studies will identify radiotoxicity-predisposing variants which could subsequently be evaluated for contribution to normal tissue reactions in clinical studies. Alternatively, any susceptibility genes identified in clinical studies can be assessed functionally in a mouse model of controlled environment and genetic background. Clinical radiogenomics has changed considerably in the last 20 years. Until mid-1990s the driving hypothesis was that the effects of radiation are solely due to cell death and inability of the tissue to compensate for cell loss. Based on this “target cell hypothesis” early efforts were concentrated on predicting late tissue response based on in vitro irradiation of fibroblasts or lymphocytes but despite promising initial results [285, 286], larger subsequent studies [287, 288] failed to confirm any correlation between cell sensitivity and tissue reactions to radiation. The lack of correlation occurs because the DNA damage and cell death *in vitro* cannot explain the remodeling, cytokine

cascades and collagen deposition which occurs at the tissue level [166, 289]. Thus the ability to study whole-organ pathology, integrating physiological and genetic parameters is another advantage of animal models.

Subsequently, clinical research focused on discovering variants in genes relevant to radiotoxicity. Using the hypothesis-driven candidate gene approach, the association between SNPs in *TGFβ1*, *XRCC1&3*, *ATM* and *SOD2* with tissue response were evaluated, yielding both positive and negative results (reviewed in [290]). Such studies however lack the ability to discover SNPs in new genes, previously unrelated to the disease.

This drawback, together with recent advances in high throughput technologies, has driven radiation research towards GWAS which offer the possibility to perform hypothesis-free surveys of SNP-phenotype associations. In 2010 three such studies were completed, in patients and lymphoblastoid cell lines [179, 291, 292] and although the results remain to be validated these findings offer a preview of the new directions in radiation biology. Studies underway regard radiotherapy side-effects as a polygenic phenotype and integrate gene association, gene expression and molecular data. The use of such high-throughput assays requires large sample sizes to ensure sufficient statistical power as well as standardized methods for reporting treatment and clinical outcome data. Therefore large databases and tissue banks are being established by international consortia like GENEPI (Genetic Pathways for the Prediction of the Effects of Radiation) from ESTRO (European Society for Radiotherapy and Oncology) [293], RAPPER (Radiogenomics: Assessment of Polymorphisms for Predicting the Effects of Radiotherapy) [294], RadGenomics [295, 296] Gene PARE [297] and the Radiogenomics Consortium [298].

Mouse studies represent an additional avenue in the community's efforts to detect underlying genes for radiotoxicity. Mice are more amenable to the study of a multitude of physiological and genetic parameters, thus in our experiments we adopted an approach focused on the mechanistic and functional immune

aspects as well as gene expression profiles and SNP association. Integrating these data pointed to the importance of Il17, Tlr and Cell adhesion molecule signaling in the development of fibrosis and identified previously unknown *Cadm1*, *Slamf6* and *Btnl1* genes as potential candidates.

Recently many groups focused on discovering radio-sensitizing genes at the transcriptome level, using microarrays [299-301] and found that changes in transcript levels correlate with susceptibility to radiation side-effects in humans. Similarly to clinical experiments we performed a gene expression study in three strains of mice with distinct phenotypes following thoracic irradiation. Both A/J and C3H strains succumb to alveolitis but do so at different times post treatment and this difference is reflected in the significantly altered pathways in each strain: a majority of inflammatory and immune pathways in C3H mice and pathways related to cell survival, proliferation and differentiation in the A/J strain.

It is unclear at this point which of the 40 cell types in the lung are affected by the proliferative genetic profiles in A/J mice. However, this strain has a high susceptibility to urethane-induced lung cancer whereas C3H and B6 mice have moderate and low susceptibilities respectively [302]. Also, the genetic profile of low inflammation in A/J is mirrored in the low numbers of Th cells populations (Figure 24) – A/J mice have the lowest numbers of Th1/2/17 cells of all six strains studied. Therefore it stands to reason that epithelial cells of A/J mice may have a higher proliferative capacity which confers susceptibility to cancer but also an increased ability to repopulate the tissue after radiation damage.

The gene expression pattern of C3H mice revealed an altered Tlr signaling pathway (Figure 8) which reflects the involvement of these receptors in radiation response. Indeed, the study of *Tlr2,4*-deficient mice showed that absence of this pathway worsens the response to radiation of B6 mice (Figure 18). Unlike in bleomycin-induced fibrosis [77] we did not observe the augmented disease to be caused by increased apoptosis of epithelial cells in knockout mice; instead in the absence of Tlr signaling decreased amounts of anti-fibrotic cytokines and higher

amounts of Il6-Tgfβ-Il17 contribute to more severe fibrosis (Figure 33). Indeed, the Il6 level in plasma is a biomarker for radiation alveolitis in patients [246]. Reports concerning Tgfβ have shown both the presence and absence of an association with fibrosis [249, 303] but these results might reflect the pleiotropic roles of this cytokine in both tissue homeostasis and late stage fibrosis [9]. Our results add to this complexity by showing that Tgfβ not only contributes to Th17 differentiation but that its production is dependent on the presence of Il17.

The gene expression profiles revealed Cell adhesion molecule (CAM) signaling as the most significantly altered pathway following irradiation in all three strains. This path includes several classes of CAMs acting on various cell types and having pro- or anti-fibrotic effects: co-stimulatory molecules and vascular CAMs which mediate leukocyte migration and activation [304-306], intracellular and vascular CAMs, cadherins, integrins, claudins and selectins which participate in controlling epithelial permeability and integrity, EMT and crosstalk with the Tgfβ pathway [192, 307-313].

Interestingly protective E- and detrimental L-selectins are over- and underexpressed respectively in A/J mice only. E-selectins protect against pulmonary fibrosis by recruiting Ifnγ-producing Th1 cells by binding to Psgl1 on their surface [265]. This agrees with the findings in Chapter V of increased numbers of CD4+Ifnγ+ in A/J mice after irradiation (Figure 24).

The GWAS in Chapter IV revealed a group of significantly associated SNPs and haplotypes within the previously determined QTL on chromosome 9. Located in an intergenic region, these are likely regulatory SNPs (*cis*- or *trans*- acting) which dictate transcript levels. Indeed, for any organism it is estimated that 10-50% of transcripts will vary due to heritable factors [314] and strong impact regulatory SNPs have a tendency to act in *cis* [315, 316]. Thus we speculate that the locus on chromosome 9 is a *cis*-eQTL influencing the expression of a nearby gene which itself contributes to the development of pulmonary fibrosis. The closest annotated gene in the locus is cell adhesion molecule *Cadm1* which is downregulated in all

three strains in our transcriptome analysis and is a member of the Cell adhesion molecule signaling pathway. Cadm1 is a tumor suppressor [317-323] and its inactivation promotes disruption of cell polarity and cell-cell adhesion [324], events which are required for metastasis but also for EMT and fibrogenesis. Moreover Cadm1 promotes Ifnγ production through its interaction with receptors on adaptive immune cells [324, 325], which downmodulates fibrogenesis as shown in Chapter V. These findings make *Cadm1* a good candidate for pulmonary fibrosis, but since radiosensitivity is a multi-genic trait, other candidates must exist.

In addition to the locus on chromosome 9, our GWAS revealed highly significant SNPs on chromosomes 5 and 6 located outside of the previously determined QTLs. One potential explanation for these results is genetic heterogeneity, with several candidate genes for radiosensitivity relevant to the majority of the 27 strains, but less so to B6 and C3H mice. The genetic heterogeneity is mirrored by the diverse T cell populations of the six strains analyzed in Chapter V. Our results indicate that development of alveolitis or fibrosis is dictated by a delicate balance of cytokines. Il17 shows the best association with fibrosis, but the severity and time to onset of fibrosis is dampened or potentiated by the presence of Ifnγ or Il13 respectively. Thus diverse genetic backgrounds translate to variations in cytokine levels which further drive the fibrotic response.

The results in Chapter V prove that Il17 is a key cytokine to the development of fibrosis. Members of the Il17 pathway should therefore be prioritized in the search for candidate genes. Interestingly the GWAS in Chapter 4 revealed epistatic interactions between SNPs in different QTLs (Figure 16). One such interaction is between polymorphisms in *Slamf6* and *Btnl1*. They are both co-stimulatory molecules but while Btnl1 inhibits T cell proliferation [199] and reduces Il6 production [326], Slamf6 promotes Th17 differentiation [327, 328], an important component of the radiation response in mice. It is possible that these

two molecules cooperate in modulating T cell proliferation and differentiation leading to fibrosis development.

Using a multi-angle approach we discovered several variants associated with radiation-induced fibrosis and provided evidence for the role of Il17 and Tlr2&4 in the development and severity of the disease. Our findings reflect the complexity of the phenotype and generate many additional questions which would have to be answered in the future. Other studies are needed to confirm the altered expression of *Cadm1*, *Slamf6* and *Btnl1* in the mouse panel and their putative role in fibrogenesis. The post-radiation phenotype and cytokine profile of mice lacking or overexpressing these genes would indicate whether these proteins are involved in the Il17/Ifnγ pathways. Since our results indicate opposing roles of Th1 and Th17 cytokines in the lung reaction to radiation, the analysis of *Ifnγ*-deficient mice would confirm the protective role of this cytokine. In the same line of reasoning Il17 blockade in mice following irradiation and monitoring the eventual disease reversal may offer a promising therapeutic strategy in preventing radiation-induced fibrosis. Moreover, studying the response to radiation of *Ifnγ*-/-*Il17*-/- double knockout mice would refine our knowledge of the crosstalk between these opposing cytokines.

Studies in both mice [279, 329] and humans [330, 331] have shown the potential therapeutic effects of Ifnγ, and since the severe phenotype of *Tlr2,4*-/- mice is due in part to the absence of this cytokine, determining whether Ifnγ administration in these animals reverses or prevents fibrosis would add to our understanding of the disease.

Advances in molecular pathology but also the advent of new high throughput technologies have improved the understanding of radiotherapy side-effects in normal tissues. It is now clear that late effects are due to an abnormal wound healing-like response, rather than solely parenchymal cell loss. Both genetic and functional approaches are needed to shed light on the complexity of radiation-induced changes at the tissue level. Mechanistic understanding of

pulmonary fibrosis in an animal model could be the first step in developing new therapeutics. New treatment modalities for this disease would limit the radiotherapy-associated morbidity and would contribute to fine-tuned, personalized cancer treatments.

REFERENCES

1. Abou-Jawde, R.M., et al., Impact of induction concurrent chemoradiotherapy on pulmonary function and postoperative acute respiratory complications in esophageal cancer. Chest, 2005. 128(1): p. 250-5.

2. Maranzano, E., et al., Long-term results of induction chemotherapy followed by concurrent chemotherapy and thoracic irradiation in limited small cell lung cancer. Lung Cancer, 2002. 37(1): p. 79-85.

3. Yu, T.K., et al., Clinically relevant pneumonitis after sequential paclitaxel-based chemotherapy and radiotherapy in breast cancer patients. J Natl Cancer Inst, 2004. 96(22): p. 1676-81.

4. Loyer, E., et al., Radiographic appearance of the chest following therapy for Hodgkin disease. Eur J Radiol, 2000. 35(2): p. 136-48.

5. Hassink, E.A., et al., Pulmonary morbidity 10-18 years after irradiation for Hodgkin's disease. Eur J Cancer, 1993. 29A(3): p. 343-7.

6. Canadian Centre for Occupational Health and Safety. Quantities and Units of Ionizing Radiation. 2007 [cited 2013 May 7].

7. Thompson, L.H. and H.D. Suit, Proliferation kinetics of x-irradiated mouse L cells studied WITH TIME-lapse photography. II. Int J Radiat Biol Relat Stud Phys Chem Med, 1969. 15(4): p. 347-62.

8. Dewey, W.C., S.C. Furman, and H.H. Miller, Comparison of lethality and chromosomal damage induced by x-rays in synchronized Chinese hamster cells in vitro. Radiat Res, 1970. 43(3): p. 561-81.

9. Martin, M., J. Lefaix, and S. Delanian, TGF-beta1 and radiation fibrosis: a master switch and a specific therapeutic target? Int J Radiat Oncol Biol Phys, 2000. 47(2): p. 277-90.

10. Abid, S.H., V. Malhotra, and M.C. Perry, Radiation-induced and chemotherapy-induced pulmonary injury. Curr Opin Oncol, 2001. 13(4): p. 242-8.

11. Abratt, R.P., et al., Pulmonary complications of radiation therapy. Clin Chest Med, 2004. 25(1): p. 167-77.

12. Marks, L.B., et al., Radiation-induced lung injury. Semin Radiat Oncol, 2003. 13(3): p. 333-45.

13. Reckzeh, B., et al., Severe lymphocytopenia and interstitial pneumonia in patients treated with paclitaxel and simultaneous radiotherapy for non-small-cell lung cancer. J Clin Oncol, 1996. 14(4): p. 1071-6.

14. Kong, F.M., et al., Non-small cell lung cancer therapy-related pulmonary toxicity: an update on radiation pneumonitis and fibrosis. Semin Oncol, 2005. 32(2 Suppl 3): p. S42-54.

15. Anscher, M.S. and Z. Vujaskovic, Mechanisms and potential targets for prevention and treatment of normal tissue injury after radiation therapy. Semin Oncol, 2005. 32(2 Suppl 3): p. S86-91.

16. Kong, F.M., et al., High-dose radiation improved local tumor control and overall survival in patients with inoperable/unresectable non-small-cell lung cancer: long-term results of a radiation dose escalation study. Int J Radiat Oncol Biol Phys, 2005. 63(2): p. 324-33.

17. Tsoutsou, P.G. and M.I. Koukourakis, Radiation pneumonitis and fibrosis: mechanisms underlying its pathogenesis and implications for future research. Int J Radiat Oncol Biol Phys, 2006. 66(5): p. 1281-93.

18. Kosaka, Y., et al., Avascular necrosis of bilateral femoral head as a result of long-term steroid administration for radiation pneumonitis after tangential irradiation of the breast. Int J Clin Oncol, 2006. 11(6): p. 482-6.

19. Morgan, G.W. and S.N. Breit, Radiation and the lung: a reevaluation of the mechanisms mediating pulmonary injury. Int J Radiat Oncol Biol Phys, 1995. 31(2): p. 361-9.

20. Johnston, C.J., et al., Inflammatory cell recruitment following thoracic irradiation. Exp Lung Res, 2004. 30(5): p. 369-82.

21. McDonald, S., et al., Injury to the lung from cancer therapy: clinical syndromes, measurable endpoints, and potential scoring systems. Int J Radiat Oncol Biol Phys, 1995. 31(5): p. 1187-203.

22. Nesbitt, L.T., Jr., Minimizing complications from systemic glucocorticosteroid use. Dermatol Clin, 1995. 13(4): p. 925-39.

23. Korfei, M., et al., Epithelial endoplasmic reticulum stress and apoptosis in sporadic idiopathic pulmonary fibrosis. Am J Respir Crit Care Med, 2008. 178(8): p. 838-46.

24. Morishima, Y., et al., Triggering the induction of myofibroblast and fibrogenesis by airway epithelial shedding. Am J Respir Cell Mol Biol, 2001. 24(1): p. 1-11.

25. Sisson, T.H., et al., Targeted injury of type II alveolar epithelial cells induces pulmonary fibrosis. Am J Respir Crit Care Med, 2010. 181(3): p. 254-63.

26. Selman, M. and A. Pardo, Role of epithelial cells in idiopathic pulmonary fibrosis: from innocent targets to serial killers. Proc Am Thorac Soc, 2006. 3(4): p. 364-72.

27. Desmouliere, A., I.A. Darby, and G. Gabbiani, Normal and pathologic soft tissue remodeling: role of the myofibroblast, with special emphasis on liver and kidney fibrosis. Lab Invest, 2003. 83(12): p. 1689-707.

28. Duffield, J.S., et al., Selective depletion of macrophages reveals distinct, opposing roles during liver injury and repair. J Clin Invest, 2005. 115(1): p. 56-65.

29. Gibbons, M.A., et al., Ly6Chi monocytes direct alternatively activated profibrotic macrophage regulation of lung fibrosis. Am J Respir Crit Care Med, 2011. 184(5): p. 569-81.

30. Borregaard, N., et al., Human neutrophil granules and secretory vesicles. Eur J Haematol, 1993. 51(4): p. 187-98.

31. Thrall, R.S., et al., The development of bleomycin-induced pulmonary fibrosis in neutrophil-depleted and complement-depleted rats. Am J Pathol, 1981. 105(1): p. 76-81.

32. Thrall, R.S., et al., Differential cellular analysis of bronchoalveolar lavage fluid obtained at various stages during the development of bleomycin-induced pulmonary fibrosis in the rat. Am Rev Respir Dis, 1982. 126(3): p. 488-92.

33. Haslett, C., et al., 111Indium-labeled neutrophil migration into the lungs of bleomycin-treated rabbits assessed noninvasively by external scintigraphy. Am Rev Respir Dis, 1989. 140(3): p. 756-63.

34. Bowden, D.H. and I.Y. Adamson, The role of cell injury and the continuing inflammatory response in the generation of silicotic pulmonary fibrosis. J Pathol, 1984. 144(3): p. 149-61.

35. Haston, C.K., et al., Distinct loci influence radiation-induced alveolitis from fibrosing alveolitis in the mouse. Cancer Res, 2007. 67(22): p. 10796-803.

36. Roberts, C.M., et al., Radiation pneumonitis: a possible lymphocyte-mediated hypersensitivity reaction. Ann Intern Med, 1993. 118(9): p. 696-700.

37. Martin, C., et al., Bilateral lymphocytic alveolitis: a common reaction after unilateral thoracic irradiation. Eur Respir J, 1999. 13(4): p. 727-32.

38. McBride, W.H. and V. Vegesna, The role of T-cells in radiation pneumonitis after bone marrow transplantation. Int J Radiat Biol, 2000. 76(4): p. 517-21.

39. Miwa, S., et al., The incidence and clinical characteristics of bronchiolitis obliterans organizing pneumonia syndrome after radiation therapy for breast cancer. Sarcoidosis Vasc Diffuse Lung Dis, 2004. 21(3): p. 212-8.

40. Majori, M., et al., Bronchoalveolar lavage in bronchiolitis obliterans organizing pneumonia primed by radiation therapy to the breast. J Allergy Clin Immunol, 2000. 105(2 Pt 1): p. 239-44.

41. Chiang, C.S., et al., Compartmental responses after thoracic irradiation of mice: strain differences. Int J Radiat Oncol Biol Phys, 2005. 62(3): p. 862-71.

42. Williams, J.P., et al., Effect of administration of lovastatin on the development of late pulmonary effects after whole-lung irradiation in a murine model. Radiat Res, 2004. 161(5): p. 560-7.

43. Hong, J.H., et al., Bronchoalveolar lavage and interstitial cells have different roles in radiation-induced lung injury. Int J Radiat Biol, 2003. 79(3): p. 159-67.

44. Westermann, W., et al., Th2 cells as effectors in postirradiation pulmonary damage preceding fibrosis in the rat. Int J Radiat Biol, 1999. 75(5): p. 629-38.

45. Postlethwaite, A.E. and J.M. Seyer, Fibroblast chemotaxis induction by human recombinant interleukin-4. Identification by synthetic peptide analysis of two chemotactic domains residing in amino acid sequences 70-88 and 89-122. J Clin Invest, 1991. 87(6): p. 2147-52.

46. Jakubzick, C., et al., Impact of interleukin-13 responsiveness on the synthetic and proliferative properties of Th1- and Th2-type pulmonary granuloma fibroblasts. Am J Pathol, 2003. 162(5): p. 1475-86.

47. Postlethwaite, A.E., et al., Human fibroblasts synthesize elevated levels of extracellular matrix proteins in response to interleukin 4. J Clin Invest, 1992. 90(4): p. 1479-85.

48. Makhluf, H.A., et al., IL-4 upregulates tenascin synthesis in scleroderma and healthy skin fibroblasts. J Invest Dermatol, 1996. 107(6): p. 856-9.

49. Lee, C.G., et al., Interleukin-13 induces tissue fibrosis by selectively stimulating and activating transforming growth factor beta(1). J Exp Med, 2001. 194(6): p. 809-21.

50. Han, G., et al., Th2-like immune response in radiation-induced lung fibrosis. Oncol Rep, 2011. 26(2): p. 383-8.

51. Abbas, A.K., K.M. Murphy, and A. Sher, Functional diversity of helper T lymphocytes. Nature, 1996. 383(6603): p. 787-93.

52. Narayanan, A.S., et al., Effect of gamma-interferon on collagen synthesis by normal and fibrotic human lung fibroblasts. Chest, 1992. 101(5): p. 1326-31.

53. Eickelberg, O., et al., Molecular mechanisms of TGF-(beta) antagonism by interferon (gamma) and cyclosporine A in lung fibroblasts. FASEB J, 2001. 15(3): p. 797-806.

54. Raghu, G., et al., A placebo-controlled trial of interferon gamma-1b in patients with idiopathic pulmonary fibrosis. N Engl J Med, 2004. 350(2): p. 125-33.

55. King, T.E., Jr., et al., Effect of interferon gamma-1b on survival in patients with idiopathic pulmonary fibrosis (INSPIRE): a multicentre, randomised, placebo-controlled trial. Lancet, 2009. 374(9685): p. 222-8.

56. Wilson, M.S., et al., Bleomycin and IL-1beta-mediated pulmonary fibrosis is IL-17A dependent. J Exp Med, 2010. 207(3): p. 535-52.

57. Gasse, P., et al., IL-1 and IL-23 mediate early IL-17A production in pulmonary inflammation leading to late fibrosis. PLoS One, 2011. 6(8): p. e23185.

58. Simonian, P.L., et al., Gammadelta T cells and Th17 cytokines in hypersensitivity pneumonitis and lung fibrosis. Transl Res, 2009. 154(5): p. 222-7.

59. Zhao, J.Q., et al., The role of interleukin-17 in murine cytomegalovirus interstitial pneumonia in mice with skin transplants. Transpl Int, 2011. 24(8): p. 845-55.

60. Liu, Y., et al., IL-17 contributes to cardiac fibrosis following experimental autoimmune myocarditis by a PKCbeta/Erk1/2/NF-kappaB-dependent signaling pathway. Int Immunol, 2012. 24(10): p. 605-12.

61. Ouyang, W., J.K. Kolls, and Y. Zheng, The biological functions of T helper 17 cell effector cytokines in inflammation. Immunity, 2008. 28(4): p. 454-67.

62. Kinder, B.W., et al., Baseline BAL neutrophilia predicts early mortality in idiopathic pulmonary fibrosis. Chest, 2008. 133(1): p. 226-32.

63. Mi, S., et al., Blocking IL-17A promotes the resolution of pulmonary inflammation and fibrosis via TGF-beta1-dependent and -independent mechanisms. J Immunol, 2011. 187(6): p. 3003-14.

64. Michel, M.L., et al., Identification of an IL-17-producing NK1.1(neg) iNKT cell population involved in airway neutrophilia. J Exp Med, 2007. 204(5): p. 995-1001.

65. Cua, D.J. and C.M. Tato, Innate IL-17-producing cells: the sentinels of the immune system. Nat Rev Immunol, 2010. 10(7): p. 479-89.

66. O'Brien, R.L., C.L. Roark, and W.K. Born, IL-17-producing gammadelta T cells. Eur J Immunol, 2009. 39(3): p. 662-6.

67. Huber, M., et al., IL-17A secretion by CD8+ T cells supports Th17-mediated autoimmune encephalomyelitis. J Clin Invest, 2013. 123(1): p. 247-60.

68. He, D., et al., CD8+ IL-17-producing T cells are important in effector functions for the elicitation of contact hypersensitivity responses. J Immunol, 2006. 177(10): p. 6852-8.

69. Saxena, A., et al., Tc17 CD8+ T cells potentiate Th1-mediated autoimmune diabetes in a mouse model. J Immunol, 2012. 189(6): p. 3140-9.

70. Vabulas, R.M., et al., HSP70 as endogenous stimulus of the Toll/interleukin-1 receptor signal pathway. J Biol Chem, 2002. 277(17): p. 15107-12.

71. Ohashi, K., et al., Cutting edge: heat shock protein 60 is a putative endogenous ligand of the toll-like receptor-4 complex. J Immunol, 2000. 164(2): p. 558-61.

72. Scaffidi, P., T. Misteli, and M.E. Bianchi, Release of chromatin protein HMGB1 by necrotic cells triggers inflammation. Nature, 2002. 418(6894): p. 191-5.

73. Urbonaviciute, V., et al., Induction of inflammatory and immune responses by HMGB1-nucleosome complexes: implications for the pathogenesis of SLE. J Exp Med, 2008. 205(13): p. 3007-18.

74. Park, J.S., et al., Involvement of toll-like receptors 2 and 4 in cellular activation by high mobility group box 1 protein. J Biol Chem, 2004. 279(9): p. 7370-7.

75. Okamura, Y., et al., The extra domain A of fibronectin activates Toll-like receptor 4. J Biol Chem, 2001. 276(13): p. 10229-33.

76. Johnson, G.B., et al., Receptor-mediated monitoring of tissue well-being via detection of soluble heparan sulfate by Toll-like receptor 4. J Immunol, 2002. 168(10): p. 5233-9.

77. Jiang, D., et al., Regulation of lung injury and repair by Toll-like receptors and hyaluronan. Nat Med, 2005. 11(11): p. 1173-9.

78. Inoue, K., et al., The role of toll-like receptor 4 in airway inflammation induced by diesel exhaust particles. Arch Toxicol, 2006. 80(5): p. 275-9.

79. Kleeberger, S.R., et al., Genetic susceptibility to ozone-induced lung hyperpermeability: role of toll-like receptor 4. Am J Respir Cell Mol Biol, 2000. 22(5): p. 620-7.

80. Barsness, K.A., et al., Hemorrhage-induced acute lung injury is TLR-4 dependent. Am J Physiol Regul Integr Comp Physiol, 2004. 287(3): p. R592-9.

81. Sarir, H., et al., Cigarette smoke regulates the expression of TLR4 and IL-8 production by human macrophages. J Inflamm (Lond), 2009. 6: p. 12.

82. Mortaz, E., et al., Cigarette smoke induces the release of CXCL-8 from human bronchial epithelial cells via TLRs and induction of the inflammasome. Biochim Biophys Acta, 2011. 1812(9): p. 1104-10.

83. Nadigel, J., et al., Cigarette smoke increases TLR4 and TLR9 expression and induces cytokine production from CD8(+) T cells in chronic obstructive pulmonary disease. Respir Res, 2011. 12: p. 149.

84. Fan, J., et al., Hemorrhagic shock-activated neutrophils augment TLR4 signaling-induced TLR2 upregulation in alveolar macrophages: role in hemorrhage-primed lung inflammation. Am J Physiol Lung Cell Mol Physiol, 2006. 290(4): p. L738-L746.

85. Liu, C., et al., TLR4 knockout protects mice from radiation-induced thymic lymphoma by downregulation of IL6 and miR-21. Leukemia, 2011. 25(9): p. 1516-9.

86. Shan, Y.X., et al., Ionizing radiation stimulates secretion of pro-inflammatory cytokines: dose-response relationship, mechanisms and implications. Radiat Environ Biophys, 2007. 46(1): p. 21-9.

87. Brickey, W.J., et al., MyD88 provides a protective role in long-term radiation-induced lung injury. Int J Radiat Biol, 2012. 88(4): p. 335-47.

88. Wiebe E, Rodrigues G., Radiation-induced lung injury: Strategies for reducing damage while optimizing therapeutic dosage. Oncology Exchange, 2006. Vol. 5 No. 2

89. Loyd, J.E., Pulmonary fibrosis in families. Am J Respir Cell Mol Biol, 2003. 29(3 Suppl): p. S47-50.

90. Garcia-Sancho, C., et al., Familial pulmonary fibrosis is the strongest risk factor for idiopathic pulmonary fibrosis. Respir Med, 2011. 105(12): p. 1902-7.

91. Girard, P.M., et al., Radiosensitivity in Nijmegen Breakage Syndrome cells is attributable to a repair defect and not cell cycle checkpoint defects. Cancer Res, 2000. 60(17): p. 4881-8.

92. Paterson, M.C., et al., Enhanced radiosensitivity of cultured fibroblasts from ataxia telangiectasia heterozygotes manifested by defective colony-forming ability and reduced DNA repair replication after hypoxic gamma-irradiation. Cancer Res, 1979. 39(9): p. 3725-34.

93. Painter, R.B. and B.R. Young, Radiosensitivity in ataxia-telangiectasia: a new explanation. Proc Natl Acad Sci U S A, 1980. 77(12): p. 7315-7.

94. Nuyten, D.S. and M.J. van de Vijver, Using microarray analysis as a prognostic and predictive tool in oncology: focus on breast cancer and normal tissue toxicity. Semin Radiat Oncol, 2008. 18(2): p. 105-14.

95. Li, C., et al., TGF-beta1 levels in pre-treatment plasma identify breast cancer patients at risk of developing post-radiotherapy fibrosis. Int J Cancer, 1999. 84(2): p. 155-9.

96. Quarmby, S., et al., Differential expression of cytokine genes in fibroblasts derived from skin biopsies of patients who developed minimal or severe normal tissue damage after radiotherapy. Radiat Res, 2002. 157(3): p. 243-8.

97. Svensson, J.P., et al., Analysis of gene expression using gene sets discriminates cancer patients with and without late radiation toxicity. PLoS Med, 2006. 3(10): p. e422.

98. Kuptsova, N., et al., Genetic predictors of long-term toxicities after radiation therapy for breast cancer. Int J Cancer, 2008. 122(6): p. 1333-9.

99. Mak, R.H., et al., A single-nucleotide polymorphism in the methylene tetrahydrofolate reductase (MTHFR) gene is associated with risk of radiation pneumonitis in lung cancer patients treated with thoracic radiation therapy. Cancer, 2012. 118(14): p. 3654-65.

100. Zhang, L., et al., ATM polymorphisms are associated with risk of radiation-induced pneumonitis. Int J Radiat Oncol Biol Phys, 2010. 77(5): p. 1360-8.

101. Andreassen, C.N., et al., Prediction of normal tissue radiosensitivity from polymorphisms in candidate genes. Radiother Oncol, 2003. 69(2): p. 127-35.

102. O'Brien, T.J., S. Letuve, and C.K. Haston, Radiation-induced strain differences in mouse alveolar inflammatory cell apoptosis. Can J Physiol Pharmacol, 2005. 83(1): p. 117-22.

103. Sharplin, J. and A.J. Franko, A quantitative histological study of strain-dependent differences in the effects of irradiation on mouse lung during the early phase. Radiat Res, 1989. 119(1): p. 1-14.

104. Sharplin, J. and A.J. Franko, A quantitative histological study of strain-dependent differences in the effects of irradiation on mouse lung during the intermediate and late phases. Radiat Res, 1989. 119(1): p. 15-31.

105. Haston, C.K., et al., Universal and radiation-specific loci influence murine susceptibility to radiation-induced pulmonary fibrosis. Cancer Res, 2002. 62(13): p. 3782-8.

106. Manenti, G., et al., Mouse genome-wide association mapping needs linkage analysis to avoid false-positive Loci. PLoS Genet, 2009. 5(1): p. e1000331.

107. Liu, P., et al., Candidate lung tumor susceptibility genes identified through whole-genome association analyses in inbred mice. Nat Genet, 2006. 38(8): p. 888-95.

108. Szatkiewicz, J.P., et al., An imputed genotype resource for the laboratory mouse. Mamm Genome, 2008. 19(3): p. 199-208.

109. Kang, H.M., et al., Efficient control of population structure in model organism association mapping. Genetics, 2008. 178(3): p. 1709-23.

110. Ramirez-Aquino, R., et al., Identification of loci controlling restriction of parasite growth in experimental Taenia crassiceps cysticercosis. PLoS Negl Trop Dis, 2011. 5(12): p. e1435.

111. Radovanovic, I., A. Mullick, and P. Gros, Genetic control of susceptibility to infection with Candida albicans in mice. PLoS One, 2011. 6(4): p. e18957.

112. Farber, C.R., et al., Mouse genome-wide association and systems genetics identify Asxl2 as a regulator of bone mineral density and osteoclastogenesis. PLoS Genet, 2011. 7(4): p. e1002038.

113. Benton, C.S., et al., Evaluating genetic markers and neurobiochemical analytes for fluoxetine response using a panel of mouse inbred strains. Psychopharmacology (Berl), 2012. 221(2): p. 297-315.

114. Berndt, A., et al., Identification of fat4 and tsc22d1 as novel candidate genes for spontaneous pulmonary adenomas. Cancer Res, 2011. 71(17): p. 5779-91.

115. Bopp, S.E., et al., Genome wide analysis of inbred mouse lines identifies a locus containing Ppar-gamma as contributing to enhanced malaria survival. PLoS One, 2010. 5(5): p. e10903.

116. Cervino, A.C., et al., Integrating QTL and high-density SNP analyses in mice to identify Insig2 as a susceptibility gene for plasma cholesterol levels. Genomics, 2005. 86(5): p. 505-17.

117. Hillebrandt, S., et al., Complement factor 5 is a quantitative trait gene that modifies liver fibrogenesis in mice and humans. Nat Genet, 2005. 37(8): p. 835-43.

118. Rangnekar, A.S., et al., Quantitative trait loci analysis of mice administered the methionine-choline deficient dietary model of experimental steatohepatitis. Liver Int, 2006. 26(8): p. 1000-5.

119. Draghici, S., et al., A systems biology approach for pathway level analysis. Genome Res, 2007. 17(10): p. 1537-45.

120. Tanner, M.J., et al., Effects of androgen receptor and androgen on gene expression in prostate stromal fibroblasts and paracrine signaling to prostate cancer cells. PLoS One, 2011. 6(1): p. e16027.

121. Turner, D.P., et al., Global gene expression analysis identifies PDEF transcriptional networks regulating cell migration during cancer progression. Mol Biol Cell, 2008. 19(9): p. 3745-57.

122. Eftang, L.L., et al., Interleukin-8 is the single most up-regulated gene in whole genome profiling of H. pylori exposed gastric epithelial cells. BMC Microbiol, 2012. 12: p. 9.

123. Wang, W., et al., Identification of deregulated miRNAs and their targets in hepatitis B virus-associated hepatocellular carcinoma. World J Gastroenterol, 2012. 18(38): p. 5442-53.

124. Carver, J.R., et al., American Society of Clinical Oncology clinical evidence review on the ongoing care of adult cancer survivors: cardiac and pulmonary late effects. J Clin Oncol, 2007. 25(25): p. 3991-4008.

125. Burkhardt, A., Alveolitis and collapse in the pathogenesis of pulmonary fibrosis. Am Rev Respir Dis, 1989. 140(2): p. 513-24.

126. Mehta, V., Radiation pneumonitis and pulmonary fibrosis in non-small-cell lung cancer: pulmonary function, prediction, and prevention. Int J Radiat Oncol Biol Phys, 2005. 63(1): p. 5-24.

127. Lee, H.J., et al., Differential gene signatures in rat mammary tumors induced by DMBA and those induced by fractionated gamma radiation. Radiat Res, 2008. 170(5): p. 579-90.

128. Kalm, M., et al., Transient inflammation in neurogenic regions after irradiation of the developing brain. Radiat Res, 2009. 171(1): p. 66-76.

129. Yang, I.V., et al., Gene expression profiling of familial and sporadic interstitial pneumonia. Am J Respir Crit Care Med, 2007. 175(1): p. 45-54.

130. Johnston, C.J., et al., Alterations in the expression of chemokine mRNA levels in fibrosis-resistant and -sensitive mice after thoracic irradiation. Exp Lung Res, 1998. 24(3): p. 321-37.

131. Lemay, A.M. and C.K. Haston, Radiation-induced lung response of AcB/BcA recombinant congenic mice. Radiat Res, 2008. 170(3): p. 299-306.

132. Johnston, C.J., et al., Radiation-induced pulmonary fibrosis: examination of chemokine and chemokine receptor families. Radiat Res, 2002. 157(3): p. 256-65.

133. Hong, J.H., et al., Rapid induction of cytokine gene expression in the lung after single and fractionated doses of radiation. Int J Radiat Biol, 1999. 75(11): p. 1421-7.

134. Iwakawa, M., et al., Strain dependent differences in a histological study of CD44 and collagen fibers with an expression analysis of inflammatory response-related genes in irradiated murine lung. J Radiat Res, 2004. 45(3): p. 423-33.

135. Lemay, A.M. and C.K. Haston, Bleomycin-induced pulmonary fibrosis susceptibility genes in AcB/BcA recombinant congenic mice. Physiol Genomics, 2005. 23(1): p. 54-61.

136. Haston, C.K., et al., Murine candidate bleomycin induced pulmonary fibrosis susceptibility genes identified by gene expression and sequence analysis of linkage regions. J Med Genet, 2005. 42(6): p. 464-73.

137. Canale-Zambrano, J.C., et al., Intestinal phenotype of variable-weight cystic fibrosis knockout mice. Am J Physiol Gastrointest Liver Physiol, 2007. 293(1): p. G222-9.

138. Gentleman, R.C., et al., Bioconductor: open software development for computational biology and bioinformatics. Genome Biol, 2004. 5(10): p. R80.

139. Irizarry, R.A., et al., Summaries of Affymetrix GeneChip probe level data. Nucleic Acids Res, 2003. 31(4): p. e15.

140. Sun, H., et al., GOFFA: gene ontology for functional analysis--a FDA gene ontology tool for analysis of genomic and proteomic data. BMC Bioinformatics, 2006. 7 Suppl 2: p. S23.

141. Kim, C.C., et al., Experimental malaria infection triggers early expansion of natural killer cells. Infect Immun, 2008. 76(12): p. 5873-82.

142. Kim, M.J., et al., Villitis of unknown etiology is associated with a distinct pattern of chemokine up-regulation in the feto-maternal and placental compartments: implications for conjoint maternal allograft rejection and maternal anti-fetal graft-versus-host disease. J Immunol, 2009. 182(6): p. 3919-27.

143. Hicks, J.T., et al., Analysis of complement-dependent antibody-mediated lysis of target cells acutely infected with measles. J Immunol, 1976. 117(1): p. 208-15.

144. Addis-Lieser, E., J. Kohl, and M.G. Chiaramonte, Opposing regulatory roles of complement factor 5 in the development of bleomycin-induced pulmonary fibrosis. J Immunol, 2005. 175(3): p. 1894-902.

145. Komura, K., et al., CD19 regulates the development of bleomycin-induced pulmonary fibrosis in a mouse model. Arthritis Rheum, 2008. 58(11): p. 3574-84.

146. Hsu, E. and C.A. Feghali-Bostwick, Insulin-like growth factor-II is increased in systemic sclerosis-associated pulmonary fibrosis and contributes to the fibrotic process via Jun N-terminal kinase- and phosphatidylinositol-3 kinase-dependent pathways. Am J Pathol, 2008. 172(6): p. 1580-90.

147. Xia, H., et al., Pathological integrin signaling enhances proliferation of primary lung fibroblasts from patients with idiopathic pulmonary fibrosis. J Exp Med, 2008. 205(7): p. 1659-72.

148. Strieter, R.M., What differentiates normal lung repair and fibrosis? Inflammation, resolution of repair, and fibrosis. Proc Am Thorac Soc, 2008. 5(3): p. 305-10.

149. Sun, X., et al., Cytokine and chemokine transcription profile during Mycoplasma pulmonis infection in susceptible and resistant strains of mice: macrophage inflammatory protein 1beta (CCL4) and monocyte chemoattractant protein 2 (CCL8) and accumulation of CCR5+ Th cells. Infect Immun, 2006. 74(10): p. 5943-54.

150. Starnes, T., et al., The chemokine CXCL14 (BRAK) stimulates activated NK cell migration: implications for the downregulation of CXCL14 in malignancy. Exp Hematol, 2006. 34(8): p. 1101-5.

151. Arpin, D., et al., Early variations of circulating interleukin-6 and interleukin-10 levels during thoracic radiotherapy are predictive for radiation pneumonitis. J Clin Oncol, 2005. 23(34): p. 8748-56.

152. Hartsell, W.F., et al., Can serum markers be used to predict acute and late toxicity in patients with lung cancer? Analysis of RTOG 91-03. Am J Clin Oncol, 2007. 30(4): p. 368-76.

153. Barthelemy-Brichant, N., et al., Increased IL-6 and TGF-beta1 concentrations in bronchoalveolar lavage fluid associated with thoracic radiotherapy. Int J Radiat Oncol Biol Phys, 2004. 58(3): p. 758-67.

154. Bauer, A.K., et al., Toll-like receptor 4 in butylated hydroxytoluene-induced mouse pulmonary inflammation and tumorigenesis. J Natl Cancer Inst, 2005. 97(23): p. 1778-81.

155. Adcock, I.M., et al., Kinase inhibitors and airway inflammation. Eur J Pharmacol, 2006. 533(1-3): p. 118-32.

156. Staal, F.J., T.C. Luis, and M.M. Tiemessen, WNT signalling in the immune system: WNT is spreading its wings. Nat Rev Immunol, 2008. 8(8): p. 581-93.

157. Bonner, A.E., W.J. Lemon, and M. You, Gene expression signatures identify novel regulatory pathways during murine lung development: implications for lung tumorigenesis. J Med Genet, 2003. 40(6): p. 408-17.

158. Lee, P.D., et al., Mapping cis-acting regulatory variation in recombinant congenic strains. Physiol Genomics, 2006. 25(2): p. 294-302.

159. Lemon, W.J., et al., Identification of candidate lung cancer susceptibility genes in mouse using oligonucleotide arrays. J Med Genet, 2002. 39(9): p. 644-55.

160. Kruse, J.J. and F.A. Stewart, Gene expression arrays as a tool to unravel mechanisms of normal tissue radiation injury and prediction of response. World J Gastroenterol, 2007. 13(19): p. 2669-74.

161. Kaminski, N. and I.O. Rosas, Gene expression profiling as a window into idiopathic pulmonary fibrosis pathogenesis: can we identify the right target genes? Proc Am Thorac Soc, 2006. 3(4): p. 339-44.

162. Marquis, J.F., et al., Genetic and functional characterization of the mouse Trl3 locus in defense against tuberculosis. J Immunol, 2009. 182(6): p. 3757-67.

163. Puthawala, K., et al., Inhibition of integrin alpha(v)beta6, an activator of latent transforming growth factor-beta, prevents radiation-induced lung fibrosis. Am J Respir Crit Care Med, 2008. 177(1): p. 82-90.

164. Westbury, C.B., et al., Genome-wide transcriptomic profiling of microdissected human breast tissue reveals differential expression of KIT (c-Kit, CD117) and oestrogen receptor-alpha (ERalpha) in response to therapeutic radiation. J Pathol, 2009. 219(1): p. 131-40.

165. Graves, P.R., et al., Radiation pulmonary toxicity: from mechanisms to management. Semin Radiat Oncol, 2010. 20(3): p. 201-7.

166. Barnett, G.C., et al., Normal tissue reactions to radiotherapy: towards tailoring treatment dose by genotype. Nat Rev Cancer, 2009. 9(2): p. 134-42.

167. Paun, A., A.M. Lemay, and C.K. Haston, Gene expression profiling distinguishes radiation-induced fibrosing alveolitis from alveolitis in mice. Radiat Res, 2010. 173(4): p. 512-21.

168. Thomas, D.M., J. Fox, and C.K. Haston, Imatinib therapy reduces radiation-induced pulmonary mast cell influx and delays lung disease in the mouse. Int J Radiat Biol, 2010. 86(6): p. 436-44.

169. Jackson, I.L., Z. Vujaskovic, and J.D. Down, Revisiting strain-related differences in radiation sensitivity of the mouse lung: recognizing and avoiding the confounding effects of pleural effusions. Radiat Res, 2010. 173(1): p. 10-20.

170. Frazer, K.A., et al., A sequence-based variation map of 8.27 million SNPs in inbred mouse strains. Nature, 2007. 448(7157): p. 1050-3.

171. Harrill, A.H., et al., Mouse population-guided resequencing reveals that variants in CD44 contribute to acetaminophen-induced liver injury in humans. Genome Res, 2009. 19(9): p. 1507-15.

172. Leikauf, G.D., et al., Haplotype association mapping of acute lung injury in mice implicates activin a receptor, type 1. Am J Respir Crit Care Med, 2011. 183(11): p. 1499-509.

173. Liu, P.Y., et al., Identification of Las2, a major modifier gene affecting the Pas1 mouse lung tumor susceptibility locus. Cancer Res, 2009. 69(15): p. 6290-8.

174. Lu, Y., et al., Genetic variants cis-regulating Xrn2 expression contribute to the risk of spontaneous lung tumor. Oncogene, 2010. 29(7): p. 1041-9.

175. Nissenbaum, J., et al., Susceptibility to chronic pain following nerve injury is genetically affected by CACNG2. Genome Res, 2010. 20(9): p. 1180-90.

176. Singer, J.B., et al., Mapping quantitative trait loci for anxiety in chromosome substitution strains of mice. Genetics, 2005. 169(2): p. 855-62.

177. Yang, H., et al., Subspecific origin and haplotype diversity in the laboratory mouse. Nat Genet, 2011. 43(7): p. 648-55.

178. Bennett, B.J., et al., A high-resolution association mapping panel for the dissection of complex traits in mice. Genome Res, 2010. 20(2): p. 281-90.

179. Niu, N., et al., Radiation pharmacogenomics: a genome-wide association approach to identify radiation response biomarkers using human lymphoblastoid cell lines. Genome Res, 2010. 20(11): p. 1482-92.

180. Cahan, P. and T.A. Graubert, Integrated genomics of susceptibility to alkylator-induced leukemia in mice. BMC Genomics, 2010. 11: p. 638.

181. Stearman, R.S., et al., Analysis of orthologous gene expression between human pulmonary adenocarcinoma and a carcinogen-induced murine model. Am J Pathol, 2005. 167(6): p. 1763-75.

182. Sudbery, I., et al., Deep short-read sequencing of chromosome 17 from the mouse strains A/J and CAST/Ei identifies significant germline variation and candidate genes that regulate liver triglyceride levels. Genome Biol, 2009. 10(10): p. R112.

183. Blanchette, M., et al., Aligning multiple genomic sequences with the threaded blockset aligner. Genome Res, 2004. 14(4): p. 708-15.

184. Siepel, A., et al., Evolutionarily conserved elements in vertebrate, insect, worm, and yeast genomes. Genome Res, 2005. 15(8): p. 1034-50.

185. Loots, G.G., et al., Identification of a coordinate regulator of interleukins 4, 13, and 5 by cross-species sequence comparisons. Science, 2000. 288(5463): p. 136-40.

186. Li, Q., S. Harju, and K.R. Peterson, Locus control regions: coming of age at a decade plus. Trends Genet, 1999. 15(10): p. 403-8.

187. Barnett, G.C., et al., Independent validation of genes and polymorphisms reported to be associated with radiation toxicity: a prospective analysis study. Lancet Oncol, 2012. 13(1): p. 65-77.

188. Sinke, A.P., et al., Genetic analysis of mouse strains with variable serum sodium concentrations identifies the Nalcn sodium channel as a novel player in osmoregulation. Physiol Genomics, 2011. 43(5): p. 265-70.

189. Keane, T.M., et al., Mouse genomic variation and its effect on phenotypes and gene regulation. Nature, 2011. 477(7364): p. 289-94.

190. Freedman, M.L., et al., Principles for the post-GWAS functional characterization of cancer risk loci. Nat Genet, 2011. 43(6): p. 513-8.

191. Forton, J.T., et al., Localization of a long-range cis-regulatory element of IL13 by allelic transcript ratio mapping. Genome Res, 2007. 17(1): p. 82-7.

192. Hallahan, D.E., L. Geng, and Y. Shyr, Effects of intercellular adhesion molecule 1 (ICAM-1) null mutation on radiation-induced pulmonary fibrosis and respiratory insufficiency in mice. J Natl Cancer Inst, 2002. 94(10): p. 733-41.

193. Konigshoff, M., Lung cancer in pulmonary fibrosis: tales of epithelial cell plasticity. Respiration, 2011. 81(5): p. 353-8.

194. Roberts, M.E., et al., Discoidin domain receptor 1 regulates bronchial epithelial repair and matrix metalloproteinase production. Eur Respir J, 2011. 37(6): p. 1482-93.

195. Peacock, J.G., et al., The Abl-related gene tyrosine kinase acts through p190RhoGAP to inhibit actomyosin contractility and regulate focal adhesion dynamics upon adhesion to fibronectin. Mol Biol Cell, 2007. 18(10): p. 3860-72.

196. Avivi-Green, C., M. Singal, and W.F. Vogel, Discoidin domain receptor 1-deficient mice are resistant to bleomycin-induced lung fibrosis. Am J Respir Crit Care Med, 2006. 174(4): p. 420-7.

197. Guerrot, D., et al., Discoidin domain receptor 1 is a major mediator of inflammation and fibrosis in obstructive nephropathy. Am J Pathol, 2011. 179(1): p. 83-91.

198. Barron, L. and T.A. Wynn, Fibrosis is regulated by Th2 and Th17 responses and by dynamic interactions between fibroblasts and macrophages. Am J Physiol Gastrointest Liver Physiol, 2011. 300(5): p. G723-8.

199. Yamazaki, T., et al., A butyrophilin family member critically inhibits T cell activation. J Immunol, 2010. 185(10): p. 5907-14.

200. Zhong, M.C. and A. Veillette, Control of T lymphocyte signaling by Ly108, a signaling lymphocytic activation molecule family receptor implicated in autoimmunity. J Biol Chem, 2008. 283(28): p. 19255-64.

201. Chapman, H.A., Epithelial-mesenchymal interactions in pulmonary fibrosis. Annu Rev Physiol, 2011. 73: p. 413-35.

202. Anscher, M.S., et al., Small molecular inhibitor of transforming growth factor-beta protects against development of radiation-induced lung injury. Int J Radiat Oncol Biol Phys, 2008. 71(3): p. 829-37.

203. Yamasaki, M., et al., P21 regulates TGF-beta1-induced pulmonary responses via a TNF-alpha-signaling pathway. Am J Respir Cell Mol Biol, 2008. 38(3): p. 346-53.

204. Shen, Z.J., et al., Pin1 regulates TGF-beta1 production by activated human and murine eosinophils and contributes to allergic lung fibrosis. J Clin Invest, 2008. 118(2): p. 479-90.

205. Lin, J.R., et al., SHPRH and HLTF act in a damage-specific manner to coordinate different forms of postreplication repair and prevent mutagenesis. Mol Cell, 2011. 42(2): p. 237-49.

206. Smirnov, D.A., et al., Genetic analysis of radiation-induced changes in human gene expression. Nature, 2009. 459(7246): p. 587-91.

207. Miyake, K., Innate immune sensing of pathogens and danger signals by cell surface Toll-like receptors. Semin Immunol, 2007. 19(1): p. 3-10.

208. Rahman, A.H., D.K. Taylor, and L.A. Turka, The contribution of direct TLR signaling to T cell responses. Immunol Res, 2009. 45(1): p. 25-36.

209. Beg, A.A., Endogenous ligands of Toll-like receptors: implications for regulating inflammatory and immune responses. Trends Immunol, 2002. 23(11): p. 509-12.

210. Muro, A.F., et al., An essential role for fibronectin extra type III domain A in pulmonary fibrosis. Am J Respir Crit Care Med, 2008. 177(6): p. 638-45.

211. Wang, Y., et al., Genetic defects in surfactant protein A2 are associated with pulmonary fibrosis and lung cancer. Am J Hum Genet, 2009. 84(1): p. 52-9.

212. Rube, C.E., et al., Irradiation induces a biphasic expression of pro-inflammatory cytokines in the lung. Strahlenther Onkol, 2004. 180(7): p. 442-8.

213. Haston, C.K. and E.L. Travis, Murine susceptibility to radiation-induced pulmonary fibrosis is influenced by a genetic factor implicated in susceptibility to bleomycin-induced pulmonary fibrosis. Cancer Res, 1997. 57(23): p. 5286-91.

214. Rubin, P., et al., A perpetual cascade of cytokines postirradiation leads to pulmonary fibrosis. Int J Radiat Oncol Biol Phys, 1995. 33(1): p. 99-109.

215. Li, Y., et al., Irradiation-induced expression of hyaluronan (HA) synthase 2 and hyaluronidase 2 genes in rat lung tissue accompanies active turnover of HA and induction of types I and III collagen gene expression. Am J Respir Cell Mol Biol, 2000. 23(3): p. 411-8.

216. Gasse, P., et al., IL-1R1/MyD88 signaling and the inflammasome are essential in pulmonary inflammation and fibrosis in mice. J Clin Invest, 2007. 117(12): p. 3786-99.

217. Trinchieri, G., Interleukin-12 and the regulation of innate resistance and adaptive immunity. Nat Rev Immunol, 2003. 3(2): p. 133-46.

218. Netea, M.G., et al., From the Th1/Th2 paradigm towards a Toll-like receptor/T-helper bias. Antimicrob Agents Chemother, 2005. 49(10): p. 3991-6.

219. Amati, L., et al., Toll-like receptor signaling mechanisms involved in dendritic cell activation: potential therapeutic control of T cell polarization. Curr Pharm Des, 2006. 12(32): p. 4247-54.

220. Akira, S., K. Takeda, and T. Kaisho, Toll-like receptors: critical proteins linking innate and acquired immunity. Nat Immunol, 2001. 2(8): p. 675-80.

221. Hoebe, K., E. Janssen, and B. Beutler, The interface between innate and adaptive immunity. Nat Immunol, 2004. 5(10): p. 971-4.

222. Mazza, C. and B. Malissen, What guides MHC-restricted TCR recognition? Semin Immunol, 2007. 19(4): p. 225-35.

223. Wynn, T.A., Fibrotic disease and the T(H)1/T(H)2 paradigm. Nat Rev Immunol, 2004. 4(8): p. 583-94.

224. Du, M., et al., H2-Ea deficiency is a risk factor for bleomycin-induced lung fibrosis in mice. Cancer Res, 2004. 64(19): p. 6835-9.

225. Sokolova, E. and G. Reiser, A novel therapeutic target in various lung diseases: airway proteases and protease-activated receptors. Pharmacol Ther, 2007. 115(1): p. 70-83.

226. Martin, S.F., et al., Toll-like receptor and IL-12 signaling control susceptibility to contact hypersensitivity. J Exp Med, 2008. 205(9): p. 2151-62.

227. Lampropoulou, V., et al., TLR-activated B cells suppress T cell-mediated autoimmunity. J Immunol, 2008. 180(7): p. 4763-73.

228. Barr, T.A., et al., TLR-mediated stimulation of APC: Distinct cytokine responses of B cells and dendritic cells. Eur J Immunol, 2007. 37(11): p. 3040-53.

229. Hayashi, F., T.K. Means, and A.D. Luster, Toll-like receptors stimulate human neutrophil function. Blood, 2003. 102(7): p. 2660-9.

230. Li, M., et al., An essential role of the NF-kappa B/Toll-like receptor pathway in induction of inflammatory and tissue-repair gene expression by necrotic cells. J Immunol, 2001. 166(12): p. 7128-35.

231. Sabroe, I., et al., Selective roles for Toll-like receptor (TLR)2 and TLR4 in the regulation of neutrophil activation and life span. J Immunol, 2003. 170(10): p. 5268-75.

232. DeGrendele, H.C., P. Estess, and M.H. Siegelman, Requirement for CD44 in activated T cell extravasation into an inflammatory site. Science, 1997. 278(5338): p. 672-5.

233. Bollyky, P.L., et al., Cutting edge: high molecular weight hyaluronan promotes the suppressive effects of CD4+CD25+ regulatory T cells. J Immunol, 2007. 179(2): p. 744-7.

234. Bjermer, L., R. Lundgren, and R. Hallgren, Hyaluronan and type III procollagen peptide concentrations in bronchoalveolar lavage fluid in idiopathic pulmonary fibrosis. Thorax, 1989. 44(2): p. 126-31.

235. Nilsson, K., et al., Hyaluronan reflects the pre-fibrotic inflammation in irradiated rat lung: concomitant analysis of parenchymal tissues and bronchoalveolar lavage. Int J Radiat Biol, 1990. 58(3): p. 519-30.

236. Rosenbaum, D., et al., Hyaluronan in radiation-induced lung disease in the rat. Radiat Res, 1997. 147(5): p. 585-91.

237. Teder, P., et al., Resolution of lung inflammation by CD44. Science, 2002. 296(5565): p. 155-8.

238. Stern, R., A.A. Asari, and K.N. Sugahara, Hyaluronan fragments: an information-rich system. Eur J Cell Biol, 2006. 85(8): p. 699-715.

239. Jayawardana, S.T., et al., Monomeric IgE and lipopolysaccharide synergistically prevent mast-cell apoptosis. Biochem Biophys Res Commun, 2008. 365(1): p. 137-42.

240. Yoshikawa, H. and K. Tasaka, Caspase-dependent and -independent apoptosis of mast cells induced by withdrawal of IL-3 is prevented by Toll-like receptor 4-mediated lipopolysaccharide stimulation. Eur J Immunol, 2003. 33(8): p. 2149-59.

241. Azzam, E.I., J.P. Jay-Gerin, and D. Pain, Ionizing radiation-induced metabolic oxidative stress and prolonged cell injury. Cancer Lett, 2012. 327(1-2): p. 48-60.

242. Zhao, W. and M.E. Robbins, Inflammation and chronic oxidative stress in radiation-induced late normal tissue injury: therapeutic implications. Curr Med Chem, 2009. 16(2): p. 130-43.

243. Ghafoori, P., et al., Radiation-induced lung injury. Assessment, management, and prevention. Oncology (Williston Park), 2008. 22(1): p. 37-47; discussion 52-3.

244. McBride, W.H., et al., A sense of danger from radiation. Radiat Res, 2004. 162(1): p. 1-19.

245. Pan, L.H., et al., Co-expression of TNF alpha and IL-1 beta in human acute pulmonary fibrotic diseases: an immunohistochemical analysis. Pathol Int, 1996. 46(2): p. 91-9.

246. Chen, Y., et al., Radiation pneumonitis and early circulatory cytokine markers. Semin Radiat Oncol, 2002. 12(1 Suppl 1): p. 26-33.

247. Chen, Y., et al., Interleukin (IL)-1A and IL-6: applications to the predictive diagnostic testing of radiation pneumonitis. Int J Radiat Oncol Biol Phys, 2005. 62(1): p. 260-6.

248. Kong, F., et al., Plasma transforming growth factor-beta1 level before radiotherapy correlates with long term outcome of patients with lung carcinoma. Cancer, 1999. 86(9): p. 1712-9.

249. Fu, X.L., et al., Predicting the risk of symptomatic radiation-induced lung injury using both the physical and biologic parameters V(30) and transforming growth factor beta. Int J Radiat Oncol Biol Phys, 2001. 50(4): p. 899-908.

250. Paun, A. and C.K. Haston, Genomic and genome-wide association of susceptibility to radiation-induced fibrotic lung disease in mice. Radiother Oncol, 2012. 105(3): p. 350-7.

251. Paun, A., et al., Combined Tlr2 and Tlr4 deficiency increases radiation-induced pulmonary fibrosis in mice. Int J Radiat Oncol Biol Phys, 2010. 77(4): p. 1198-205.

252. Joshi, A.D., et al., Interleukin-17-mediated immunopathogenesis in experimental hypersensitivity pneumonitis. Am J Respir Crit Care Med, 2009. 179(8): p. 705-16.

253. Fox, J. and C.K. Haston, CXC receptor 1 and 2 and neutrophil elastase inhibitors alter radiation-induced lung disease in the mouse. Int J Radiat Oncol Biol Phys, 2013. 85(1): p. 215-22.

254. Fox, J., J.R. Gordon, and C.K. Haston, Combined CXCR1/CXCR2 antagonism decreases radiation-induced alveolitis in the mouse. Radiat Res, 2011. 175(5): p. 657-64.

255. Bettelli, E., et al., Reciprocal developmental pathways for the generation of pathogenic effector TH17 and regulatory T cells. Nature, 2006. 441(7090): p. 235-8.

256. Mangan, P.R., et al., Transforming growth factor-beta induces development of the T(H)17 lineage. Nature, 2006. 441(7090): p. 231-4.

257. Veldhoen, M. and B. Stockinger, TGFbeta1, a "Jack of all trades": the link with pro-inflammatory IL-17-producing T cells. Trends Immunol, 2006. 27(8): p. 358-61.

258. Veldhoen, M., et al., TGFbeta in the context of an inflammatory cytokine milieu supports de novo differentiation of IL-17-producing T cells. Immunity, 2006. 24(2): p. 179-89.

259. Nakagome, K., et al., In vivo IL-10 gene delivery attenuates bleomycin induced pulmonary fibrosis by inhibiting the production and activation of TGF-beta in the lung. Thorax, 2006. 61(10): p. 886-94.

260. Pelletier, M., et al., Evidence for a cross-talk between human neutrophils and Th17 cells. Blood, 2010. 115(2): p. 335-43.

261. Laan, M., et al., Neutrophil recruitment by human IL-17 via C-X-C chemokine release in the airways. J Immunol, 1999. 162(4): p. 2347-52.

262. Miyamoto, M., et al., Endogenous IL-17 as a mediator of neutrophil recruitment caused by endotoxin exposure in mouse airways. J Immunol, 2003. 170(9): p. 4665-72.

263. Witowski, J., et al., IL-17 stimulates intraperitoneal neutrophil infiltration through the release of GRO alpha chemokine from mesothelial cells. J Immunol, 2000. 165(10): p. 5814-21.

264. Wilson, R.H., et al., Allergic sensitization through the airway primes Th17-dependent neutrophilia and airway hyperresponsiveness. Am J Respir Crit Care Med, 2009. 180(8): p. 720-30.

265. Yoshizaki, A., et al., Cell adhesion molecules regulate fibrotic process via Th1/Th2/Th17 cell balance in a bleomycin-induced scleroderma model. J Immunol, 2010. 185(4): p. 2502-15.

266. Rivera, A., et al., Dectin-1 diversifies Aspergillus fumigatus-specific T cell responses by inhibiting T helper type 1 CD4 T cell differentiation. J Exp Med, 2011. 208(2): p. 369-81.

267. O'Connor, W., Jr., et al., A protective function for interleukin 17A in T cell-mediated intestinal inflammation. Nat Immunol, 2009. 10(6): p. 603-9.

268. Mosser, D.M., The many faces of macrophage activation. J Leukoc Biol, 2003. 73(2): p. 209-12.

269. Shearer, J.D., et al., Differential regulation of macrophage arginine metabolism: a proposed role in wound healing. Am J Physiol, 1997. 272(2 Pt 1): p. E181-90.

270. Keane, M.P., The role of chemokines and cytokines in lung fibrosis. Eur Respir Rev, 2008. 17(109): p. 151-156.

271. Wynn, T.A., Integrating mechanisms of pulmonary fibrosis. J Exp Med, 2011. 208(7): p. 1339-50.

272. Lo Re, S., D. Lison, and F. Huaux, CD4+ T lymphocytes in lung fibrosis: diverse subsets, diverse functions. J Leukoc Biol, 2013. 93(4): p. 499-510.

273. Johnston, C.J., et al., Early and persistent alterations in the expression of interleukin-1 alpha, interleukin-1 beta and tumor necrosis factor alpha mRNA levels in fibrosis-resistant and sensitive mice after thoracic irradiation. Radiat Res, 1996. 145(6): p. 762-7.

274. Yang, X., et al., The chemokine, CCL3, and its receptor, CCR1, mediate thoracic radiation-induced pulmonary fibrosis. Am J Respir Cell Mol Biol, 2011. 45(1): p. 127-35.

275. Hyde, D.M., et al., Effect of murine gamma interferon on the cellular responses to bleomycin in mice. Exp Lung Res, 1988. 14(5): p. 687-704.

276. Yi, T., et al., Absence of donor Th17 leads to augmented Th1 differentiation and exacerbated acute graft-versus-host disease. Blood, 2008. 112(5): p. 2101-10.

277. Lo Re, S., et al., IL-17A-producing gammadelta T and Th17 lymphocytes mediate lung inflammation but not fibrosis in experimental silicosis. J Immunol, 2010. 184(11): p. 6367-77.

278. Braun, R.K., et al., IL-17 producing gammadelta T cells are required for a controlled inflammatory response after bleomycin-induced lung injury. Inflammation, 2008. 31(3): p. 167-79.

279. Kim, J.H., et al., Natural killer T (NKT) cells attenuate bleomycin-induced pulmonary fibrosis by producing interferon-gamma. Am J Pathol, 2005. 167(5): p. 1231-41.

280. Kim, J.H. and D.H. Chung, CD1d-restricted IFN-gamma-secreting NKT cells promote immune complex-induced acute lung injury by regulating macrophage-inflammatory protein-1alpha production and activation of macrophages and dendritic cells. J Immunol, 2011. 186(3): p. 1432-41.

281. Sharma, A.K., et al., Natural killer T cell-derived IL-17 mediates lung ischemia-reperfusion injury. Am J Respir Crit Care Med, 2011. 183(11): p. 1539-49.

282. Pichavant, M., et al., Ozone exposure in a mouse model induces airway hyperreactivity that requires the presence of natural killer T cells and IL-17. J Exp Med, 2008. 205(2): p. 385-93.

283. Bold, T.D. and J.D. Ernst, CD4+ T cell-dependent IFN-gamma production by CD8+ effector T cells in Mycobacterium tuberculosis infection. J Immunol, 2012. 189(5): p. 2530-6.

284. Chang, Y., et al., CD8 positive T cells express IL-17 in patients with chronic obstructive pulmonary disease. Respir Res, 2011. 12: p. 43.

285. Johansen, J., et al., Relationship between the in vitro radiosensitivity of skin fibroblasts and the expression of subcutaneous fibrosis, telangiectasia, and skin erythema after radiotherapy. Radiother Oncol, 1996. 40(2): p. 101-9.

286. West, C.M., et al., Lymphocyte radiosensitivity is a significant prognostic factor for morbidity in carcinoma of the cervix. Int J Radiat Oncol Biol Phys, 2001. 51(1): p. 10-5.

287. Sullivan, E.R., Molecular genetics of biosurfactant production. Curr Opin Biotechnol, 1998. 9(3): p. 263-9.

288. Peacock, J., et al., Cellular radiosensitivity and complication risk after curative radiotherapy. Radiother Oncol, 2000. 55(2): p. 173-8.

289. Dickson, J., et al., Relationship between residual radiation-induced DNA double-strand breaks in cultured fibroblasts and late radiation reactions: a comparison of training and validation cohorts of breast cancer patients. Radiother Oncol, 2002. 62(3): p. 321-6.

290. Alsner, J., C.N. Andreassen, and J. Overgaard, Genetic markers for prediction of normal tissue toxicity after radiotherapy. Semin Radiat Oncol, 2008. 18(2): p. 126-35.

291. Kerns, S.L., et al., Genome-wide association study to identify single nucleotide polymorphisms (SNPs) associated with the development of erectile dysfunction in African-American men after radiotherapy for prostate cancer. Int J Radiat Oncol Biol Phys, 2010. 78(5): p. 1292-300.

292. Michikawa, Y., et al., Genome wide screen identifies microsatellite markers associated with acute adverse effects following radiotherapy in cancer patients. BMC Med Genet, 2010. 11: p. 123.

293. De Ruysscher, D., et al., First report on the patient database for the identification of the genetic pathways involved in patients over-reacting to radiotherapy: GENEPI-II. Radiother Oncol, 2010. 97(1): p. 36-9.

294. Barnett, G.C., et al., No association between SNPs regulating TGF-beta1 secretion and late radiotherapy toxicity to the breast: results from the RAPPER study. Radiother Oncol, 2010. 97(1): p. 9-14.

295. Iwakawa, M., et al., [RadGenomics project]. Nihon Igaku Hoshasen Gakkai Zasshi, 2002. 62(9): p. 484-9.

296. Suga, T., et al., Influence of multiple genetic polymorphisms on genitourinary morbidity after carbon ion radiotherapy for prostate cancer. Int J Radiat Oncol Biol Phys, 2008. 72(3): p. 808-13.

297. Ho, A.Y., et al., Genetic predictors of adverse radiotherapy effects: the Gene-PARE project. Int J Radiat Oncol Biol Phys, 2006. 65(3): p. 646-55.

298. West, C., et al., Establishment of a Radiogenomics Consortium. Int J Radiat Oncol Biol Phys, 2010. 76(5): p. 1295-6.

299. Rieger, K.E., et al., Toxicity from radiation therapy associated with abnormal transcriptional responses to DNA damage. Proc Natl Acad Sci U S A, 2004. 101(17): p. 6635-40.

300. Jen, K.Y. and V.G. Cheung, Transcriptional response of lymphoblastoid cells to ionizing radiation. Genome Res, 2003. 13(9): p. 2092-100.

301. Rieger, K.E. and G. Chu, Portrait of transcriptional responses to ultraviolet and ionizing radiation in human cells. Nucleic Acids Res, 2004. 32(16): p. 4786-803.

302. Meuwissen, R. and A. Berns, Mouse models for human lung cancer. Genes Dev, 2005. 19(6): p. 643-64.

303. De Jaeger, K., et al., Significance of plasma transforming growth factor-beta levels in radiotherapy for non-small-cell lung cancer. Int J Radiat Oncol Biol Phys, 2004. 58(5): p. 1378-87.

304. Moore, T.V., et al., Inducible costimulator controls migration of T cells to the lungs via down-regulation of CCR7 and CD62L. Am J Respir Cell Mol Biol, 2011. 45(4): p. 843-50.

305. Tager, A.M., et al., Accessory cells with immunophenotypic and functional features of monocyte-derived dendritic cells are recruited to the lung during pulmonary inflammation. J Leukoc Biol, 1999. 66(6): p. 901-8.

306. Okazaki, T., et al., Impairment of bleomycin-induced lung fibrosis in CD28-deficient mice. J Immunol, 2001. 167(4): p. 1977-81.

307. Hamaguchi, Y., et al., Intercellular adhesion molecule-1 and L-selectin regulate bleomycin-induced lung fibrosis. Am J Pathol, 2002. 161(5): p. 1607-18.

308. Matsuse, T., et al., ICAM-1 mediates lung leukocyte recruitment but not pulmonary fibrosis in a murine model of bleomycin-induced lung injury. Eur Respir J, 1999. 13(1): p. 71-7.

309. Horikawa, M., et al., E- and P-selectins synergistically inhibit bleomycin-induced pulmonary fibrosis. Am J Pathol, 2006. 169(3): p. 740-9.

310. Wray, C., et al., Claudin-4 augments alveolar epithelial barrier function and is induced in acute lung injury. Am J Physiol Lung Cell Mol Physiol, 2009. 297(2): p. L219-27.

311. Bryan, C.S., Penicillin mastics in the treatment of chronic streptococcic mastitis. Vet Med, 1946. 41(12): p. 429-32.

312. Gammon, A., et al., Hamartomatous polyposis syndromes. Best Pract Res Clin Gastroenterol, 2009. 23(2): p. 219-31.

313. Schneider, D.J., et al., Cadherin-11 contributes to pulmonary fibrosis: potential role in TGF-beta production and epithelial to mesenchymal transition. FASEB J, 2012. 26(2): p. 503-12.

314. Stamatoyannopoulos, J.A., The genomics of gene expression. Genomics, 2004. 84(3): p. 449-57.

315. Schadt, E.E., et al., Genetics of gene expression surveyed in maize, mouse and man. Nature, 2003. 422(6929): p. 297-302.

316. Ronald, J. and J.M. Akey, The evolution of gene expression QTL in Saccharomyces cerevisiae. PLoS One, 2007. 2(7): p. e678.

317. Murakami, Y., et al., Localization of tumor suppressor activity important in nonsmall cell lung carcinoma on chromosome 11q. Proc Natl Acad Sci U S A, 1998. 95(14): p. 8153-8.

318. Kuramochi, M., et al., TSLC1 is a tumor-suppressor gene in human non-small-cell lung cancer. Nat Genet, 2001. 27(4): p. 427-30.

319. Fukami, T., et al., Promoter methylation of the TSLC1 gene in advanced lung tumors and various cancer cell lines. Int J Cancer, 2003. 107(1): p. 53-9.

320. Fukuhara, H., et al., Promoter methylation of TSLC1 and tumor suppression by its gene product in human prostate cancer. Jpn J Cancer Res, 2002. 93(6): p. 605-9.

321. Honda, T., et al., Hypermethylation of the TSLC1 gene promoter in primary gastric cancers and gastric cancer cell lines. Jpn J Cancer Res, 2002. 93(8): p. 857-60.

322. Allinen, M., et al., Analysis of 11q21-24 loss of heterozygosity candidate target genes in breast cancer: indications of TSLC1 promoter hypermethylation. Genes Chromosomes Cancer, 2002. 34(4): p. 384-9.

323. Jansen, M., et al., Aberrant methylation of the 5' CpG island of TSLC1 is common in pancreatic ductal adenocarcinoma and is first manifest in high-grade PanINs. Cancer Biol Ther, 2002. 1(3): p. 293-6.

324. Boles, K.S., et al., The tumor suppressor TSLC1/NECL-2 triggers NK-cell and CD8+ T-cell responses through the cell-surface receptor CRTAM. Blood, 2005. 106(3): p. 779-86.

325. Giangreco, A., et al., Epidermal Cadm1 expression promotes autoimmune alopecia via enhanced T cell adhesion and cytotoxicity. J Immunol, 2012. 188(3): p. 1514-22.

326. Bas, A., et al., Butyrophilin-like 1 encodes an enterocyte protein that selectively regulates functional interactions with T lymphocytes. Proc Natl Acad Sci U S A, 2011. 108(11): p. 4376-81.

327. Chatterjee, M., et al., CD3-T cell receptor co-stimulation through SLAMF3 and SLAMF6 receptors enhances RORgammat recruitment to the IL17A promoter in human T lymphocytes. J Biol Chem, 2012. 287(45): p. 38168-77.

328. Chatterjee, M., et al., Increased expression of SLAM receptors SLAMF3 and SLAMF6 in systemic lupus erythematosus T lymphocytes promotes Th17 differentiation. J Immunol, 2012. 188(3): p. 1206-12.

329. Gurujeyalakshmi, G. and S.N. Giri, Molecular mechanisms of antifibrotic effect of interferon gamma in bleomycin-mouse model of lung fibrosis: downregulation of TGF-beta and procollagen I and III gene expression. Exp Lung Res, 1995. 21(5): p. 791-808.

330. Gottlober, P., et al., Interferon-gamma in 5 patients with cutaneous radiation syndrome after radiation therapy. Int J Radiat Oncol Biol Phys, 2001. 50(1): p. 159-66.

331. Ziesche, R., et al., A preliminary study of long-term treatment with interferon gamma-1b and low-dose prednisolone in patients with idiopathic pulmonary fibrosis. N Engl J Med, 1999. 341(17): p. 1264-9.

APPENDIX

Chapter II

Due to the large number of entries per table, Supplementary Tables 1-5 have not been included in this thesis, but can be accessed online at http://dx.doi.org/10.1667/RR1798.1.

Supplementary Table 1-3: Detailed gene expression profiles after thoracic irradiation in A/J, C57Bl/6J and C3H/HeJ mice. File 10.1667_rr1798.1.s1.xls (927 kB).

Supplementary Table 4: Gene expression profiles from inter-strain comparisons. File 10.1667_rr1798.1.s3.xls (1 MB).

Supplementary Table 5: A complete listing of GO terms represented in each strain's response to thoracic irradiation. File 10.1667_rr1798.1.s2.xls (68 kB).

Chapter III

Supplementary Table 6: Significantly interacting SNP pairs in *Radpf1* and *Radpf2*

***Radpf1* SNP**	***Radpf2* SNP**	**p-value**	**FDR**	***Radpf1* nearest gene**	***Radpf2* nearest gene**
rs50253706	rs31168022	2.67E-09	0.01	*Ddr1*	*Tpr* intron 9
rs51899510	rs31168022	2.60E-09	0.01	*Ddr1*	Tpr intron 9
rs33801987	rs31168022	1.01E-08	0.025	*Btbd9* intron 4	*Tpr* intron 9
rs46654461	rs31272943	1.75E-07	0.134	*Myo1f*	*Abl2* 3'UTR
rs49838267	rs31272943	1.96E-07	0.134	*Myo1f* intron 1	*Abl2* 3'UTR
rs33444918	rs31529220	1.72E-07	0.134	*Btnl1*	*Slamf6* intron 1
rs33444918	rs31528128	2.66E-07	0.134	*Btnl1*	*Slamf6* intron 1
rs47182407	rs31168022	2.35E-07	0.134	*Mrps18b* intron 1	*Tpr* intron 9
rs51682784	rs31168022	2.03E-07	0.134	*Ddr1* intron 7	*Tpr* intron 9
rs29518121	rs46915727	2.17E-07	0.134	*Notch4* intron 17	intergenic

A linear model was fitted to the phenotypic data with *Radpf1* and *Radpf2* SNPs as covariates. The significance of the interaction term between each pair of SNPs was determined by comparing the model with interaction versus a simple additive model. The first 10 significant interacting SNP pairs are shown together with the false discovery rates and the gene containing or located near the SNP.